THE ASTRONOMICAL JOURNAL VOLUME 89, NUMBER 6 JUNE 1984

NEUTRAL HYDROGEN IN ISOLATED GALAXIES. IV. RESULTS FOR THE ARECIBO SAMPLE

MARTHA P. HAYNES
Astronomy Department, Cornell University, Ithaca, New York 14853
and National Astronomy and Ionosphere Center,[a] Ithaca, New York 14853

RICCARDO GIOVANELLI
Arecibo Observatory, National Astronomy and Ionosphere Center, Arecibo, Puerto Rico 00613
Received 28 December 1983; revised 21 February 1984

ABSTRACT

Neutral hydrogen observations of 324 isolated galaxies have been made in order to define a standard sample for the comparison of the H I content of galaxies in differing intergalactic environments. The observational sample is comprised of galaxies which are contained both in the Karachentseva *Catalog of Isolated Galaxies* and in the *Uppsala General Catalog* and which lie in the declination range accessible to the Arecibo 305-m telescope. A total observational data base composed of both mapping and single-point spectra has been used to compute the integral properties of the galaxies in the sample. The derivation of such properties is described in detail. Corrections for the absorption of both optical brightness and H I flux within the galaxian disk are determined and can be expressed in similar form. Of the 324 galaxies surveyed, neutral hydrogen emission has been detected in 288 with certainty. Neutral hydrogen absorption is seen in one, UGC 11905. A definite increase in the nondetection rate occurs for the earliest types, although some E–S0 galaxies have abundant hydrogen masses. For galaxies of unknown redshift, the H I may be undetected because its emission lies outside the frequency range covered by the observations. It is shown that the optical diameter of a spiral disk is better correlated with the hydrogen mass than is the morphological type. When used to define a measure of H I content, the isolated galaxy sample can predict "normalcy" with an accuracy carrying a standard error of about 0.20 in the log of the H I mass, if a dependence on the size of the disk, as well as the type, is properly taken into account. While the sample is not complete in any magnitude-limited sense and suffers from a Malmquist bias, it does contain a healthy population of distant objects and is thus suitable for comparison with galaxies of similar optical characteristics at relatively large distances.

I. INTRODUCTION

Observations of catastrophic tidal interactions, gradients in the distribution of morphological types in clusters, head-tail radio sources, x-ray emission from the intracluster medium, as well as the deficiency in the H I content of spiral galaxies in some (but not all) clusters imply that the present state of spiral galaxies can be strongly influenced by their environment. Except in the most obvious examples of ongoing interaction between a galaxy and its neighbors or surroundings, it is, however, as yet uncertain what relative roles in the evolution of a galaxy are played by the conditions at the time of galaxy formation or by more recent disruptive phenomena (Haynes, Giovanelli, and Chincarini 1984a).

Galaxies which would be expected to testify only minimally to the effects of their surroundings are those located in the far peripheries of superclusters, or truly in the "field," if such exist. Attempts to single out the truly isolated galaxies among nearby samples of galaxies have been made by numerous authors (e. g., Karachentseva 1973; Turner and Gott 1976; Huchra and Thuan 1977), who have based their definitions of isolation on widely varying criteria. In the absence of distance measures for most galaxies, these criteria mainly rest on magnitude or angular diameter and separation of a galaxy from its potential neighbors. The sparsity of field galaxies, or conversely, the vast expanse of supercluster aggregations has been demonstrated repeatedly (Chincarini and Rood 1979; Einasto *et al.* 1980; Kirschner *et al.* 1981). For any magnitude-limited sample, Soneira and Peebles (1977) estimate that the proportion of field galaxies is always less than 18%; Fesenko (1977) estimates that the true field is comprised of fewer than 10% of all.

The identification of an observational sample of isolated galaxies is important not only as possible evidence of the existence of field galaxies but also as a comparison of the properties of galaxies in different density environments. For example, the measure by which the H I content of galaxies in the cores of clusters is depleted is thought to be indicative of the physical conditions of the intracluster medium. An absolute measure of the magnitude of such depletion necessitates a carefully defined comparison sample of galaxies which must be, on the one hand, as unperturbed as possible by mechanisms characteristic of the environment being probed, and, on the other hand, sufficiently similar that the outcome of the comparison will be relatively independent of potential observational biases. The requirement of a well-chosen comparison data set has led us to define a sample of 324 isolated galaxies which we have then observed in the 21-cm line of neutral hydrogen; these galaxies have roughly the same characteristics of type, optical dimensions, and apparent magnitude as the galaxies in nearby clusters also being observed.

Preliminary results for five H I-rich early-type isolated galaxies have been reported previously (Haynes and Giovanelli 1980, hereafter Paper I). Arecibo mapping and NRAO* 91.4-m telescope observations of the large angular diameter ($a \geqslant 2.5$ arcmin) galaxies are included in Hewitt *et al.* (1983,

[a] The National Astronomy and Ionosphere Center is operated by Cornell University under contract with the National Science Foundation.

*The National Radio Astronomy Observatory is operated by Associated Universities, Inc., under contract with the National Science Foundation.

 0004-6256/84/060758-43$00.90

hereafter Paper II). The redshift distribution and its reflection of structure within the local universe is discussed in Haynes and Giovanelli (1983, hereafter Paper III). Here we present the results for the entire survey, making use of the data reported earlier and including all observations made with the Arecibo circular feed system which is described in Sec. II.

The H I observations of the isolated galaxy sample allow a statistical investigation of the H I properties and of the relation between the optical and H I characteristics derived from a homogeneous set of data. In Sec. IV, we present the observational data and describe in detail how the galaxy properties have been derived. Section V contains an examination of the distribution of intrinsic galaxy characteristics; the derived correlations are used to define in Sec. VI a standard of "normal" H I content for the future comparison of cluster and isolated galaxies.

II. THE SAMPLE

A list of isolated galaxies covering the appropriate magnitude range ($m \leqslant +15.7$) is given by Karachentseva (1973) in her *Catalog of Isolated Galaxies* (CIG). She searched the Palomar Sky Survey prints, trying to identify those galaxies in the Zwicky *et al.* (1960–1968) *Catalog of Galaxies and Clusters of Galaxies* (CGCG) which have no near neighbors. Her isolation criterion is based on angular diameter: a galaxy of angular diameter d is considered to be isolated if it cannot be identified as the neighbor of any galaxy of angular diameter d_1 with $\frac{1}{4}d \leqslant d_1 \leqslant 4d$, that is, the isolated galaxy must lie at a projected distance of more than $20d_1$ from all potential neighbors. The CIG contains 1052 galaxies, or roughly 3% of the galaxies included in the CGCG. An evaluation of the isolated galaxy criterion of this sample has been presented by Karachentseva (1980).

Even without redshift information, the strictness of this isolation criterion can still be estimated to be quite conservative. However, as pointed out by Stocke (1978), the angular separation definition weakens for the very nearby galaxies, where the area searched for potential companions exceeds the dimensions of a Sky Survey field, and several of the brighter galaxies in the CIG are actually members of nearby de Vaucouleurs (1975) groups. In Paper III, an examination of the redshift distribution shows that many of these galaxies lie in the peripheries of nearby superclusters and do not represent a true field population. At least, these galaxies should populate very low-density regions of intergalactic space and should show little or no evidence of interaction with their surroundings.

In order to make use of already compiled optical data, we have restricted our observing sample to those galaxies in the CIG which are also included in the *Uppsala General Catalog of Galaxies* (Nilson 1973, hereafter UGC). A complete list of the galaxies which are common to both catalogs is given in Haynes (1978). Our final sample has been further confined by the declination range accessible to the traveling feed system of the Arecibo 305-m telescope: $-1° < \delta < +38°$. One object, UGC 10642, was eliminated because it may be a star cluster rather than a resolved dwarf system. The final Arecibo isolated galaxy sample then contains 324 galaxies.

III. OBSERVATIONS

The observational material included in this survey of isolated galaxies has been obtained using several telescopes and systems. The 91.4-m telescope of the National Radio Astronomy Observatory at Green Bank has been used to reobserve some of the galaxies in order to prove the reliability of the flux-scale calibration and correction (Paper II). Optical redshifts have been measured for a very few of the galaxies with the 2.1-m telescope and IIDS of the Kitt Peak National Observatory* (Haynes, Giovanelli, and Chincarini 1984b), but the Arecibo 305-m telescope has been used for the majority of the observations. The mapping technique discussed in Paper II employed the 40-ft linearly polarized feed; dubbed the "flat" feed, this system is characterized by a lower gain, larger beamwidth, and higher system temperature (Paper II; Briggs 1982), but has a significantly milder sidelobe response than its alternative at Arecibo, the "dual circular" feed. It is the latter system that is discussed here.

The workhorse of extragalactic 21-cm observations since its installation in 1975, the dual circular feed is a 40-ft line feed of circular cross section, sensitive to both circular polarizations. Because 21-cm line radiation is randomly polarized, the integration time can be effectively doubled by combining measurements of incoming signals at the two orthogonal polarization ports, under the valid assumption that these two signals are independent. Hence, the receiver system is dual channel. These observations were conducted over numerous observing periods between August 1978 and June 1981, except in a few instances where better profiles have been obtained more recently for clarification. Prior to December 1980, the receiver system consisted of two room-temperature parametric amplifiers showing a system temperature of about 70 and 90 K, respectively, at optimum. Since that time, a system temperature of better than 40 K at optimum is provided in both channels by cooled FET amplifiers.

The dual circular feed illuminates an annulus on the dish 700 ft in diameter; it is tapered to attain a beamwidth (full width at half-power) of 3.3 ± 0.1 arcmin. This tapering creates a relatively high sidelobe response that can be seen in Fig. 1, a representative map of the source 3C133.0, made with the feed tuned to 1360 MHz. In Fig. 1, the contours are measured in dB below the peak response. The first sidelobe ring, at a level of about -10 dB, has a radius of about 5.6 arcmin. Sidelobe leakage can cause spurious signals to appear, particularly in regions close to bright sources. The sidelobe response varies with telescope configuration. It is because of the danger of sidelobe contamination that we used the flat feed for the mapping observations (Paper II). The circular feed observations consisted of single (center) point observations of the small angular diameter ($a \leqslant 2.5$ arcmin) galaxies. For such measurements, use of the circular feed is entirely acceptable. In the isolated galaxy case in particular, sidelobe contamination is not expected, because, by definition, isolated galaxies should not have any nearby companions which might intercept the sidelobe ring.

Vignetting causes a contribution to the system temperature from ground radiation at zenith angles greater than ten degrees. Similarly, the gain, beamwidth, and sidelobe response all degrade with increasing zenith angle beyond ten degrees. Figure 2 shows the degradation of system temperature, sensitivity, and beamwidth with increasing zenith angle.

Because the phase velocity inside the feed is a function of frequency, the correction for spherical aberration made by

*The Kitt Peak National Observatory is operated by Associated Universities for Research in Astronomy under contract with the National Science Foundation.

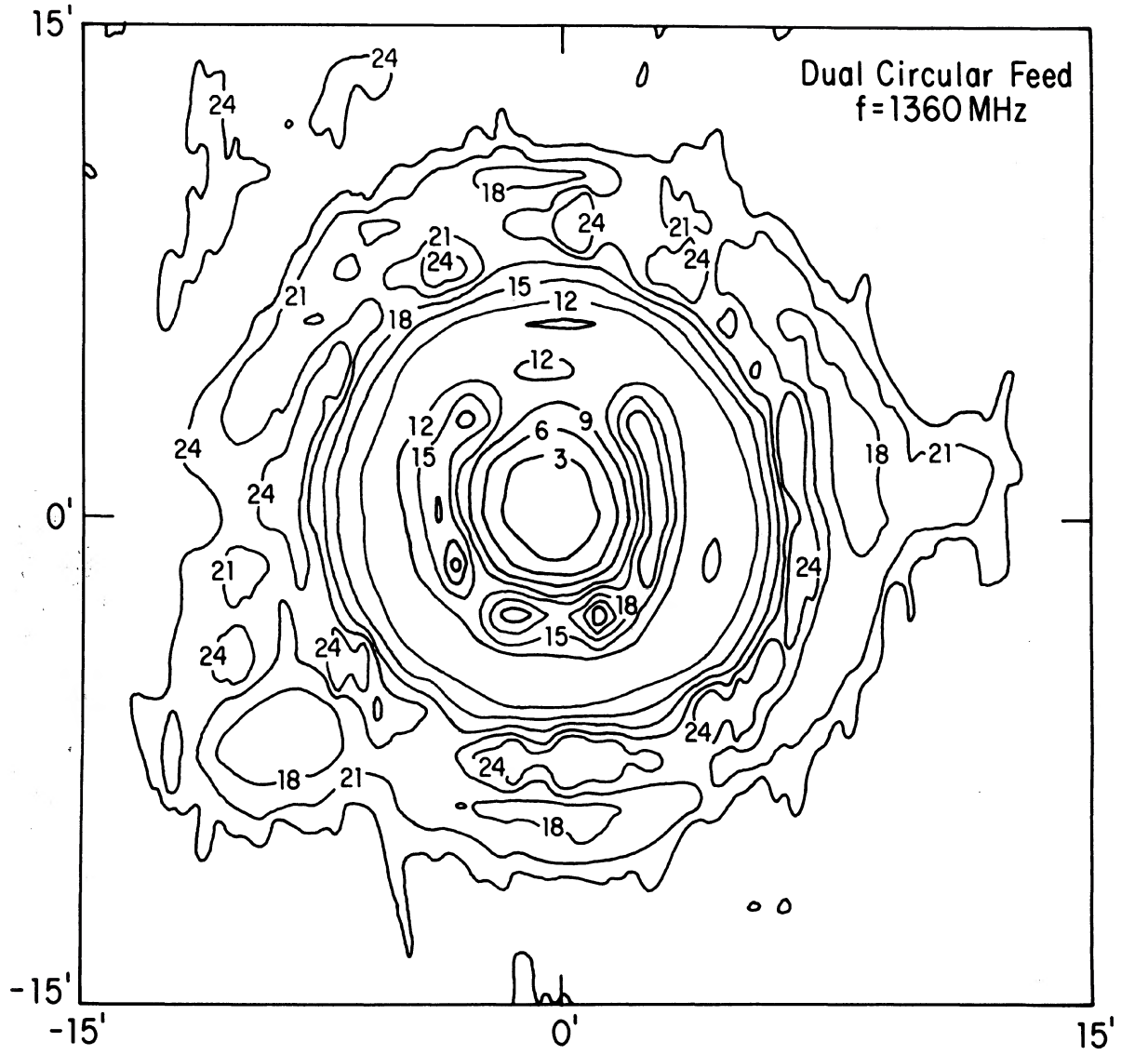

FIG. 1. Representative map of the Arecibo 21-cm dual circular feed beam obtained on the source 3C133.0 with the feed and system tuned to 1360 MHz. Contour units are dB below the peak. The first sidelobe ring, at a radius of about 5.6 arcmin, is approximately 10 dB below the peak response. Both the structure of the beam and the intensity of the sidelobes vary with the telescope orientation.

the line feed will be complete for only one frequency. Moving the feed up and down with respect to the paraxial surface shifts the frequency of maximum response. Thus the feed can be "tuned" in frequency by raising or lowering it mechanically to one of 19 mounting points, spaced at one-inch intervals, giving a frequency shift of about 4 MHz between successive mounts. The half-power point of the frequency response at any tuning is about 45 MHz, and the gain decreases from a maximum of about 8 K Jy^{-1} at the nominal optimum tuning of 1410 MHz to about 6 K Jy^{-1} at 1360 MHz.

The rms pointing error of the circular feed under normal conditions was about 20 arcsec. Pointing inaccuracies increase at very high and very low zenith angles, and tracking becomes difficult at very low zenith angles when the tracking speed of the azimuth arm is too slow to keep up with the rate of change of azimuth. In isolated cases, pointing errors of up to one minute may have occurred. The consistency of fluxes measured with this system and with the 91.4-m telescope at Green Bank (Paper II) testifies that pointing errors are not a limitation of these data.

More than half of these observations were made during filler time or when other experiments were cancelled because of equipment failure; each of the 26 observing periods had to be calibrated separately. The determination of the flux scale was achieved by comparing the noise diode to several strong radio sources taken from the catalog of Bridle *et al.* (1972), after accounting for the zenith-angle correction. A frequency response curve was derived for each tuning slot by observing sources while changing the frequency over a wide range.

The 21-cm line observations were made in a four-correlator quadrant mode, employing the 1008-channel autocorrelation spectrometer system in a two-level sampling mode. Normally, each polarization was split into two so that a total of four spectra were obtained by feeding each 10 MHz band into a separate quadrant of the autocorrelator. The resultant

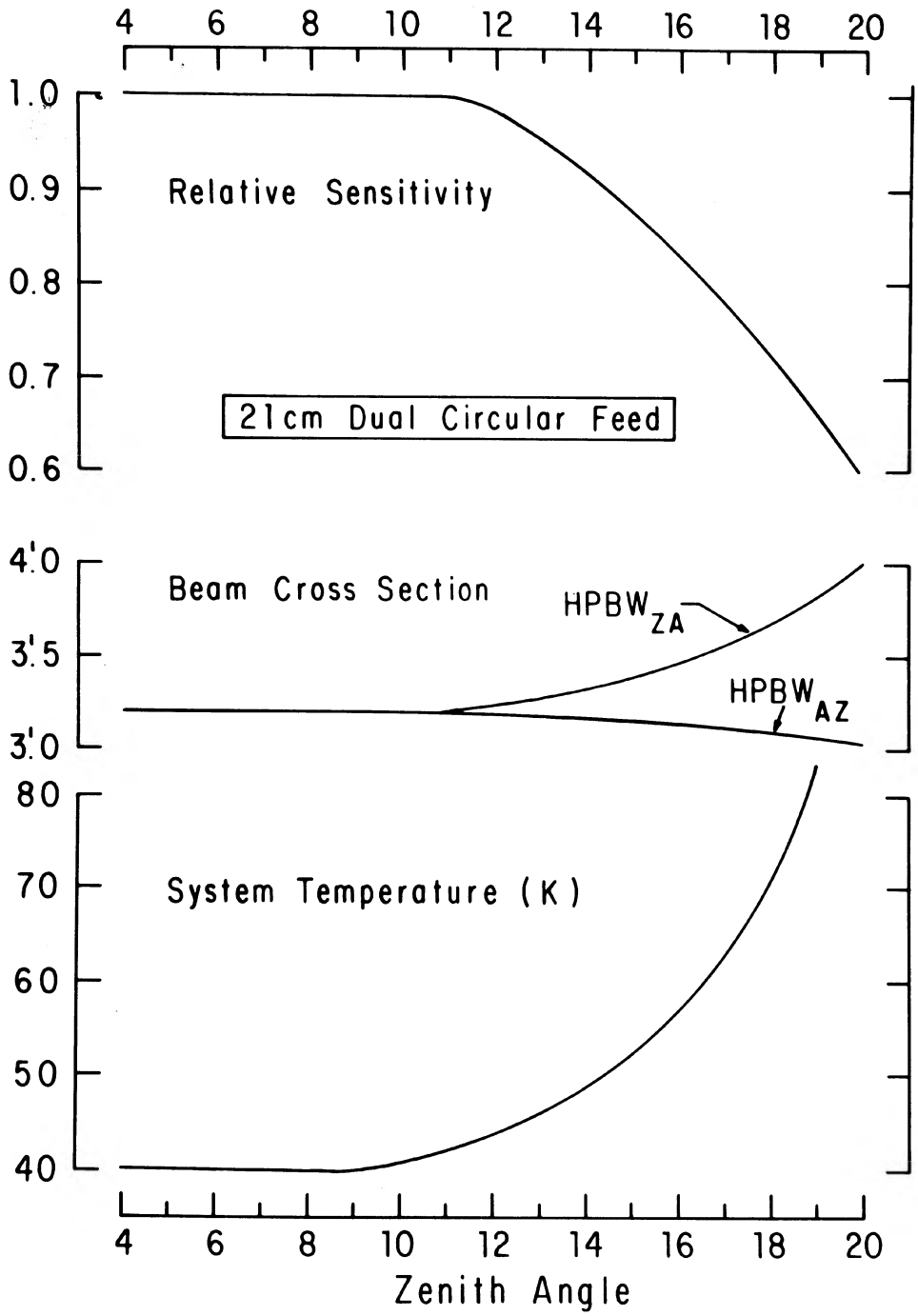

FIG. 2. Variation of the relative sensitivity, the beam cross section and the system temperature of the Arecibo 21-cm dual circular feed system caused by increased vignetting at high zenith angles.

252-channel spectra had a channel spacing of 39.1 kHz. When the observations were begun in 1978, redshifts were available for fewer than 25% of the galaxies. A search mode was used, consisting of offsetting quadrants by 7.5 MHz (to allow overlap on the band edges). This allowed a total coverage of 32.5 MHz or about 7000 km s^{-1}; if a galaxy were not detected, the four spectra were shifted again, usually by 22.5 MHz so that the entire velocity range 0–12 700 km s^{-1} was searched. Of the 324 galaxies, redshifts are now available for 306, and only 17 of those were not detected.

Once a detection was made, or if the redshift were known from some other source, all quadrants were centered on the same appropriate frequency. The redundancy of recording four spectra from only two independent incoming signals (the two polarizations) allowed the recovery of some of the noise introduced within the back end, as well as the combination of all data with the same resolution.

The observations were made in a total-power mode, alternating five-minute ON–source scans with OFF scans taken with the same telescope configuration in azimuth and zenith

angle. The final spectra, shown in Fig. 3, are the averaged accumulations of individual differenced ON-OFF pairs, with weighting performed for variations in the system temperature and gain (caused by both zenith angle and frequency degradation). The spectra have been weighted according to the inverse square of the three corrections, f_{za} (zenith-angle gain), f_{fre} (frequency response), f_T (system temperature), so that the final weight used for the ith difference spectrum is

$$w_i = (f_{za} f_{fre} f_T)^{-2}. \quad (1)$$

As a function of feed mounting, the frequency correction must be derived for each observing session. The zenith-angle correction as shown in Fig. 2 is given by

$$f_{za} = \exp[0.00512(ZA - 10°)^2], \quad (2)$$

where ZA is the zenith angle in degrees of the source at the midpoint of the ON scan. The total ON-source integration times varied from a minimum of ten minutes to several hours, depending on the required signal-to-noise ratio. The successful application of the calibration procedure has been demonstrated in Paper II, in which fluxes measured with the circular feed and with the 91.4-m telescope are shown to agree to better than 25% after correction for the fact that the angular extent of the source is not negligible when compared to the telescope beam.

Figure 3 shows the unbaselined smoothed spectra for all galaxies which are considered detections or suspected detections from the circular feed data, with the exception of four galaxies—UGC 1503, 2357, 2774, and 6777—which have been reported previously in Paper I. A new interference-free spectrum is shown for UGC 12541, also discussed in Paper I. The spectra of galaxies which were mapped at Arecibo (Paper II) are not included in Fig. 3. The weighted average spectra have been smoothed with a rectangular function three channels wide and with a Hanning function to give a final velocity resolution of about 15 km s^{-1}. The smooth curve superimposed on the spectrum in each panel is the polynomial baseline subtracted from the observed profile before measurement of the flux integral. Each spectrum is identified by its entry number in the UGC.

IV. DERIVATION OF GALAXY PROPERTIES

The total observational base composed of both mapping and circular feed data has been used to derive the fundamental galaxy properties which we summarize in Table I. Because we shall use these galaxies to set a standard of normal H I content, we describe here in detail how we have derived these parameters. This discussion and that contained in the appendices are meant to be sufficiently complete that others may retrace the steps used to derive the tabulated properties. The more casual reader may wish to gloss over the more esoteric details; we will not be offended. The tabulated entries are referenced by column and line number below.

a) Galaxy Identification

Columns (1) to (3) contain the names assigned to the galaxies by the various authors. Column (1) gives the entry number in the CIG, while column (2) is the entry number in the UGC. Column (3) contains the corresponding NGC or IC number or other common name, where applicable.

b) Positions

The 1950.0 coordinates of the galaxy are given in column (4). Line (1) contains the right ascension in hhmmss.s, and line (2), the declination in $\pm$ ddmmss. Coordinates come from Dressel and Condon (1976) for galaxies brighter than + 14.5 or were measured by us from overlays for the Palomar Sky Survey prints. The latter are accurate to within 5″.

c) Morphological Types

The morphological type of each galaxy is indicated in column (5). The original restriction of the observing sample to CIG galaxies which are also in the UGC was motivated by the prior availability of morphological classifications in the latter catalog; these type codings as recorded on a tape version of the UGC are included in line (1).

The morphological classification of small angular diameter galaxies is difficult and uncertain; ideally, classification should be performed using high-quality plates obtained specifically for that purpose with adequate scale. However, in practice, this is not feasible for a sky-wide sample. The UGC types were obtained by examination of the Palomar Sky Survey prints; we have performed our own classification making use of plate reproductions of the Palomar Sky Survey at Cornell University; these have an image quality (dynamic range) superior to that of the prints. For some of the brighter galaxies, overexposure on the Palomar Sky Survey material favors an earlier classification than given by other authors, and we retain the morphology assigned in the RSA by Sandage and Tammann (1981), who used superior plate material for the 32 galaxies in common with our sample.

In line (2), we assign a numerical type coding as follows:

0—Elliptical	6—Sbc
1—S0	7—Sc
2—S0/a	8—Scd, Sd
3—Sa	9—Irr, Sm, Sdm, dwarf sp
4—Sab	10—Pec
5—Sb	

This index is based on our examination of the plate reproductions or, where available, the classifications done by Sandage and Tammann. Overall, we have found reassuring agreement with the UGC classification, so that for statistical purposes at least, the morphological type coding we employ is probably accurate to $T \pm 1$, although for individual galaxies the error may be larger. Bars are indicated by a "B" next to the type code; for the small, faint galaxies, the identification of a bar is impossible for even moderate inclinations, and the analysis includes no distinction between barred and unbarred spirals. Misclassification has already been discussed in Paper I as a possible explanation for the large hydrogen mass to luminosity ratios of those five early-type galaxies, yet they would still be distinctive among the isolated galaxy sample as spirals with low disk luminosities. Because we feel that the plate reproductions are superior for classification, and because we have attempted to refine the classification of galaxies listed only as "S . . . " or " Peculiar" in the UGC, the typing given by the index T is used throughout.

d) Dimensions

Column (6), line (1) contains the blue major and minor diameters, $a \times b$, in arc minutes from the UGC. The possible effects of galactic extinction on apparent dimensions are discussed in Appendix C. UGC diameters are visual estimates;

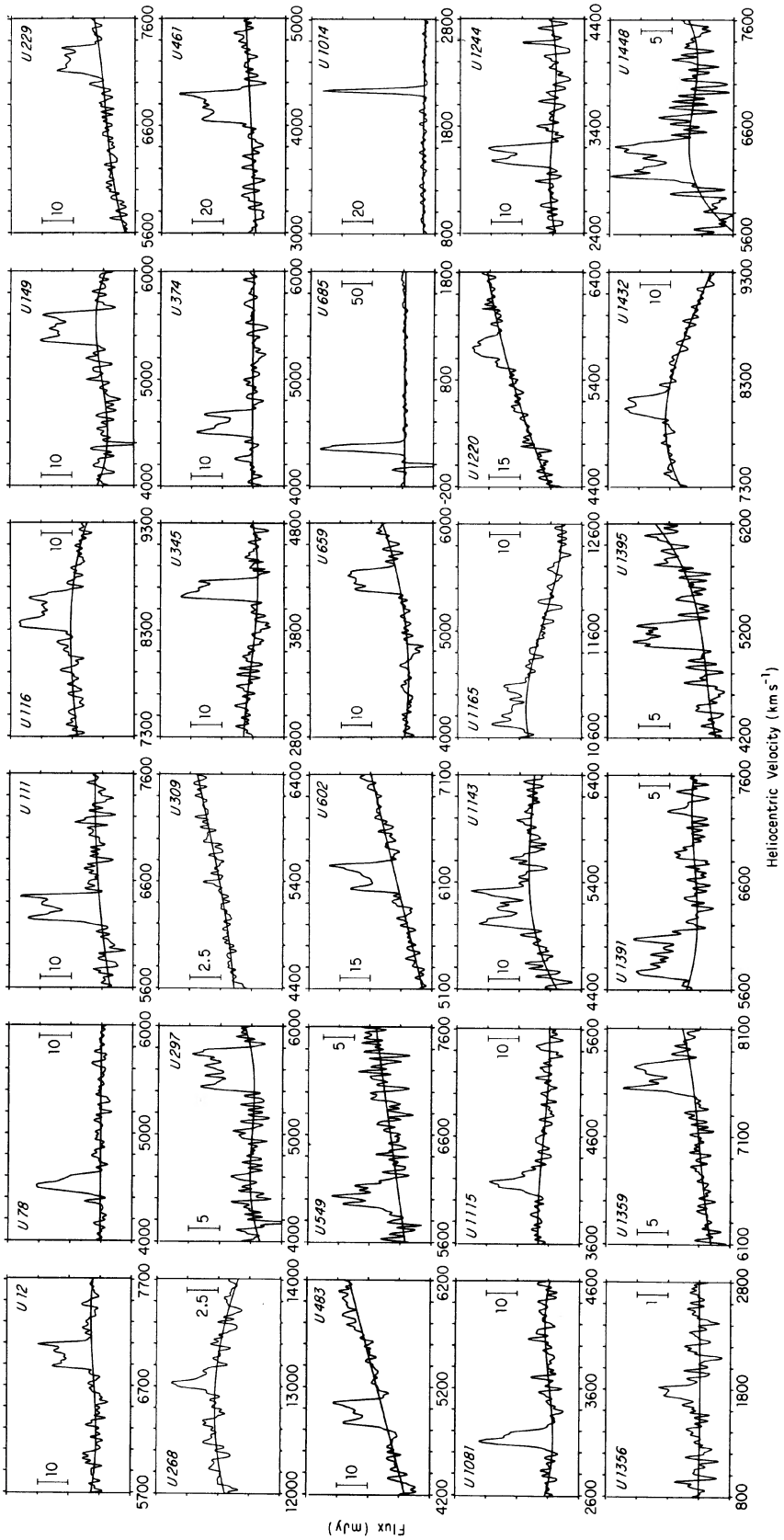

FIG. 3. (a) 21-cm line spectra obtained with the Arecibo 21-cm dual circular feed system. The scale (between tic marks) in mJy on the flux axis is indicated by the vertical bar in each plot. The velocity axis is heliocentric. Superimposed on each spectrum is the polynomial baseline which was removed before parameters were measured. The UGC number is given for identification.

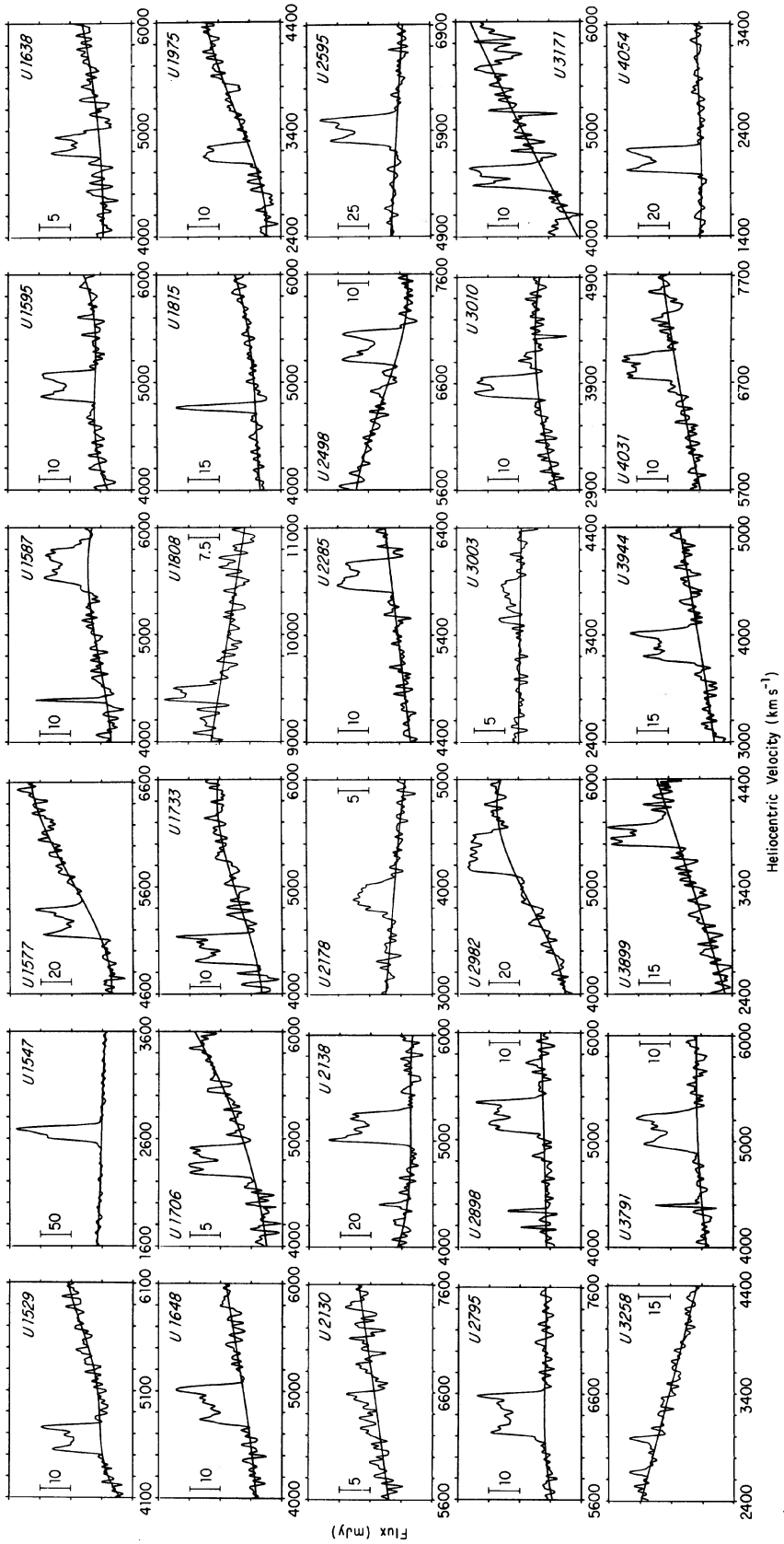

FIG. 3. (a) (continued)

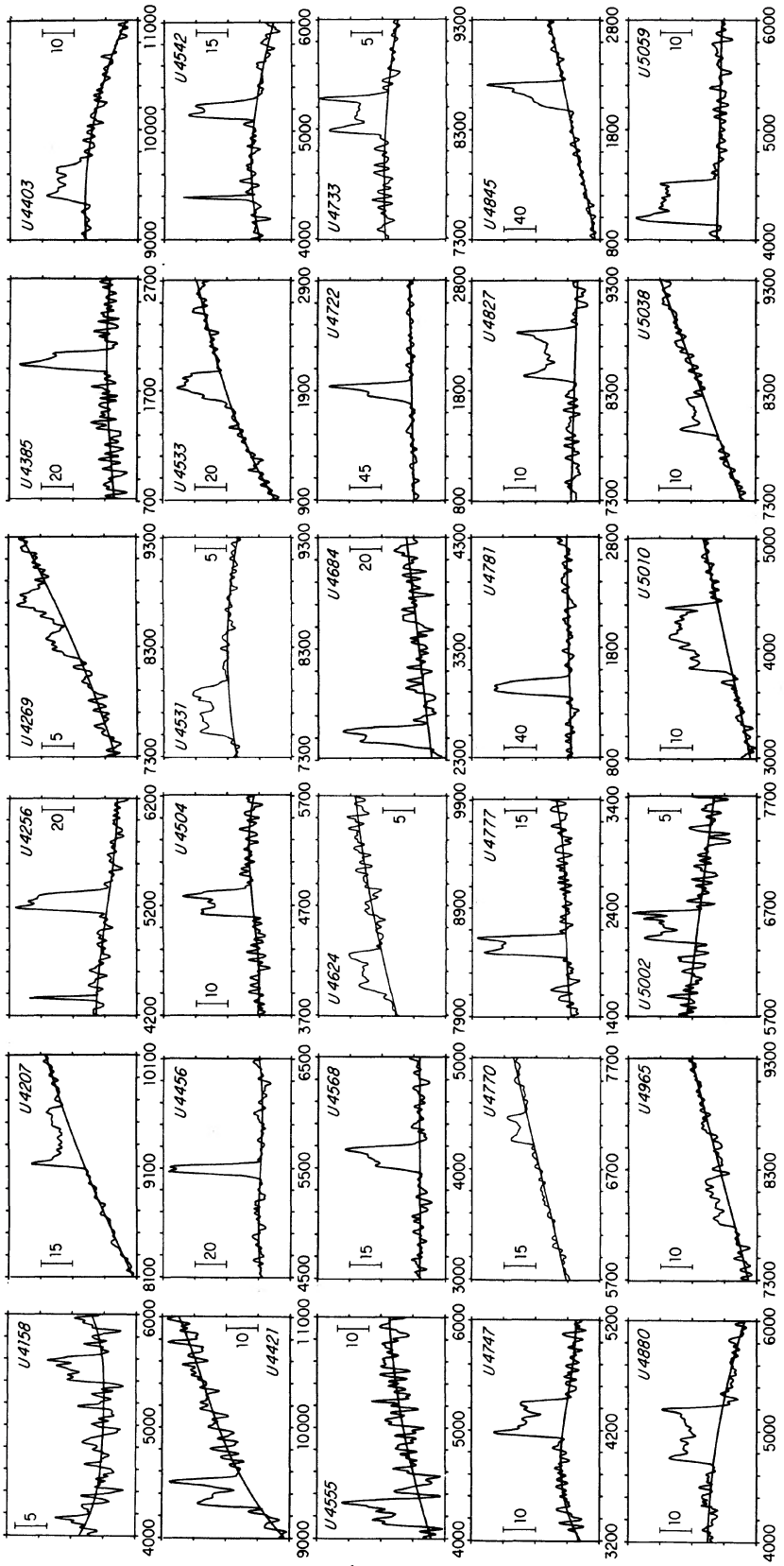

FIG. 3. (a) (continued)

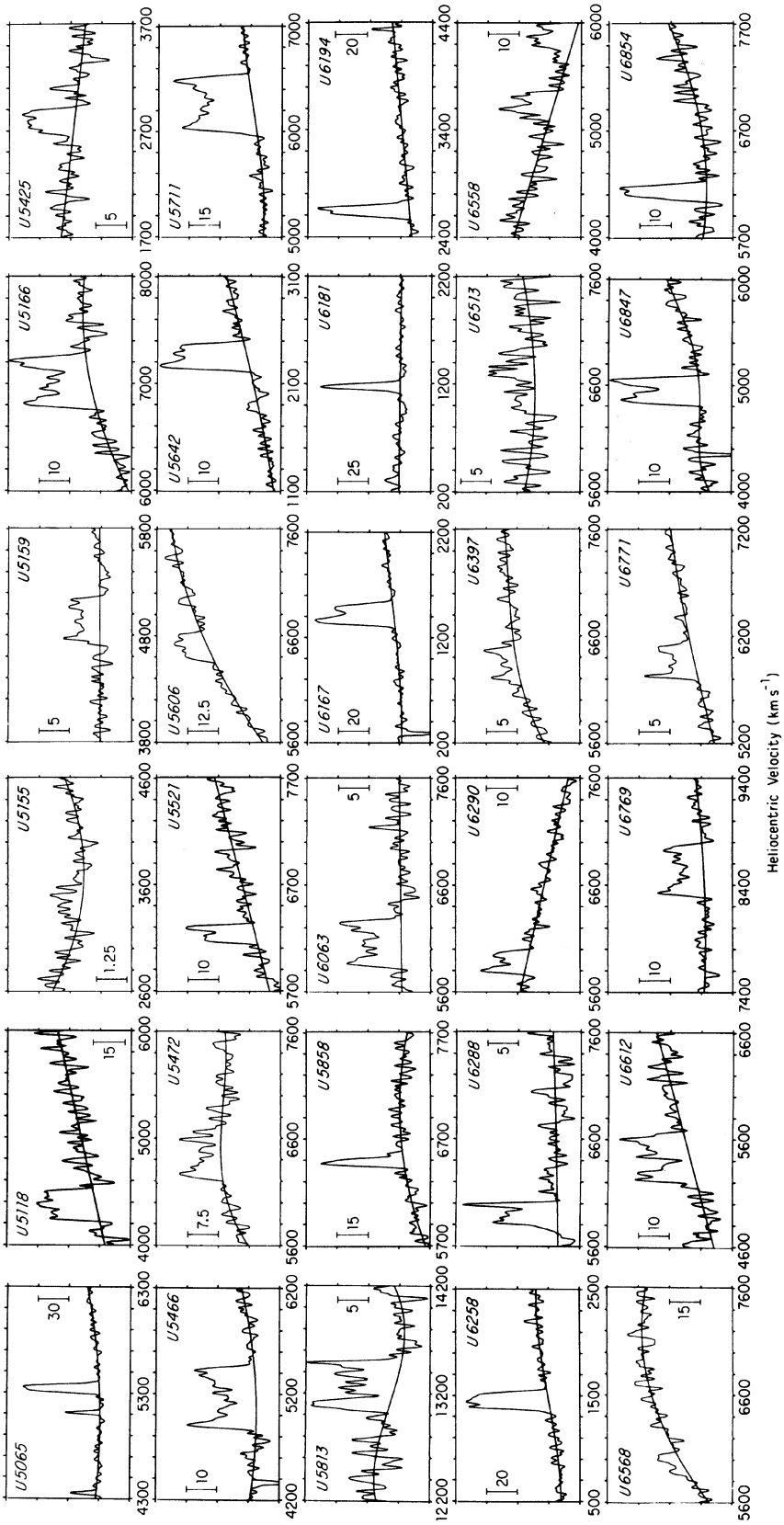

FIG. 3. (a) (continued)

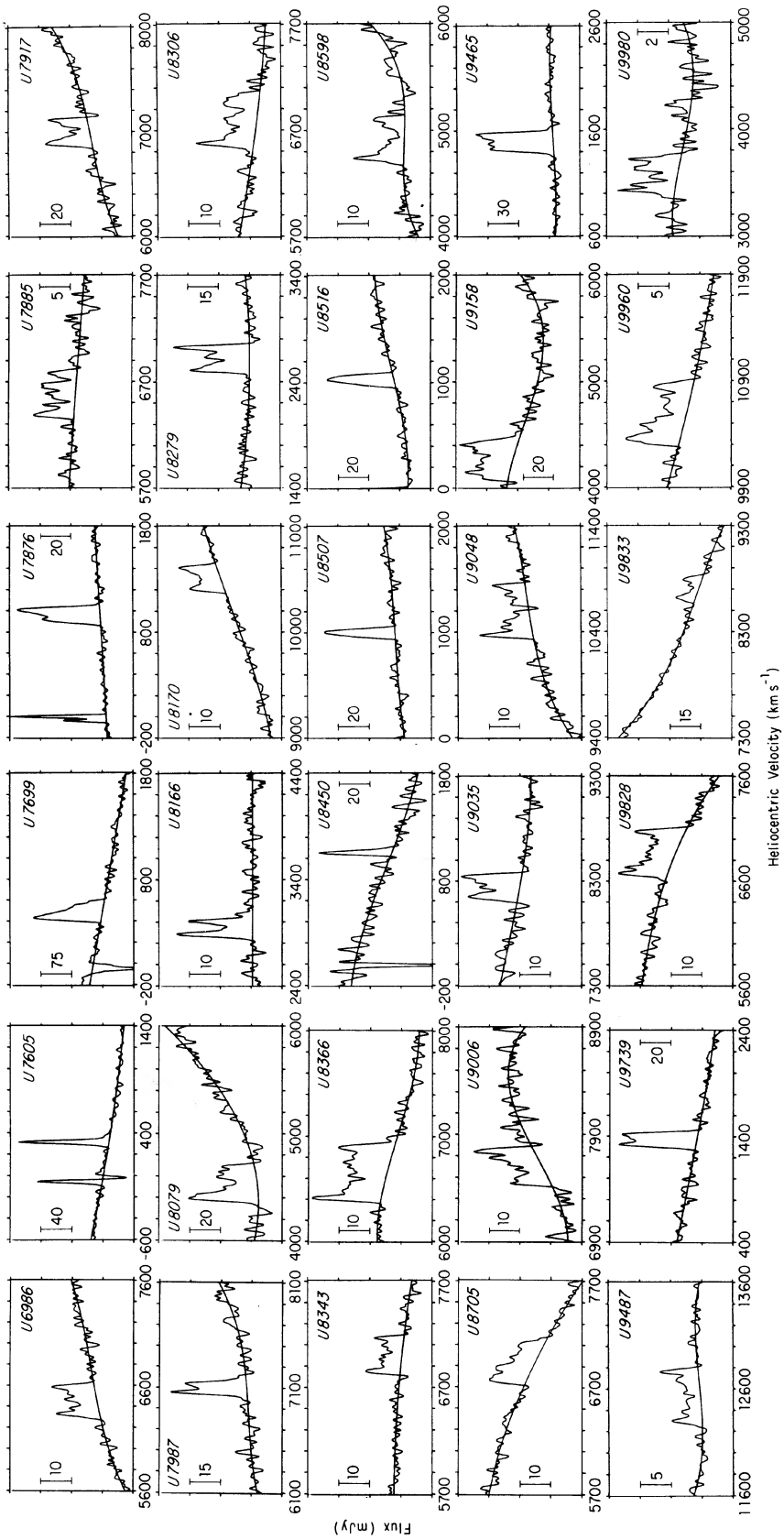

FIG. 3. (a) (continued)

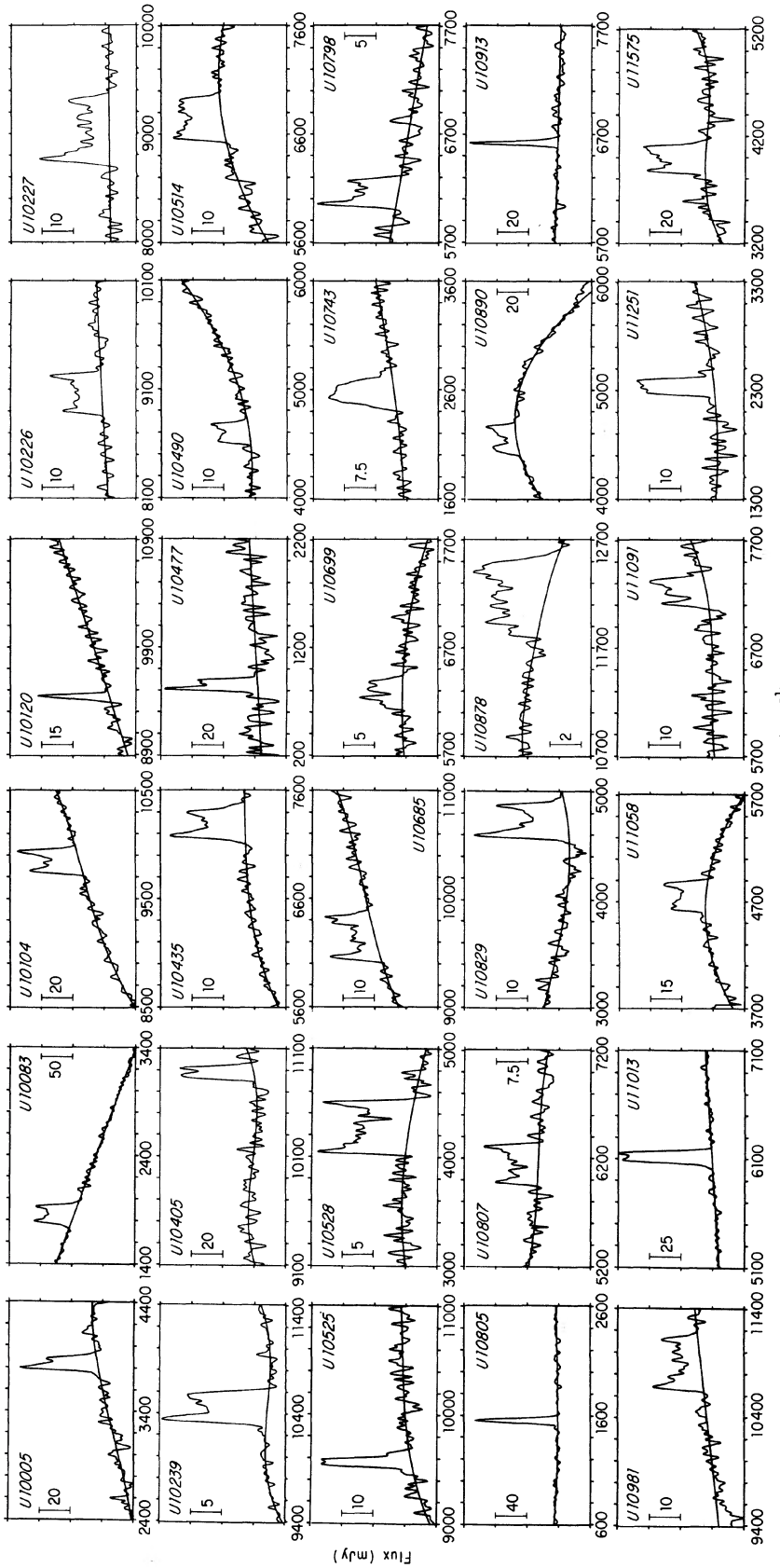

FIG. 3. (a) (continued)

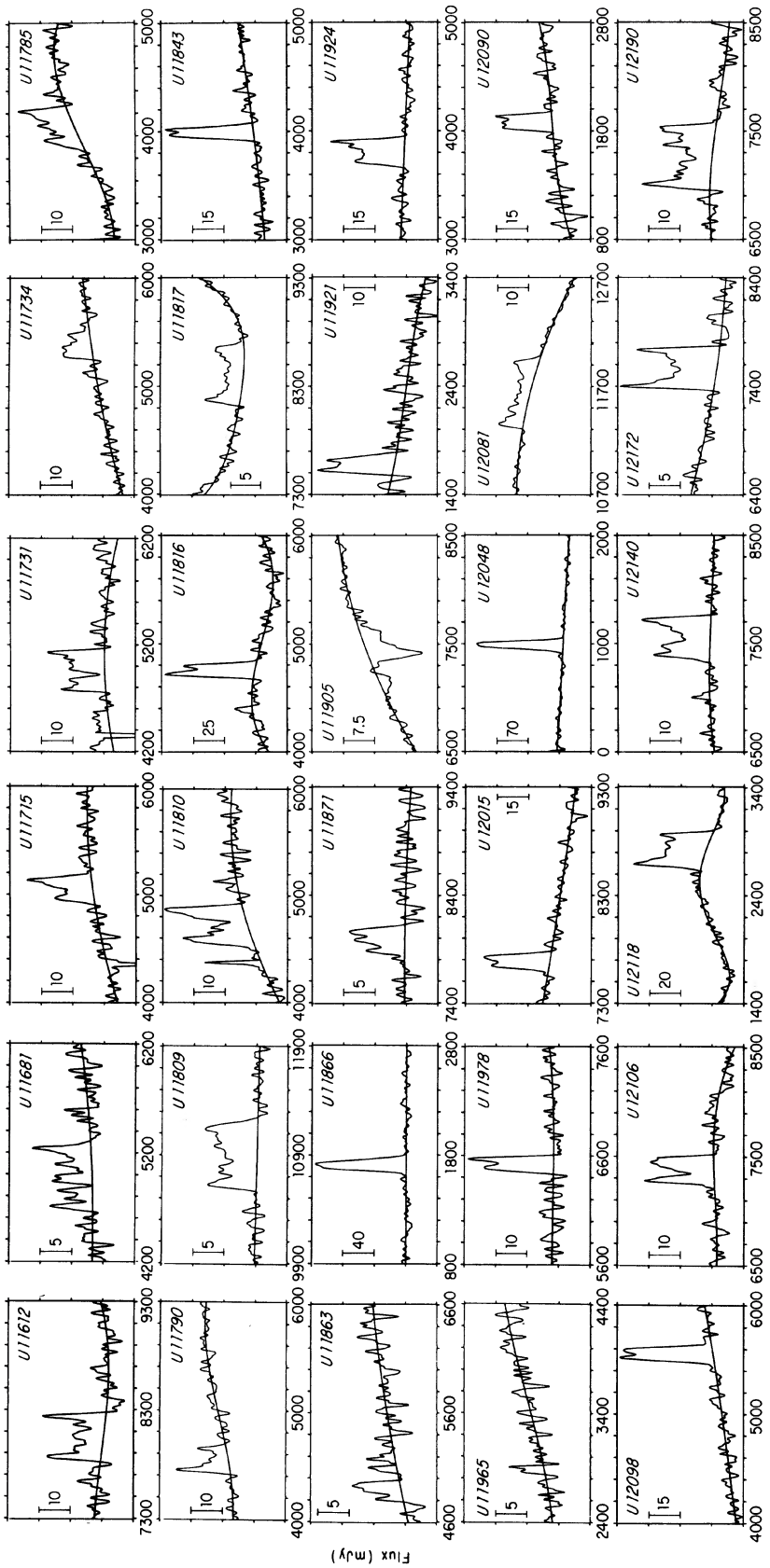

FIG. 3. (a) (continued)

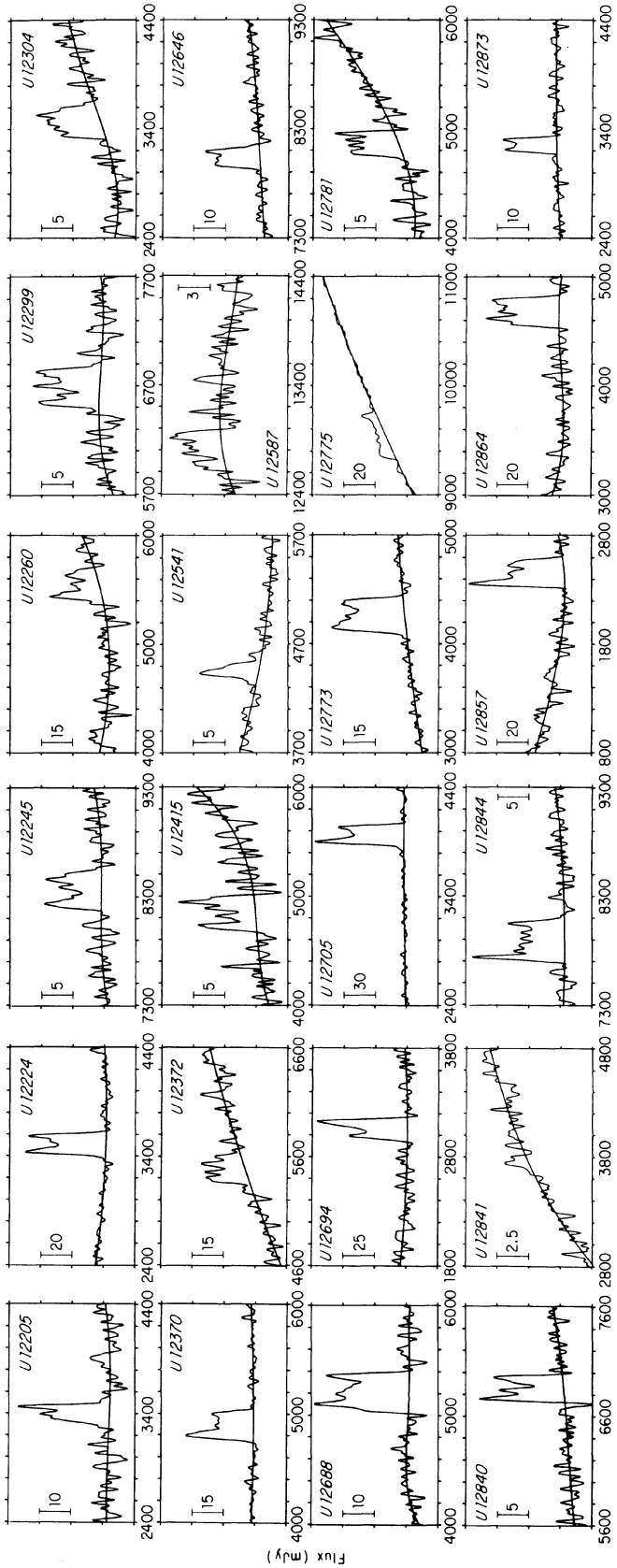

FIG. 3. (a) (continued)

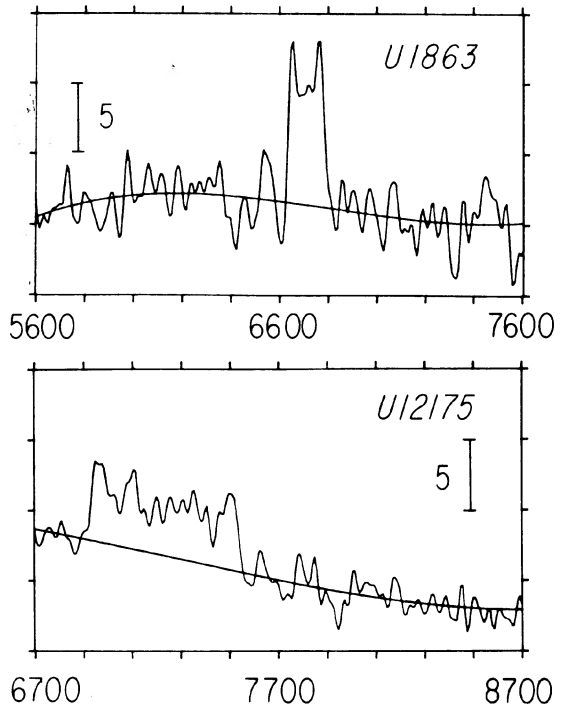

FIG. 3(b). Spectra of galaxies U 1863 and U 12175. See caption to Fig. 3(a).

they are fairly accurate, but the isophotal levels to which they correspond are dependent on the average surface brightness. In Appendix D, we discuss the dependence of UGC diameter on surface brightness and use the resultant correction to the UGC blue diameter a wherever diameters are used in the correlations investigated in Secs. V and VI.

e) Inclination

The inclination i, in degrees, is given in column (6), line (2). We have derived i using Holmberg's (1946) description of galaxies as oblate spheroids:

$$\cos^2 i = (r_i^2 - p^2)(1 - p^2)^{-1}, \quad (3)$$

where $r_i = b'/a'$ and $p = c'/a'$, and a', b', and c' are the spheroid's three axes. Lewis (1980) has discussed the visual underestimate of the intrinsic axial ratio r_i with decreasing r_i as apparent in the UGC major and minor diameters, and we adopt his corrections to $r_{\rm UGC} = b/a$. He has also shown that p itself is type dependent, and we apply his values of p, interpolating to all types:

$$\begin{aligned} p &= 0.23 \quad T \leqslant 3 \\ &\quad 0.20 \quad = 4 \\ &\quad 0.175 = 5 \text{ and } 10 \\ &\quad 0.14 \quad = 6 \\ &\quad 0.103 = 7 \\ &\quad 0.10 \quad = 8 \text{ and } 9 \end{aligned}$$

If $b/a < p$, i is set to 90°; however, in order to avoid division by zero in $(\cos i)^{-1}$ terms, a maximum value of 85° is used in the calculations. No inclination is given for ellipticals; for irregulars, the inclinations may be unreliable.

f) Apparent Magnitudes

Column (7), line (1) gives the apparent magnitude m_z taken from the UGC. Nilson used Zwicky magnitudes for galaxies in the CGCG ($m_z \leqslant +15.7$). A number of corrections must be applied to the apparent magnitude in order to derive the corrected apparent magnitude m_c given in line (2) which is to be used throughout. This magnitude has been derived from the Zwicky magnitude m_z after correction for a number of effects.

1) Correction for Systematic Effects in the CGCG—Δm_s

The possibility of systematic errors in the CGCG magnitudes has been discussed by numerous authors (Kron and Shane 1976; Peterson 1979; Bothun and Schommer 1982; Auman *et al.* 1982; Giovanelli and Haynes 1984). Several of these authors, as well as others, present recursion relations to convert Zwicky magnitudes to those of other systems, most notably to the photographic magnitudes in the Holmberg (1958) system, or to the B_T system of de Vaucouleurs *et al.* (1976). Because of the sparse overlap between any of the other systems and the CGCG at the faint-magnitude end, these recursion relations are probably unsatisfactory for magnitudes much fainter than +14.0. Moreover, the majority of galaxies in the isolated galaxy sample are fainter than that limit. For this reason, we choose not to convert to another system, but rather we adopt the Zwicky scale. On the other hand, Kron and Shane (1976) have shown that there are indeed systematic errors within the Zwicky system, particularly a dependence on the volume of the CGCG in which a galaxy appears. This effect has been discussed by others (Peterson 1979; Auman *et al.* 1982), who identified it as a declination dependence. Kron and Shane have shown the deviation to be isolated to Volume I of the CGCG, the other volumes being similar to one another but distinct from the first. We adopt the mean corrections to the raw Zwicky magnitudes reflecting both the volume effect and the systematic discrepancies based on magnitude range as given in Tables III and IV of Kron and Shane. In a separate paper (Giovanelli and Haynes 1984), we have shown that if systematic errors are removed from the CGCG according to the analysis of Kron and Shane, the Zwicky magnitude scale closely approaches a Pogson standard one, at least in the range from $+14.0 \leqslant m_z \leqslant +15.4$, characterized by a scatter of 0.2–0.3 mag and systematic errors of less than half that large.

2) Correction for Galactic Extinction—Δm_g

Burstein and Heiles (1978) have derived a measure of the galactic extinction based on H I column densities $N_{\rm H}$ and Lick survey galaxy counts $N_{\rm gal}$, where available. Using a tape copy of the UGC kindly provided by D. Burstein, complete with entries for $N_{\rm H}$ and $N_{\rm gal}$, we have derived the correction to m_z for galactic extinction by employing the relations given by those authors in their Table 3 to estimate the reddening from H I column densities and galaxy counts.

3) Correction for Redshift—Δm_K

The K-correction accounts for the magnitude difference between spectral energy distributions which are redshifted by different amounts and observed over the same spectral interval. We derive K corrections for the B filter as tabulated by Pence (1976) for different morphological types and low redshift ($z < 0.05$), using the z dependence as given in Giovanelli *et al.* (1981).

TABLE I. Galaxy properties.

K #	UGC #	NGC/IC Name	R.A. Dec.	Type T	a x b i	m_z m_c^c	V^{opt} Ref.	V^{21} V_o	S $S_{H,c}$	σ	W W_o	obs	h^2L	h^2M_H	hM_T
(1)	(2)	(3)	(4)	(5)	(6)	(7)	(8)	(9)	(10)	(11)	(12)	(13)	(14)	(15)	(16)
2	12		000046.2 +293100	Sc 6	1.1x0.9 35	15.7 15.38		6984 7222	2.84 3.30	2.2	249 429	1	9.72	9.61	11.62
4	19	N7817	000124.9 +202818	Sb/Sc 6	4.0x1.1 75	12.7 11.82	2598 KK79	2308 2524	13.6 16.2		422 436	10	10.22	9.39	11.50
6	78	N9	000620.1 +233224	Pec 4	1.3x0.7 58	14.5 13.80	4500 CfA	4528 4749	2.69 3.20	1.3	184 216	1	9.98	9.23	10.62
8	111		000933.5 +114600	Sc 5	1.3x0.4 74	15.4 14.53		6342 6527	4.85 6.53	1.9	265 276	1	9.96	9.82	10.92
9	116		001002.8 +051333	S... 5	1.2x0.5 66	15.4 14.71		8474 8636	4.08 5.21	1.7	355 388	1	10.14	9.96	11.34
12	149		001321.7 +134740	S... 3	1.3x0.3 85	15.6 14.99		5474 5663	2.84 3.36	1.0	310 311	1	9.66	9.40	10.94
13	151		001339.0 +100317	S0? 1	1.3x1.2 23	14.7 14.32				0.96		0			
18	229		002116.5 +280317	Sb 5	1.0x0.5 60	15.3 14.75		7208 7432	2.94 3.60	1.2	274 315	1	9.99	9.67	11.05
22	268	I1551	002459.3 +083553	S... 5	2.6x1.3 60	15.0 14.36	13334 KK79	13040 13204	0.36 0.55	0.55	146: 168:	1	10.65	9.35	
23	297	I1552	002705.8 +211147	S... 4	1.0x0.2 83	15.4 14.60		5600 5803	2.63 3.23	1.2	390 393	1	9.83	9.41	11.06
25	309	N137	002822.8 +095558	S0 1	1.6x1.6 0	14.2 13.80	5276 CfA	5443		0.28		0	10.10		
26	318		002912.3 +372413	SBc 7B	1.1x1.0 24	16.5 16.25				2.5		0			
29	345		003209.5 +280800	SB?c 7	1.1x0.3 77	15.6 14.70		4177 4395	3.81 5.13	1.6	196 201	1	9.55	9.37	10.63
30	374	I35	003503.7 +100447	Sc 7	1.3x1.2 22	15.0 14.65		4587 4750	2.80 3.33	1.2	234	1	9.64	9.25	
33	461	N237	004054.4 -002350	Sb-c 7	2.0x1.2 53	13.6 13.17	4139 Sa	4174 4294	9.16 12.43	3.0	300 379	1	10.14	9.73	1145
34	483		004410.5 +261206	IV-V 4	1.2x0.5 67	15.7 15.13		4956 5162	2.68 3.20	1.2	250 272	1	9.52	9.30	10.80
38	549		005156.2 +363017	Sc 7	1.1x0.1 90	15.7 14.26		6035 6259	1.79 2.73	1.1	277 277	1	10.04	9.40	10.99
39	550	I1596	005203.4 +211500	S... 3	2.5x1.2 63	15.1 14.73		2677 2864	10.7 11.0		240 269	10	9.17	9.33	10.79
40	558		005211.1 +101550	S0 3	1.7x0.7 68	15.7 15.28				0.75		0			
41	602		005537.7 +362740	Sc/SBc 8B	1.7x1.6 19	14.5 14.10		6145 6367	5.13 6.52	1.2	273	1	10.11	9.79	
42	659		010138.6 +182547	... 4	1.1x0.3 74	15.5 14.84		5463 5635	3.10 3.73	1.2	230 239	1	9.72	9.45	10.68
45	685		010443.0 +162501	Irr 9	1.9x1.3 46	14.5 14.21	113 CfA	155 318	9.95 12.57	3.0	90 126	1	7.47	7.48	9.51
49	833		011530.3 +110706	SBc 7B	2.5x1.7 47	14.3 13.79	5062 Sa	5196 5333	11.7 12.3		297 409	10	10.09	9.92	11.70
50	1014		012345.6 +060100	Irr 7	1.6x1.6 0	15.2 15.09		2132 2245	2.76 3.47	1.07	62	1	8.82	8.62	
53	1081	I1710	012802.8 +211056	SBc 7B	1.9x1.8 19	13.8 13.42	3322 KK79	3128 3289	2.76 3.69	1.7	162	1	9.81	8.97	
54	1115	I1715	013054.9 +121948	Irr 10	0.7x0.5 44	14.5 14.14		4176 4306	2.04 2.20	1.7	208 297	1	9.76	8.98	10.67
56	1143	N622	013325.6 +002435	SBb 5B	2.1x1.7 37	14.1 13.76	5249 KK79	5155 5239	4.03 5.59	2.8	372 625	1	10.08	9.56	11.77
58	1165		013542.5 +282753	Sc 5	1.4x0.2 90	15.7 14.33		10902 11079	2.45 3.74	0.78	408 409	1	10.51	10.04	11.45
59	1167		013542.1 +071647	Sc 7	2.8x2.2 38	14.8 14.43	4429 KK79	4295 4403	11.4 11.80		233 376	10	9.66	9.73	11.59
61	1194	N656	013939.9 +255330	SB0 2B	1.5x1.3 31	13.5 12.97	3916 CfA	4083		0.78		0	10.18		
62	1220	N662 VZw98	014139.4 +372643	S... 4	0.8x0.4 56	13.6 12.94	5855 KK79	5662 5858	2.78 3.15	1.9	285 342	1	10.51	9.41	10.95
64	1244		014402.0 +241300	S... 5	1.4x0.6 66	15.5 14.67		3128 3287	3.12 4.06	2.0	207 228	1	9.31	9.01	10.51
68	1356	N718	015036.5 +350703	SBa 3	2.6x2.2 33	12.5 12.25	1756 CfA	1733: 1816:	0.14: 0.21:	0.33	124	1	9.77	7.21:	
69	1359		015050.3 +294111	SB... 5B	0.9x0.8 28	14.2 13.75	7683 CfA	7658 7828	2.17 2.45	0.8	308	1	10.43	9.55	

TABLE I. (continued)

K #	UGC #	NGC/IC Name	R.A. Dec.	Type T	a x b i	m_z m_c^z	V^{opt} Ref.	V^{21} V_o	S $S_{H,c}$	σ	W W_o	obs	h^2L	h^2M_H	hM_T
(1)	(2)	(3)	(4)	(5)	(6)	(7)	(8)	(9)	(10)	(11)	(12)	(13)	(14)	(15)	(16)
71	1391		015237.7 +094600	Sc 7	1.5x0.1 88	15.5 14.13		5928 6031	2.66 4.15	1.2	445 445	1	10.06	9.55	11.49
72	1395		015244.8 +062200	Sb 5	1.7x1.5 29	14.5 14.08	5190 Sa	5164 5255	2.16 2.77	1.2	255	1	9.96	9.26	
76	1432	VV12	015442.0 +165827	Sb-c 5	1.0x0.7 45	14.8 14.31		8054 8181	2.34 2.74	1.2	216 301	1	10.25	9.64	11.08
78	1448		015533.7 +014907	Sc 7	1.3x0.3 75	15.1 14.32		6292 6363	3.05 4.09	1.7	370 384	1	10.03	9.59	11.42
80	1466	N772 Arp78	015635.3 +184550	Sb 5	8.0x5.0 51	11.3 10.82	2489 CfA	2461 2593	76.4 82.1		456 584	10	10.65	10.12	11.82
81	1482	N781	015728.1 +122448	S... 4	1.7x0.5 76	14.0 13.09	3483 CfA	3592		0.33		0	10.03		
83	1503		015824.6 +330515	E 0	1.0x0.9	14.4 13.94	5260 St	5085 5259	1.71 1.92	1.6	288	1	10.01	9.10	
84	1529	I193	015950.3 +105047	Sc 7	1.9x1.9 0	14.7 14.36		4649 4751	3.27 4.39	1.4	263	1	9.76	9.37	
85	1547	D17	020032.6 +214800	Irr 9	2.2x2.0 24	15.0 14.64	2808 KK79	2646 2785	15.0 21.1	4.0	149	1	9.18	9.59	
86	1577		020232.2 +305620	SBb 6B	2.4x1.7 45	14.0 13.47	5409 KK79	5278 5443	6.91 10.10	4.0	297 422	1	10.23	9.85	11.72
87	1587		020259.3 +063143	S... 5	1.1x0.4 70	14.6 13.75		5658 5741	4.03 5.20	2.0	368 392	1	10.17	9.61	11.13
88	1595		020336.0 +264747	Sc 6	1.4x0.8 55	15.5 14.96		4962 5114	3.69 4.59	1.9	276 337	1	9.58	9.45	11.31
89	1631	N821	020540.5 +104532	E 0	3.3x2.2	12.6 12.30	1716 CfA	1812		0.9		0	9.75		
90	1638		020606.0 +254747	Sc 5	1.0x0.5 61	15.4 14.82		4874 5021	1.20 1.47	1.0	246 283	1	9.62	8.94	10.78
91	1648		020623.2 +252006	... 2	1.2x0.8 49	14.5 13.97		4872 5017	5.06 5.73	1.8	376 498	1	9.96	9.53	11.36
94	1706		021042.2 +253707	Sc 7	1.2x0.4 71	14.7 13.83		4794 4937	2.34 3.02	1.0	289 307	1	10.00	9.24	11.11
95	1733		021231.9 +214606	Sc 7	1.7x0.2 86	15.6 14.22		4415 4544	5.51 8.58	2.2	279 280	1	9.78	9.62	11.02
96	1736	N864	021249.8 +054610	Sc 6	4.8x3.5 43	12.0 11.62		1560 1632	116. 121.		239 350	10	9.93	9.88	11.27
97	1808		021815.9 +232203	Sb 7	1.2x1.1 24	14.7 14.26		9447 9577	1.47 1.72	1.9	157	1	10.41	9.57	
98	1815		021836.0 +304840	SB IV 9B	1.4x1.3 22	15.7 15.41		4762 4915	2.29 2.74	1.5	75	1	9.37	9.19	
100	1863		022153.3 +013643	Sc 7	1.1x1.1 0	15.3 15.22		6712 6760	1.44 1.65	1.6	155	1	9.73	9.25	
103	1888	N918	022303.7 +181620	Sc 7	3.6x2.1 54	14.3 13.41		1508 1617	22.6 24.3		268 333	13	9.20	9.18	11.11
104	1903		022336.5 +293620	Sb 5	1.0x0.2 83	15.7 14.41	10769 CfA	10915		1.74		0	10.46		
105	1913	N925	022416.6 +332120	Sc/SBc 7B	13.x8.0 51	10.5 9.97		550 706	310. 331.		218 280	10	9.86	9.59	11.02
107	1975		022714.7 +325420	S... 4	1.3x0.2 90	15.3 14.18		3176 3329	2.46 3.18	1.5	187 188	1	9.52	8.92	10.23
109	1983	N949	022745.1 +365453	S... 7	3.6x2.3 51	12.0 11.66	801 KK79	612 776	16.9 16.9		193 248	13	9.26	8.38	10.30
112	2082		022822.7 +251227	Sc 7	6.3x1.1 81	14.0 12.54	840 KK79	706 830	56.0 71.1		222 225	13	8.97	9.06	10.55
113	2130		023542.9 +074627	S... 5	1.2x0.3 79	15.4 14.34		6400 6460	0.82 1.13	1.2	403 411	1	10.03	9.05	11.22
115	2138	I1825	023613.4 +085247	Sc 7	1.4x1.0 44	14.9 14.33		5124 5188	11.0 13.5	4.0	301 433	1	9.85	9.93	11.55
116	2178	N1050	023931.8 +343301	SBa 5B	1.8x1.2 48	13.5 12.92	4058 KK79	3901 4050	1.37 1.80	1.8	279 374	1	10.20	8.84	11.15
119	2285		024554.6 +061900	Sc-Irr 9	1.4x0.5 69	15.3 14.98		5959 6005	3.90 4.44	1.0	290 311	1	9.71	9.58	11.42
120	2357	I1861	025011.9 +251700	S0 1	1.8x1.3 45	14.7 13.81		6691 6802	1.79 2.23	1.1	425 604	1	10.29	9.39	11.80
121	2455	N1156	025646.8 +250221	Irr 9	3.7x3.0 36	12.0 11.25		371 476	76.4 76.4		102 175	10	9.00	8.61	10.21
122	2498		025923.6 +170853	SBc 7B	1.7x0.8 62	15.7 14.88		6930 7005	4.12 5.43	1.8	311 354	1	9.89	9.80	11.53

TABLE I. (continued)

K #	UGC #	NGC/IC Name	R.A. Dec.	Type T	a x b i	m_z m_c	V^{opt} Ref.	V^{21} V_o	S $S_{H,c}$	σ	W W_o	obs	h^2L	h^2M_H	hM_T
(1)	(2)	(3)	(4)	(5)	(6)	(7)	(8)	(9)	(10)	(11)	(12)	(13)	(14)	(15)	(16)
123	2595	I302	031013.9 +043106	SBb/SBc 7B	2.2x2.0 25	14.0 13.34		5903 5921	17.4 17.6		278	11	10.36	10.16	
128	2774	N1349	032848.9 +041233	S0 1	1.0x1.0 0	15.0 14.21		6596 6596	2.46 2.78	1.4	382	1	10.10	9.46	
130	2795		033253.2 +045340	SB:b-c 5B	1.1x0.5 64	15.6 14.49	6461 KK79	6407 6407	4.98 5.62		403 449	11	9.97	9.74	11.31
135	2898	I2002	035146.5 +103327	SBa 5B	1.4x1.1 39	15.1 14.26		5222 5227	9.49 9.99	2.0	309 493	12	9.88	9.81	11.43
138	2936		040012.4 +014933	Sc 7	2.6x0.9 70	15.7 14.49	3776 KK79	3823 3787	8.40 9.70		467 498	10	9.51	9.52	11.67
140	2964		040553.2 +270347	Sc 7	1.3x1.2 23	15.5 15.09				0.93		0			
143	2982		040942.4 +052453	S... 5	1.0x0.5 61	15.5 14.54		5311 5281	8.28 10.13	4.0	377 433	1	9.78	9.82	11.17
144	2988		041036.5 +252117	Sb: 5	3.0x1.0 72	15.5 14.37		3823 3872	29.6 35.1		466 490	13	9.57	10.09	11.47
145	3003	N1542	041434.0 +043940	Sa-b 4	1.4x0.6 66	15.1 14.10		3714 3677	0.86 1.05	0.8	416 455	1	9.64	8.52	11.16
146	3010		041618.0 +051927	SBc 7B	1.1x0.7 50	15.4 14.58		3870 3834	3.73 4.43	2.0	217 284	1	9.48	9.19	10.97
151	3059		042704.6 +033420	SAdm 8	2.4x1.0 65	15.4 14.36	4748 KK80	4811 4759	12.8 12.8		384 424	10	9.76	9.84	11.68
154	3171		044509.1 +014347	SB:c 9B	1.5x1.1 43	15.2 14.80		4553 4479	4.35 5.17	2.2	226 334	1	9.53	9.39	11.44
156	3258		050808.7 +002050	SB... 5B	0.7x0.6 31	13.9 13.25	2886 KK80	2821 2724	1.20 1.33	0.98	365 699	1	9.72	8.37	11.23
183	3791		071526.0 +271453	Sc-Irr 6	1.3x0.2 84	15.3 14.13		5098 5044	5.09 7.25	2.0	360 363	1	9.90	9.64	11.24
193	3876		072610.5 +280018	Sc 8	2.5x1.5 52	14.4 13.80		863 809	18.7 18.7		206 260	13	8.45	8.46	10.53
196	3899		072920.2 +354307	Sa-b 5	1.1x0.3 77	15.4 14.45		3885 3868	5.58 7.51	2.3	221 227	1	9.54	9.42	10.46
199	3944		073516.0 +374500	Sc 7	2.0x0.9 63	15.0 14.26		3901 3893	7.03 9.70	1.9	312 351	1	9.63	9.54	11.32
205	4031		074520.6 +232147	Sc 6	1.0x0.7 45	15.3 14.85		6852 6769	3.65 4.25	1.2	261 366	1	9.87	9.66	11.41
208	4054		074755.9 +240113	Sb 5	2.2x0.5 81	15.1 14.00	2076 KK79	2122 2042	9.74 15.16	3.0	253 257	1	9.17	9.17	10.50
222	4158	N2503	075732.1 +223213	SBb/Sc 7	1.1x1.1 0	15.0 14.66		5508 5418	1.35 1.55	1.6	234	1	9.75	9.03	
227	4207		080151.6 +205027	Sb/Sc? 6	1.7x1.0 54	14.8 14.22		9359 9260	4.86 6.29	1.0	522 648	1	10.39	10.10	12.20
232	4256	N2532	080703.1 +340621	Sc 7	2.2x1.7 40	12.9 12.47		5249 5215	8.70 12.26	2.7	188 296	1	10.59	9.90	11.38
234	4269		080907.4 +193053	S... 5	1.2x0.6 61	14.6 13.96		8533 8426	1.95 2.43	0.8	639 734	1	10.41	9.61	11.89
236	4276		081003.7 +092313	SBa 3B	1.1x0.8 44	15.1 15.16				1.78		0			
244	4341		081708.2 +271500	S0-a 3	1.1x0.6 58	15.0 14.68				1.27		0			
247	4385		082104.2 +145456	Pec 10	0.9x0.8 28	14.4 14.08		1969 1837	6.55 7.26	4.0	169	1	9.05	8.76	
252	4403		082333.0 +113953	S... 4	1.0x0.3 72	15.4 15.08		9530 9383	3.00 3.56	1.2	361 380	1	10.06	9.87	11.28
253	4421		082449.3 +020033	Sb/SBb 7	1.1x0.8 43	15.3 15.26		9412 9224	3.72 4.37	1.9	260 380	1	9.97	9.94	11.61
255	4432		082540.5 +011013	Sb-c 7	1.7x1.2 45	15.2 15.13				2.74		0			
260	4456	I509	082906.1 +241040	Sc 8	1.9x1.7 27	14.6 14.28	5514 KK79	5487 5399	5.26 6.90	2.0	110	1	9.90	9.68	
268	4504		083449.7 +204050	Sc 8	1.5x1.0 48	15.3 14.98		4724 4618	3.75 4.43	1.4	239 324	1	9.49	9.35	11.32
276	4524		083735.1 +054847	Sc 7	1.4x0.2 84	15.2 14.36				1.61		0			
278	4531		083846.0 +330253	SBb 5B	1.2x0.4 72	14.5 13.55		7728 7684	1.96 2.58	0.5	466 489	1	10.50	9.56	11.47
279	4533	N2644	083854.4 +050943	Pec 5	1.8x0.7 68	13.4 12.36	1813 KK79	1938 1761	5.52 7.62	2.0	257 277	1	9.69	8.75	10.48

TABLE I. (continued)

K #	UGC #	NGC/IC Name	R.A. Dec.	Type T	a x b i	m_z m_c	v^{opt} Ref.	v^{21} V_o	S $S_{H,c}$	σ	W W_o	obs	h^2L	h^2M_H	hM_T
(1)	(2)	(3)	(4)	(5)	(6)	(7)	(8)	(9)	(10)	(11)	(12)	(13)	(14)	(15)	(16)
280	4542		083955.0 +251453	SAm 9	1.5x1.5 0	15.5 15.42		5190 5106	4.11 5.06	3.0	163	1	9.40	9.49	
281	4555	N2649	084059.1 +345356	SBb/Sc 7	1.7x1.6 20	13.1 12.82	4040 KK79	4235 4200	3.50 4.48	2.2	242	1	10.27	9.27	
283	4568		084200.0 +103906	Irr 7	1.7x0.4 77	14.9 14.04		4095 3941	5.32 7.56	1.5	222 228	1	9.72	9.44	10.84
287	4624		084725.0 +260820	Sa-b 4	1.1x0.5 64	15.4 14.83		8297 8217	1.47 1.73	0.9	381 423	1	10.05	9.44	11.37
291	4684		085406.0 +003400	Sc 8	1.4x1.1 38	14.7 14.37		2519 2321	7.40 8.71	3.7	183 295	1	9.13	9.05	10.94
293	4722		085727.5 +254820	S-Irr 10	1.6x0.3 90	15.2 15.05		1794 1711	11.7 13.4	4.5	157 157	1	8.59	8.97	9.86
294	4733		085837.1 +041900	Sc 7	1.3x0.1 90	15.7 14.73		8430 8247	2.06 3.27	0.88	347 347	1	10.09	9.72	11.34
296	4747	I2428	090013.0 +304713	Sc 7	1.9x0.4 80	14.7 13.74	4220 KK79	4306 4248	4.49 6.70	1.2	334 340	1	9.91	9.45	11.01
298	4770	N2746	090253.0 +353442	SBa 7	1.8x1.7 19	14.4 14.12	7025 CfA	7066 7033	1.77 2.32	1.0	261	1	10.20	9.43	
299	4777		090334.3 +344913	Irr 7	2.4x0.4 82	15.2 14.24	2120 KK79	2055 2018	6.33 10.25	2.5	194 197	1	9.06	8.99	10.50
300	4781		090355.3 +063010	Sc 6	1.9x0.7 69	14.9 14.33		1441 1267	12.2 16.8	4.0	157 169	1	8.62	8.81	10.16
303	4791	N2765	090459.9 +033547	S0 1	1.7x1.0 55	13.3 12.57	4250 St	4064		0.36		0	10.34		
309	4820	N2775	090741.0 +071435	Sa 3	5.0x4.0 38	11.4 10.78	1135 RC2	1350 1180	4.00 8.73	3.5	418 679	14	9.98	8.46	11.48
310	4826		090813.3 +031040	Sa-b 3	1.0x0.1 90	15.3 15.00				2.18		0			
312	4827		090817.1 +133700	S... 4	1.4x0.5 71	15.0 14.45		8629 8487	4.96 6.10	1.2	454 479	1	10.23	10.02	11.55
317	4845		090943.8 +100943	SB:c 5	1.6x0.7 65	15.1 14.63		2117 1959	13.2 17.5	4.0	232 256	1	8.88	9.20	10.43
319	4880	I530	091234.0 +120538	Sa-b 3	2.1x0.7 75	14.3 13.65	4751 KK79	4973 4824	5.41 6.94	1.4	497 516	1	10.05	9.58	11.49
323	4965		091812.4 +243107	S... 3	1.1x0.3 87	15.2 14.61		8015 7926	1.92 2.23	1.1	435 436	1	10.10	9.52	11.32
328	5002		092125.3 +283030	SB... 5B	1.0x0.5 61	14.8 14.25		6518 6449	1.77 2.17	1.0	281 324	1	10.06	9.33	11.01
329	5010	N2862	092200.1 +265935	S... 6	2.4x0.6 77	13.8 12.92	4080 KK79	4099 4022	7.51 11.56	1.0	600 616	1	10.19	9.65	11.83
334	5032		092409.6 +012203	Sa-b 3	1.0x0.2 90	15.7 15.72				3.56		0			
336	5038	I2473	092424.4 +303925	SBb 5B	1.6x1.6 0	14.6 14.33		8067 8009	1.94 2.44	1.3	334	1	10.22	9.57	
340	5059	I2487	092720.2 +201834	Sb 5	1.9x0.4 80	14.2 13.13	4294 CfA	4343 4233	6.94 10.35	1.2	388 395	1	10.15	9.64	11.14
343	5065	N2900	092737.5 +042140	SBc 7B	1.6x1.3 36	14.6 14.25	5172 KK79	5341 5159	5.86 7.37	3.0	96 164	1	9.87	9.67	10.76
347	5079	N2903	092919.9 +214319	Sb/Sc 7	13.3x6.0 63	9.8 9.33	539 CfA	555 452	239. 266.		392 441	10	9.72	9.11	11.20
355	5118	N2922	093348.5 +375453	Irr 9	1.1x0.4 66	14.6 14.42		4369 4349	6.53 7.23	3.8	288 317	1	9.66	9.51	11.23
358	5155	N2954	093740.5 +150858	E 1	1.7x1.1 51	13.5 12.80	3836 CfA	3440: 3306:	0.23: 0.28:	0.3	308:	0	10.07		
359	5159	N2960	093800.5 +034815	Sa? 1	1.7x1.3 41	13.6 12.96	4781 KK79	4932 4748	1.55 1.91	0.8	435 659	1	10.32	9.01	11.70
361	5166	N2955	093815.4 +360640	Sb 7	1.5x0.7 63	13.9 13.33	7056 Sa	7013 6984	7.83 10.06	2.0	488 554	1	10.51	10.06	11.88
377	5279	N3026	094800.8 +284701	Irr 9	2.6x0.7 75	13.8 13.62	1403 KK79	1485 1419	10.90 10.90		231 240	10	9.00	8.71	10.75
383	5325	N3049	095210.3 +093055	SBb 5B	2.5x1.6 50	13.5 12.73	1410 KK79	1496 1339	12.4 13.3		211 274	13	9.31	8.75	10.50
388	5373	SexB	095722.9 +053422	Dw Irr 9	6.0x4.0 48	12.2 11.68		302 129	112. 112.		57 78	10	7.69	7.64	9.08
389	5397	N3098	095928.2 +245706	S0-a 1	2.3x0.6 81	13.0 12.52	1401 CfA	1318		0.64		0	9.38		
397	5425		100140.1 +135151	... 3	0.8x0.7 30	13.6 13.00	2743 Sa	2782 2646	5.54 6.10	1.2	295	1	9.79	9.00	

TABLE I. (continued)

K #	UGC #	NGC/IC Name	R.A. Dec.	Type T	a x b i	m_z m_c^c	V^{opt} Ref.	V^{21} V_o	S $S_{H,c}$	σ	W W_o	obs	h^2L	h^2M_H	hM_T
(1)	(2)	(3)	(4)	(5)	(6)	(7)	(8)	(9)	(10)	(11)	(12)	(13)	(14)	(15)	(16)
400	5466	N3126	100527.3 +320632	Sb 5	2.9x0.5 87	13.5 12.35	5199 CfA	5169 5123	7.77 13.79	1.8	585 587	1	10.63	9.93	11.68
401	5472	I594	100601.3 -002440	SBb-c 4	1.1x0.5 64	14.7 14.14		6447 6251	2.57 3.02	1.8	462 513	1	10.08	9.45	11.42
405	5521		101118.1 +004753	Sc 7	1.0x0.9 26	15.0 15.00		6232 6042	2.95 3.36	2.0	176	1	9.71	9.46	
410	5606	I605	101949.8 +012708	S... 4	0.7x0.6 32	14.5 14.10		6492 6307	2.88 3.16	2.2	256 488	1	10.11	9.47	11.29
416	5642		102301.8 +115930	Sb-c 7	1.7x0.2 85	14.8 13.73	2203 KK79	2349 2209	5.75 8.84	1.4	262 263	1	9.34	9.01	10.66
422	5708		102836.9 +044340	SBd-m 7B	3.4x0.6 81	14.6 13.56	1138 KK79	1175 1005	35.8 45.4		194 197	13	8.73	9.03	10.32
423	5711	N3270	102844.5 +250735	Sb 6	3.1x0.8 77	14.1 13.24	6293 CfA	6259 6183	14.49 24.61	2.0	541 557	1	10.43	10.35	12.02
432	5813		103819.1 +363740	Sc 6	1.8x0.8 64	15.3 14.79		13277 13261	4.03 5.40	2.3	464 517	1	10.48	10.35	12.15
434	5829	D84	103955.1 +344313	Dw Irr 9	5.3x4.5 32	15.1 15.01	634 RC2	627 602	58.3 58.3		90 171	10	7.71	8.70	10.41
435	5840	N3344	104046.6 +251110	Sc 6B	7.5x7.0 21	11.1 10.98	698 Sa	588 516	184. 186.		169	10	9.18	9.07	
436	5842	N3346	104059.0 +150803	SBc 7B	2.6x2.5 16	12.8 12.24	1043 KK79	1260 1140	17.3 17.4		165	10	9.37	8.73	
439	5858		104209.2 +161253	... 7	1.6x1.2 41	15.6 15.33		6481 6366	3.11 3.92	2.0	93 141	1	9.62	9.57	10.71
440	5865		104233.6 +051220	Sc? 3	1.0x1.0 0	15.7 15.90	23000: HGC	22837:		2.6		0	10.50		
443	5891	N3376	104450.6 +061838	S... 1	0.8x0.3 76	14.4 13.86	5837 CfA	5679		1.5		0	10.11		
447	5986	N3432 Arp206	104942.7 +365305	SBm 7	7.5x2.0 75	11.7 10.96		608 597	140. 168.		251 260	10	9.32	9.15	10.63
448	5995	N3437	104952.8 +231201	Sc 7	2.8x0.9 73	12.6 11.92	1120 KK79	1285 1206	20.4 23.8		338 357	13	9.54	8.91	10.91
453	6063		105024.0 +255536	S... 5	1.1x0.1 90	16.5 15.28		6052 5986	2.85 4.43	1.4	445 445	1	9.59	9.57	11.15
455	6098	N3495	105840.9 +035343	Sc 7	4.8x1.0 79	13.1 11.04	1145 Sa	1133 970	35.9 44.5		326 333	10	9.71	9.00	10.89
461	6150	N3521	110315.1 +001358	Sb 5	13.5x7.0 59	10.1 9.27		804 628	282. 312.		458 533	10	10.03	9.46	11.28
464	6167	N3526	110420.5 +072640	Sc 6	2.0x0.5 77	13.7 12.52	1318 CfA	1418 1272	8.28 12.10	1.8	219 225	1	9.35	8.66	10.39
465	6181		110506.4 +194913	Dw 8	1.0x0.9 26	15.5 15.41		1171 1081	3.90 4.38	3.0	82	1	8.05	8.08	
466	6194		110621.4 +231140	S... 7	1.6x1.6 0	14.7 14.54		2642 2569	5.86 7.37	2.0	128	1	9.15	9.06	
467	6196	N3540	110631.6 +361713	SB0 2B	1.3x1.3 0	14.6 14.33	6400: HGC	6391		1.88		0	10.03		
470	6258		111110.3 +214727	Irr 10	2.1x0.5 80	15.6 15.55	1417 KK80	1450 1372	8.32 10.17	2.0	182 185	1	8.20	8.66	10.03
472	6277	N3596	111227.9 +150338	Sc 7	4.4x4.4 0	11.7 11.23		1192 1083	34.7 34.7		144	10	9.73	8.98	
473	6288	I2672	111329.5 +102553	Sc 7	1.0x0.8 37	15.3 15.39		5895 5766	2.08 2.39	1.0	231 384	1	9.52	9.27	11.39
474	6290	I2674	111333.2 +111853	Sc 7	1.4x0.7 60	15.3 15.20		5883 5758	2.05 2.58	1.2	214 249	1	9.59	9.31	11.09
477	6397		112019.6 +344613	Sa-b 4	1.8x0.3 90	15.0 13.98		6314 6303	0.99 1.36	0.91	336 336	1	10.16	9.10	11.11
483	6513	N3716	112906.2 +034556	S0? 1	0.7x0.6 32	14.5 14.14	6636 CfA	6628 6478	1.92 2.08	2.3	597 1128	1	10.11	9.31	12.03
487	6558		113230.0 +024933	SBc 6	1.0x0.3 74	15.4 15.09		5230 5078	2.74 3.53	1.9	259 270	1	9.52	9.33	10.95
489	6568		113302.7 +002416	S... 3	1.0x0.4 66	14.4 13.88	5949 CfA	5955 5794	1.46 1.65	3.2	206 226	1	10.12	9.12	10.64
491	6608		113559.4 -005430	S... 3	1.1x0.7 51	14.5 14.09	6200: HGC	6035:		4.0		0	10.07		
492	6612	I716	113629.1 +000400	Sb 5	1.6x0.2 90	14.9 13.79		5429 5268	5.98 9.51	1.5	460 460	1	10.08	9.79	11.26
499	6769		114509.3 +020620	SB:a-b 5	1.1x0.5 64	15.0 14.59		8537 8389	4.23 5.29	1.2	470 525	1	10.16	9.94	11.56

TABLE I. (continued)

K #	UGC #	NGC/IC Name	R.A. Dec.	Type T	a x b i	m_z m_c	V^{opt} Ref.	V^{21} V_o	S $S_{H,c}$	σ	W W_o	obs	h^2L	h^2M_H	hM_T
(1)	(2)	(3)	(4)	(5)	(6)	(7)	(8)	(9)	(10)	(11)	(12)	(13)	(14)	(15)	(16)
500	6771		114526.0 +044556	SBa 5B	1.9x1.7 27	14.4 14.10	5981 CfA	5962 5825	1.48 1.98	0.7	318	1	10.04	9.20	
501	6777		114601.6 +325450	... 0	0.9x0.8	15.5 15.34		6999 6990	2.07 2.29	1.6	278	1	9.70	9.42	
507	6847		115002.9 +243507	Sb-c 5	1.7x0.3 83	15.4 14.51		4945 4898	5.62 8.36	2.0	259 262	1	9.73	9.67	10.80
508	6854	VV105	115010.0 +020103	SB... 6	1.1x1.0 25	14.4 14.10	6118 CfA	6125 5979	3.58 4.13	1.4	159	1	10.06	9.54	
512	6903		115302.7 +013046	SBc 8B	2.5x2.2 28	14.1 13.73	1812 KK79	1890 1744	19.9 19.9		190	13	9.14	9.16	
516	6986		115652.6 +180200	S... 5	1.1x0.3 73	15.3 14.60		6449 6376	3.03 3.99	2.0	324 338	1	9.92	9.58	11.03
518	7045	N4062	120130.2 +321023	Sc 7	4.8x2.0 65	11.9 11.38		767 762	23.6 26.0		309 341	10	9.36	8.56	10.86
524	7321		121502.3 +224901	Sc 7	5.5x0.3 90	14.0 12.33	428 KK79	406 365	35.9 53.6		239 239	13	8.33	8.23	10.11
530	7605		122610.3 +355927	Dw Irr 9	1.6x1.1 46	15.3 15.24		309 334	4.82 5.79	4.0	57 80	1	7.09	7.18	9.09
534	7699		123021.2 +375341	Sbc 8	4.0x1.1 74	13.4 12.67	614 KK79	486 522	19.8 32.4	4.0	189 197	1	8.51	8.32	10.18
536	7723	N4534	123138.8 +354741	Sdm 8	4.5x3.3 43	13.2 12.92	822 KK79	802 829	71.3 71.3		132 196	13	8.82	9.06	10.50
547	7876	N4635	124009.4 +201312	Sc 8	1.8x1.4 39	13.7 13.36	882 KK79	960 923	6.51 8.19	2.0	169 269	1	8.73	8.22	10.53
548	7885	I3692	124024.9 +211547	SBa 3B	1.0x0.7 46	14.8 14.44		6579 6546	1.75 1.97	0.8	450 620	1	10.00	9.30	11.61
549	7901	N4651 Arp189	124112.5 +164005	Sc 7	3.8x2.5 49	11.3 10.99	794 RC2	800 748	61.8 65.9		384 509	13	9.49	8.94	10.92
550	7917	N4662	124202.1 +372337	SBb 6B	2.5x2.0 37	14.1 13.77	6991 CfA	6994 7034	4.91 7.40	3.2	274 453	1	10.34	9.94	11.92
553	7987	N4719	124744.6 +332555	SBb 4B	1.7x1.5 29	14.2 13.87	7061 CfA	7098 7124	4.18 5.30	3.0	156 325	1	10.31	9.80	
559	8062	N4826	125416.9 +215718	Sb 4	10.0x5.0 61	8.9 8.54		410 390	51.2 54.0		354 405	10	9.92	8.29	10.73
561	8079	N4846	125526.6 +362827	S... 3	1.5x0.7 64	14.6 14.18		4534 4578	8.84 10.52	4.0	346 385	1	9.80	9.72	11.14
566	8166		130123.0 +111427	Sc 6	1.5x0.1 90	15.7 14.89		2942 2881	2.94 4.85	1.3	191 191	1	9.11	8.98	10.40
568	8170		130142.5 +092933	Sc 6	1.0x0.9 26	14.8 14.65		10505 10437	2.25 2.56	1.5	256	1	10.33	9.82	
575	8279	N5016	130942.5 +242142	Sb-c 7	1.9x1.4 43	14.3 13.94		2614 2615	5.87 7.79	1.5	265 394	1	9.41	9.10	11.27
576	8306		131106.0 +161527	Sb 5	1.6x0.3 90	14.9 13.79		6792 6759	4.86 7.46	1.5	513 513	1	10.29	9.91	11.48
579	8343		131416.8 +221420	S... 2	1.3x0.7 59	15.5 15.24		7001 6996	2.35 2.67	1.2	358 419	1	9.74	9.49	11.36
581	8366	N5081	131646.5 +284603	SBb 5B	2.2x0.7 73	14.3 13.48	6630 CfA	6656 6680	7.20 10.74	1.6	546 570	1	10.41	10.05	11.73
584	8450		132430.4 +101841	Dw Irr 9	1.1x0.9 35	17.0 17.00		1055 1007	2.14 2.42	4.0	61 107	1	7.36	7.76	9.71
588	8507	VV88	132833.8 +194141	(Irr) 9	1.6x0.9 55	14.0 13.82		994 988	3.47 4.11	2.0	103 126	1	8.61	7.98	9.94
590	8516		132928.1 +201523	Sc 5	1.1x0.8 44	13.8 13.45	990 KK79	1021 1018	4.01 4.74	2.0	124 180	1	8.78	8.06	9.76
593	8598		133416.5 +202640	Sb-c 5	1.7x0.2 90	14.8 13.53		4909 4911	3.00 4.87	1.6	439 439	1	10.12	9.44	11.20
598	8705		134411.0 +210533	Sc 5	1.1x0.6 57	14.8 14.30		6941 6953	3.65 4.46	1.4	417 496	1	10.11	9.71	11.45
605	8865	N5375	135440.6 +292426	SBb 5B	3.5x2.7 40	13.2 12.91	2477 KK79	2383 2436	13.2 13.8		294 457	13	9.76	9.29	11.33
6111	9006		140231.5 +001027	S... 1	1.3x0.7 59	15.3 15.24		7600 7542	3.98 4.52	2.0	355 415	1	9.81	9.78	11.38
612	9035		140541.5 +300640	SBb 6B	1.5x1.1 43	15.2 14.95		8241 8305	3.71 4.60	2.0	258 380	1	10.01	9.87	11.67
613	9048		140643.0 +334600	Sb-c 6	1.5x0.3 81	15.6 14.72		10594 10673	3.51 4.98	1.3	510 517	1	10.32	10.13	11.93
615	9079	N5496	140903.3 -005524	Sc 7	4.5x0.8 81	13.4 11.89	1527 RC2	1542 1486	59.9 75.8		271 275	11	9.73	9.60	10.87

TABLE I. (continued)

K #	UGC #	NGC/IC Name	R.A. Dec.	Type T	a x b i	m_z m_c	V^{opt} Ref.	V^{21} V_o	S $S_{H,c}$	σ	W W_o	obs	h^2L	h^2M_H	hM_T
(1)	(2)	(3)	(4)	(5)	(6)	(7)	(8)	(9)	(10)	(11)	(12)	(13)	(14)	(15)	(16)
621	9119	N5523	141235.4 +253500	Sc 7	4.7x1.4 75	13.4 12.65	1044 RC2	1045 1096	23.9 28.2		280 294	10	9.17	8.90	10.86
622	9158	I4403	141606.0 +315300	S... 3	1.4x0.5 73	14.9 14.49		4273 4351	8.33 9.83	3.0	393 412	1	9.63	9.64	11.13
625	9182		141826.4 +221000	Sc 6	2.6x0.5 82	14.7 13.73	4721 KK79	4655 4698	21.3 26.6		351 355	10	10.00	10.14	11.42
626	9201	N5584	141949.9 -000934	Sc 7	3.5x2.8 37	12.8 12.06	1454 KK79	1641 1596	22.8 25.5		208 346	11	9.73	9.19	11.15
638	9416	N5690	143509.3 +023014	Sc 7	3.6x1.1 72	13.1 11.91	1758 KK79	1752 1731	33.1 38.9		323 339	13	9.86	9.44	11.09
642	9465	N5727	143821.3 +341200	SABdm 9	2.3x1.2 58	14.6 14.43	1625 KK79	1492 1595	15.10 15.10		202 239	12	8.78	8.96	10.81
642	9487		144042.0 +213753	Sa-b 3	1.4x0.4 79	15.7 15.20		12528 12586	1.54 1.83	0.5	523 533	1	10.27	9.83	11.79
662	9739		150644.5 +255513	S:Bd-m 10	1.0x0.3 79	15.6 15.43		1365 1460	6.64 7.25	3.0	161 164	1	8.31	8.56	9.71
672	9828		152015.3 +192613	Sc 6	1.7x0.1 90	15.7 14.18		6871 6954	4.87 8.14	1.7	459 459	1	10.16	9.97	11.59
674	9833		152141.4 +234320	... 8	1.2x1.0 34	15.7 15.36		8705 8804	1.57 1.80	0.9	254 458	1	9.89	9.52	11.85
691	9935	N5964	153508.2 +060816	SBc 7B	4.4x3.4 40	14.2 13.65	1412 KK79	1448 1493	44.7 46.3		206 325	10	9.04	9.39	11.14
694	9960		153734.2 +020520	Sa 3	1.6x0.5 76	15.5 15.26		10596 10628	2.96 3.58	0.76	584 601	1	10.10	9.98	11.88
697	9980		154001.8 +021020	SB0 1	1.0x0.6 54	15.2 15.03		3567 3601	0.80 0.88	0.60	387 478	1	9.25	8.43	11.11
700	10005		154241.1 +005547	Sc? 7	1.6x1.5 20	15.7 15.87		3836 3868	5.06 6.35	3.8	144	1	8.97	9.35	
712	10083	N6012	155154.5 +144455	SBa 5B	2.1x1.6 41	13.1 12.36	1920 KK80	1855 1947	22.1 23.1		195 299	11	9.78	9.32	10.70
716	10104		155527.3 +301157	Sc 8	2.8x2.6 22	14.9 14.62	9849 KK79	9845 9991	6.15 10.09	2.5	234	1	10.30	10.38	
719	10120		155716.3 +351013	Sb-c 5B	1.3x1.3 0	14.9 14.67	9900 RC2	9430 9592	1.61 1.91	2.5	67	1	10.24	9.62	
723	10226		160709.2 +355520	Sb 5	1.1x0.5 64	15.4 14.89		9063 9234	3.71 4.64	1.5	373 416	1	10.12	9.97	11.40
724	10227		160708.0 +364413	SB?c 7	2.2x0.2 90	15.6 14.30	9222 KK80	9026 9199	5.99 10.24	2.3	618 618	1	10.36	10.31	12.08
726	10239		160803.6 +125707	SBa 3B	1.0x0.9 27	15.1 14.97		10457 10556	3.62 4.08	0.47	307	1	10.20	10.03	
741	10405		162639.5 +180000	Sc 6	1.7x1.3 40	15.2 14.76		10879 11010	5.63 7.21	3.6	140 217	1	10.33	10.31	11.35
743	10435		162914.4 +224813	SBb 5B	1.1x0.7 50	15.3 14.83		7295 7444	4.77 5.71	1.5	307 398	1	9.96	9.87	11.30
748	10445		163148.6 +290519	Sc 7	2.9x1.9 48	14.2 13.76	1157 KK80	956 1126	26.3 27.8		169 226	13	8.75	8.92	10.55
753	10477		163545.1 +372233	S... 3	1.8x0.3 90	15.4 14.89		851 1045	4.95 6.23	4.3	123 123	1	8.23	8.20	9.48
754	10490		163634.8 +172700	Sc 6	1.1x0.9 35	15.3 14.85		4594 4731	1.91 2.22	1.0	204 353	1	9.56	9.07	11.26
761	10514		164018.4 +251020	S-Irr 5	1.7x0.5 75	15.4 14.56		6742 6906	5.16 7.29	2.0	408 422	1	10.00	9.91	11.40
766	10521	N6207	164117.8 +365532	S... 7	3.3x1.2 72	11.9 11.26	1047 KK79	850 1046	40.0 45.9		243 261	10	9.68	9.03	10.64
767	10525		164157.3 +232913	Sb 5	1.0x0.9 26	15.7 15.41		9572 9733	2.91 3.32	2.0	119	1	9.96	9.87	
769	10528		164242.3 +223641	S0 1	2.4x1.3 59	13.5 12.99	4561 KK80	4274 4432	4.33 5.78	1.0	496 581	1	10.25	9.43	11.65
775	10606	N6255	165300.5 +363455	SBc 7B	3.5x1.4 66	13.8 13.13	1043 KK79	914 1117	31.1 35.2		206 225	10	8.99	9.01	10.56
785	10685		170231.3 +125920	S... 6	1.3x0.5 68	15.2 14.56	9788 KK79	9642 9784	3.73 4.78	1.3	441 477	1	10.30	10.03	11.83
786	10699		170357.2 +102622	SB... 5	0.5x0.4 36	14.5 13.85		6275 6409	1.20 1.33	0.9	285 490	1	10.22	9.11	11.21
791	10743		170904.9 +080307	Sa? 3	1.2x0.5 68	14.8 14.25		2567 2697	3.41 3.93	1.3	288 311	1	9.31	8.83	10.64
797	10798		171640.6 +193433	Sb-c 5	1.0x0.2 83	15.4 14.29		6167 6341	2.01 2.82	1.2	273 275	1	10.04	9.43	10.78

TABLE I. (continued)

K #	UGC #	NGC/IC Name	R.A. Dec.	Type T	a x b i	m_z m_c	V^{opt} Ref.	V^{21} V_o	S $S_{H,c}$	σ	W W_o	obs	h^2L	h^2M_H	hM_T
(1)	(2)	(3)	(4)	(5)	(6)	(7)	(8)	(9)	(10)	(11)	(12)	(13)	(14)	(15)	(16)
799	10805	D207	171734.4 +142647	Dw sp 8	1.8x1.6 27	15.3 15.05	1558 RC2	1554 1712	4.88 6.27	4.0	66	1	8.60	8.64	
800	10807	N6347	171740.6 +164237	SBb 6B	1.2x0.6 60	14.6 13.70		6146 6311	2.71 3.34	1.5	378 436	1	10.27	9.50	11.56
805	10829	I1256	172146.3 +263157	Sb 6	1.7x1.3 40	14.5 13.93		4730 4927	6.00 7.68	1.9	342 528	1	9.96	9.64	11.77
808	10862		172541.9 +072740	SBc 7B	3.3x3.0 25	15.0 14.76	1944 KK80	1690 1830	16.9 17.1		141	13	8.77	9.13	
809	10878		172744.2 +232130	Pec 10	1.1x0.5 61	15.4 14.93		12181 12373	2.23 2.48	0.34	714 820	1	10.36	9.95	12.13
810	10890		172948.3 +321600	Sc 7	1.9x0.1 90	15.6 13.92		4549 4765	3.28 5.84	1.2	275 275	1	9.93	9.50	10.99
812	10893	N6389	173025.8 +162616	Sb 7	3.2x2.0 51	13.6 12.81	3304 KK79	3115 3288	40.5 43.1		415 537	13	10.06	10.04	11.80
817	10913		173421.2 +151940	SBc 8B	1.1x1.0 25	15.6 15.65		6619 6792	2.32 2.64	2.0	58	1	9.55	9.46	
828	10972		174421.8 +263341	Sc 7	2.6x0.7 75	14.5 13.37	4912 KK80	4657 4868	6.80 8.13		409 424	13	10.17	9.66	11.62
830	10981		174516.8 +093347	Sb-c 5	1.0x0.5 61	15.3 14.51		10901 11062	4.16 5.09	1.4	490 563	1	10.43	10.17	11.72
838	11013	I1269	174958.8 +213451	Sb/Sc 7	1.7x1.3 40	14.5 13.61		6115 6317	8.19 10.49	2.5	130 202	1	10.31	9.99	11.04
840	11058		175504.0 +323827	SBb 6B	1.6x1.2 42	14.4 13.84	4749 RC2	4755 4987	4.54 5.72	1.8	293 441	1	10.01	9.53	11.60
844	11091		175855.7 +350033	Sc 7	1.1x0.6 56	15.7 15.10		7243 7481	3.49 4.21	2.3	308 370	1	9.86	9.75	11.47
853	11251		182703.8 +380047	Pec 7	1.5x0.9 52	15.7 15.30	2300: HGC	2334 2591	3.64 4.57	2.4	166 210	1	8.85	8.86	10.63
879	11575		202736.3 +025300	Sc-Irr 5	1.6x0.5 74	14.8 13.69		3991 4199	8.70 12.06	4.4	280 291	1	9.92	9.70	10.84
884	11612		203818.7 +002813	Sb-c 6	1.1x0.1 90	15.7 14.25		8047 8247	4.22 6.28	2.1	431 431	1	10.28	10.00	11.51
886	11618	N6954	204131.6 +030141	S... 1	0.9x0.5 58	14.2 13.37	4011 RC2	4221		1.14		0	10.05		
889	11633	N6969	204559.8 +073313	Sa 3	1.1x0.3 80	15.0 14.16	4000 CfA	4227		0.85		0	9.74		
897	11681	N7025	210527.6 +160803	Sa 3	2.3x1.5 50	14.1 13.42		4969 5223	2.48 3.39	1.2	593 773	1	10.21	9.34	11.97
904	11715		211524.7 +132300	Sc 6	1.0x0.1 86	15.6 14.35		5049 5295	3.08 4.35	2.0	246 247	1	9.86	9.46	10.83
910	11731	I5104	211912.2 +210138	SB?a-b 5	1.8x0.4 79	14.4 13.03		4958 5225	6.80 8.43		389 397	12	10.37	9.74	11.23
911	11734	N7056	211948.1 +182706	SBb 6B	1.0x1.0 0	13.8 13.26	5548 KK79	5378 5638	1.78 2.01	1.3	247	1	10.35	9.18	
922	11785		213652.9 +023547	Sc 7	1.4x0.1 87	15.4 14.02	4260 KK79	4074 4283	3.36 5.14	1.7	358 359	1	9.80	9.35	11.14
924	11790		213855.7 +003933	Sc 7	1.6x1.1 46	15.3 14.87		4540 4741	1.92 2.43	1.4	242 336	1	9.55	9.11	11.33
929	11809		214408.5 +080333	Sb 6	1.0x0.4 63	15.4 14.73		10897 11124	3.70 4.52	0.9	609 681	1	10.35	10.12	12.12
930	11810	I1401	214426.1 +012840	Sb 7	2.1x0.7 71	14.7 13.76	4710 RC2	4719 4923	5.82 8.36	3.0	375 398	1	10.03	9.68	11.52
931	11816		214632.5 +001240	SBb-c 7B	1.6x1.5 20	14.8 14.30		4751 4950	7.50 9.42	4.0	138	1	9.82	9.74	
932	11817	N7138	214635.3 +121640	SBa 4	1.1x0.5 64	15.4 14.69		8406 8647	1.80 2.12	0.7	554 614	1	10.15	9.57	11.72
935	11843	N7156	215201.1 +024225	Sc 6	1.6x1.4 29	13.5 13.01		3990 4197	4.40 5.52	2.0	129	1	10.19	9.36	
936	11859		215534.0 +004613	Sb 5	2.5x0.2 90	15.6 14.06	3246 KK80	3013 3212	17.1 25.4		319 319	10	9.54	9.79	10.83
937	11863		215553.8 -005853	Dw sp 9	1.0x0.8 37	15.7 15.41		4883: 5075:	0.89 0.99	1.64	176:	0	9.40:		
938	11866		215608.6 +135253	Pec 10	1.5x0.8 58	15.6 15.32		1708 1952	11.8 13.8	4.5	132 155	1	8.60	9.09	9.99
940	11871		215813.7 +101843	Dbl sys 10	1.0x0.6 53	14.7 14.26:	8400 RC2	7978 8211	1.63 1.80	1.0	253 316	1	10.27	9.46	11.11
946	11905	IIZw163	220332.2 +202347	Pec 4	1.9x0.8 67	15.1 14.28		7522 7783	abs	0.7	353:	2	10.22		

TABLE I. (continued)

K #	UGC #	NGC/IC Name	R.A. Dec.	Type T	a x b i	m_z m_c	V^{opt} Ref.	V^{21} V_o	S $S_{H,c}$	σ	W W_o	obs	h^2L	h^2M_H	hM_T
(1)	(2)	(3)	(4)	(5)	(6)	(7)	(8)	(9)	(10)	(11)	(12)	(13)	(14)	(15)	(16)
947	11914	N7217	220537.6 +310655	Sb 5	3.8x3.3 30	11.0 10.45		952 1234	15.5 15.9		353 702	10	10.15	8.76	11.45
949	11921		220649.6 +140647	Irr 9	1.9x0.8 65	14.7 14.32		1679 1922	3.27 3.98	1.9	186 206	1	8.99	8.54	10.68
950	11924		220653.3 +211607	Sc 9	1.7x1.0 53	14.8 14.33		3803 4065	5.67 6.84	1.9	245 306	1	9.63	9.43	11.34
951	11928		220727.1 +163840	SB... 5B	1.0x0.8 37	15.7 15.43				0.85		0			
956	11965	I1437	221311.9 +014853	S0-a 1	1.1x1.0 25	14.9 14.62		2875:	0.26:	1.28	72:	0			
958	11978		221521.6 +280153	Sc 7	1.3x1.3 0	15.7 15.33		6520 6795	3.05 3.62	1.5	151	1	9.68	9.60	
963	12015		222101.2 +193553	SBc 9	1.3x1.1 32	15.7 15.46		7682 7937	4.00 4.67	1.7	156 293	1	9.76	9.84	11.54
967	12048	N7292	222606.5 +300209	Irr 9	2.3x1.8 39	13.1 12.71	1254 KK80	988 1264	19.2 19.2		99 159	11	9.27	8.86	10.39
970	12081		223133.5 +095453	Sa-b 3	1.3x0.3 90	15.5 14.68	11853 KK79	11637 11860	3.09 3.68	0.6	619 619	1	10.42	10.09	11.84
971	12082	D213	223152.7 +323606	Dw sp 9	3.5x3.0 31	15.6 15.27		803 1081	31.6 31.6		82 160	10	8.11	8.94	10.47
972	12090		223220.7 +154106	Irr 9	1.0x0.4 66	15.7 15.42		1880 2121	3.53 3.87	2.8	161 177	1	8.63	8.61	10.38
974	12098	N7316	223330.6 +200350	S... 6B	1.1x0.9 35	13.7 13.25	5548 RC2	5553 5805	5.72 6.65	2.0	154 267	1	10.38	9.72	11.11
975	12106	I5233	223410.3 +253007	S... 5	1.1x0.9 36	14.8 14.32		7375 7640	4.00 4.67	1.6	252 432	1	10.18	9.81	11.41
976	12118	N7328	223459.8 +101623	Sa-b 5	2.1x0.7 72	14.3 13.32	2793 CfA	2823 3047	9.36 13.69	2.1	332 349	1	9.79	9.48	10.95
978	12140		223801.2 +154454	S... 5	1.1x0.4 70	15.3 14.50		7555 7794	5.30 6.84	1.2	392 417	1	10.13	9.99	11.32
982	12172		224126.2 +070733	Sc 7	1.2x0.6 60	15.5 14.85		7568 7779	3.31 4.08	1.2	375 435	1	9.99	9.76	11.65
984	12175	N7367	224201.8 +032246	Sa-b 4	1.6x0.4 80	14.9 13.95	7624 KK80	7235 7432	2.36 3.03	0.91	602 611	1	10.31	9.60	11.72
985	12178		224237.0 +061003	... 8	3.3x1.7 58	14.2 13.58	2235 KK79	1932 2139	28.9 28.9		241 283	13	9.37	9.49	11.10
988	12190		224543.8 +280133	Sc 5	2.2x0.2 90	15.6 14.03	7759 KK79	7263 7530	6.75 12.10	1.4	589 589	1	10.29	10.21	11.71
990	12205		224716.4 +144920	Irr 4	0.9x0.3 73	15.4 14.67		3395 3629	3.64 4.30	2.2	178 187	1	9.40	9.13	10.21
992	12224		225006.3 +054933	Sc 7	2.1x2.1 0	15.3 15.06	3693 KK80	3509 3712	7.97 11.21	2.0	204	1	9.26	9.56	
997	12245		225223.8 +213206	Sc 7	1.0x0.4 63	15.6 14.98		8360 8610	2.10 2.57	1.2	347 390	1	10.03	9.65	11.53
999	12251		225322.7 +060627	S0? 1	1.0x0.4 69	15.4 15.03				0.97		0			
1000	12260		225412.4 +372753	Sc 7	1.7x0.3 81	15.7 14.19		5540 5819	4.02 5.93	3.0	298 302	1	10.00	9.68	11.23
1002	12299	N7451	225809.4 +081153	SBb-c 5B	1.1x0.5 64	15.0 14.34		6684 6893	2.75 3.44	1.2	361 403	1	10.09	9.59	11.25
1003	12304		225835.4 +052307	S... 7	1.4x0.2 84	15.4 14.20		3465 3663	2.22 3.27	1.2	300 302	1	9.60	9.01	10.95
1004	12343	N7479	230226.8 +120306	SBb 6B	4.4x3.4 40	11.7 11.31	2392 Sa	2381 2600	42.3 43.9		381 597	10	10.45	9.85	11.91
1005	12370		230434.0 +094040	Sc 7	1.5x0.3 79	15.5 14.55		4889 5100	5.60 7.95	1.5	268 273	1	9.75	9.69	11.05
1006	12372		230438.1 +353025	S... 5	0.8x0.7 29	14.5 13.86		5480 5753	3.96 4.43	2.8	268	1	10.12	9.54	
1008	12393	I5287	230646.0 +002900	SBb 5B	1.1x1.0 25	15.2 14.97				2.01		0			
1009	12415	N7514	231001.6 +343655	S... 2	1.6x1.0 52	13.5 12.87	5227 KK80	4843 5113	2.19 2.61	1.9	317 402	1	10.41	9.21	11.27
1013	12474		231418.1 +334325	Sa 3	1.2x0.4 75	14.1 13.40				1.83		0			
1015	12541	I5315	231849.8 +250633	Compact 0	1.0x1.0	14.6 14.20	4710 St	4431 4679	0.99 1.12	1.0	180	1	9.81	8.76	
1017	12587		232221.8 +262200	Sb 6	1.1x0.8 43	15.6 15.16		12795 13045	1.24 1.46	1.1	351 512	1	10.32	9.77	12.02

TABLE I. (continued)

K #	UGC #	NGC/IC Name	R.A. Dec.	Type T	a x b i	m_z m_c	V^{opt} Ref.	V^{21} V_o	S $S_{H,c}$	σ	W W_o	obs	h^2L	h^2M_H	hM_T
(1)	(2)	(3)	(4)	(5)	(6)	(7)	(8)	(9)	(10)	(11)	(12)	(13)	(14)	(15)	(16)
1019	12598	N7664	232410.6 +244818	Sc 5	3.3x1.8 57	13.3 12.66		3477 3722	27.4 30.1		349 415	10	10.23	9.99	11.38
1020	12623	N7683	232631.2 +111007	S0 1	2.0x0.9 66	14.6 14.17				0.76		0			
1023	12646		232909.4 +254013	SBb 5B	1.9x1.7 27	14.4 13.99	7969 CfA	8028 8273	2.62 3.50	1.3	190	1	10.39	9.75	
1027	12688		233253.3 +070250	Pec 5	1.6x0.4 79	14.4 13.26	5207 CfA	5207 5396	7.45 10.66	1.4	356 364	1	10.31	9.86	11.12
1028	12694	N7712	233320.8 +232032	Pec 10	0.9x0.8 28	13.7 13.36	3033 CfA	3055 3293	9.04 10.02	3.3	190	1	9.84	9.41	
1030	12705		233404.9 +135247	SBc 6B	1.5x1.0 48	15.7 15.30		3966 4177	11.1 13.8	2.0	188 254	1	9.27	9.76	11.01
1032	12729		233746.6 +005753	S0-a 1	1.3x0.5 70	15.2 14.85				1.54		0			
1036	12773	I1508	234322.0 +114700	S-Irr 5	1.8x0.4 81	14.6 13.52		4261 4461	8.86 13.18	1.3	321 325	1	10.04	9.79	10.97
1037	12775		234339.9 +053506	S... 4	1.0x0.4 68	15.5 14.67		9536 9714	2.66 3.13	0.8	407 439	1	10.26	9.84	11.43
1038	12776		234341.3 +330526	SBb 7B	2.8x2.2 38	14.2 13.63	5193 KK80	4925 5199	18.2 18.8		285 458	13	10.13	10.08	11.83
1039	12781	I5355	234444.1 +323021	SBc 5	1.1x0.6 57	14.4 13.65		4859 5111	1.65 2.01	1.2	234 278	1	10.10	9.09	10.81
1042	12794	N7760	234640.3 +304213	... 0	1.1x1.1	14.8 14.41	5000 St	5248		0.44		0	9.82		
1044	12840		235156.7 +283538	SB0 3B	1.2x1.0 35	14.3 13.84	6841 CfA	6856 7097	2.13 2.46	1.0	244 430	1	10.32	9.47	11.40
1045	12841	N7785	235245.5 +053811	E 0	1.8x1.2	13.0 12.64	3833 CfA	4006		0.59		0	10.30		
1046	12844		235306.8 +191400	Sc 7	1.6x0.5 72	15.4 14.69		7886 8103	2.79 3.79	1.0	371 391	1	10.09	9.77	11.63
1047	12857		235413.0 +010427	S... 5	1.9x0.4 82	14.7 13.66		2459 2614	9.71 14.73	4.0	265 268	1	9.52	9.38	10.59
1048	12864		235450.6 +304240	SBb 5	1.8x1.0 57	14.7 14.07		4681 4925	9.64 12.84	4.0	271 325	1	9.90	9.87	11.10
1050	12873		235558.8 +255607	Sm 9	1.5x1.3 30	15.6 15.44		3252 3485	2.07 2.50	1.4	146 292	1	9.06	8.86	11.23

Notes to Table I

U 149—Interference spike in spectrum does not affect observed parameters.
U 151—No known velocity; not detected.
U 268—Optical velocity for observations kindly provided by G. L. Chincarini. The detection is of low signal-to-noise and derived parameters are uncertain.
U 309—The narrow feature seen in the spectrum in Fig. 3 is probably spurious, and the galaxy is considered to be undetected.
U 318—No known velocity; not detected.
U 461—Type appears earlier on PSS material than Sandage and Tammann (1981) because of burned-out center. Sandage and Tammann type used.
U 558—No known velocity; not detected.
U 685—Zero-velocity spike caused by galactic H I; two concentrations?
U 1194—Early-type galaxy; not detected.
U 1220—V Zw 98.
U 1356—Possibly detected at low level. H I parameters uncertain.
U 1432—VV 12; M51 case.
U 1466—Arp 78; companion with U 1463.
U 1482—Not detected.
U 1503—Isolated early-type galaxy reported in Paper I.
U 1547—DDO 17; dwarf Magellanic type.
U 1587—Interference spike in spectrum does not affect observed parameters.
U 1631—Early-type galaxy; not detected; also previously not detected by Knapp *et al.* (1978).
U 1863—Detected after Fig. 3 was prepared. Profile included in Fig. 3(b).
U 1903—Not detected; optical velocity not available at time of observations.
U 2130—Probable detection, but H I parameters uncertain.
U 2357—Isolated early-type galaxy reported in Paper I.
U 2774—Isolated early-type galaxy reported in Paper I.
U 2898—Interference spike in spectrum does not affect observed parameters.
U 2964—No known velocity; not detected.
U 3010—Interference spike in spectrum does not affect observed parameters.
U 3258—Probable detection, but H I parameters uncertain.
U 3791—Interference spike in spectrum does not affect observed parameters.
U 4256—Interference spike in spectrum does not affect observed parameters.
U 4269—Peculiar H I profile.
U 4276—No known velocity; not detected.
U 4341—No known velocity; not detected.
U 4432—No known velocity; not detected.
U 4524—No known velocity; not detected.
U 4542—Interference spike in spectrum does not affect observed parameters.
U 4791—Early-type galaxy; not detected.
U 4820—In interacting pair with U 4823 (Haynes 1981).
U 4826—No known velocity; not detected.
U 5032—No known velocity; not detected.
U 5065—Interference spikes in spectrum do not affect observed parameters.
U 5155—Possible detection; H I parameters very uncertain.
U 5373—DDO 70.
U 5397—Early-type galaxy; not detected.
U 5865—No known velocity; not detected.
U 5829—DDO 84.
U 5891—Early-type galaxy; not detected.
U 5986—VV 11; Arp 206.
U 6196—Not detected; optical velocity unavailable at time of observations.
U 6513—Probable detection; H I parameters uncertain.
U 6558—Probable detection; H I parameters uncertain.
U 6568—Probable detection; H I parameters uncertain.
U 6608—Not detected; optical velocity unavailable at time of observations.
U 6777—Isolated early-type galaxy reported in Paper I.
U 6854—VV 105.

Notes to Table I. (continued)

U 6903—Outlying member of Virgo cluster (Giovanelli and Haynes 1983.)
U 7045—Outlying member of Virgo cluster.
U 7321—Outlying member of Virgo cluster.
U 7605—Zero-velocity spike caused by galactic H I.
U 7699—Zero-velocity spike caused by galactic H I.
U 7723—Outlying member of Virgo cluster.
U 7876—Zero-velocity spike caused by galactic H I. Outlying member of Virgo cluster.
U 7901—Outlying member of Virgo cluster; VV 56; Arp 189.
U 8062—Outlying member of Virgo cluster; discussed in Giovanelli and Haynes (1983).
U 8450—Zero-velocity spike caused by galactic H I.
U 8507—VV 88.
U 9201—Flux from 91-m telescope obtained by Haynes and Giovanelli (unpublished).
U 10805—DDO 207.
U 11618—Early-type galaxy; not detected.
U 11633—Not detected; optical velocity unavailable at time of observations.
U 11731—Interference spike in spectrum at $+4375$ km s^{-1} does not affect observed parameters.
U 11810—Interference spike in spectrum does not affect observed parameters.
U 11863—Possible detection; H I parameters very uncertain.
U 11871—Double system in UGC. Appears as peculiar on Sky Survey plate.
U 11905—H I detected in absorption; continuum flux measured at 1410 MHz is 76 mJy; 6-cm flux is 31 ± 5 mJy (Adams *et al.* 1980).
U 11928—No known velocity; not detected.
U 11965—No known velocity; feature at $+2875$ km s^{-1} is probably spurious; considered as not detected.
U 12175—Detected after Fig. 3 was prepared. Profile included in Fig. 3(b).
U 12251—No known velocity; not detected.
U 12393—No known velocity; not detected.
U 12474—No known velocity; not detected.
U 12541—Isolated early-type galaxy reported in Paper I. New profile shown here in Fig. 3 is free of interference.
U 12623—Early-type galaxy; no known velocity; not detected.
U 12729—Early-type galaxy; no known velocity; not detected.
U 12794—Early-type galaxy; not detected.
U 12841—Nearby early-type galaxy; not detected; previously observed by Knapp *et al.* (1978).

4) Correction for Internal Absorption—Δm_i

A correction for internal absorption $\Delta m_i = c_2 \log r_i$, where c_2 is the appropriate coefficient from Table VII and r_i is the intrinsic axial ratio, is derived in Appendix A by examining, for different morphological types, the relationship between the axial ratio r_i and the surface magnitude that would be observed if the galaxy were face-on and with no internal absorption correction defined as

$$\mathrm{SM} = m_z + \Delta m_s + \Delta m_g + \Delta m_k + 5 \log a \,. \quad (4)$$

The corrected apparent magnitude m_c then is obtained by applying all four corrections:

$$m_c = m_z + \Delta m_s + \Delta m_g + \Delta m_K + \Delta m_i. \quad (5)$$

g) Velocities

Column (8), line (1) contains the optical heliocentric velocity V^{opt} in km s^{-1} whenever available. The source for V^{opt} is given in line (2). The code corresponds to the following citations:

Cfa	Huchra *et al.* (1983)
RC2	de Vaucouleurs *et al.* (1976)
HGC	Haynes *et al.* (1983)
KK79	Karachentseva and Karachentsev (1979)
KK80	Karachentseva and Karachentsev (1980)
Sa	Sandage (1978)
St	Stocke (1979)

The heliocentric velocity V^{21} in km s^{-1} given in column (9), line (1) is measured from the 21-cm data source indicated in column (13) and defined as the midpoint at a level having a flux equal to 50% of the mean flux over the range of detected emission. Line (2) contains the adopted velocity V_0 corrected for the motion of the Sun with respect to the Local Group and using as the heliocentric velocity $V_\odot$ the 21-cm velocity V^{21}, except in those cases where only an optical velocity V^{opt} is available:

$$V_0 = V_\odot + 300 \sin l \cos b, \quad (6)$$

where l and b are the galactic longitude and latitude.

h) H I Flux

For galaxies observed with the Arecibo circular feed, column (10), line (1) contains the H I line flux integrated over the observed signal $\int S\,dV$ in Jy km s^{-1}, corresponding to the spectra shown in Fig. 3. Observed fluxes must be corrected for the effects of random pointing errors, source extent, and internal H I absorption. The corrected H I line flux $S_{H,c}$, after accounting for random pointing errors, the source to beam size ratio, depending on the telescope and feed used for each observation as specified in column (13), and the effect of internal H I absorption within the galaxy's disk, is given in line (2).

To account for random pointing errors, we adopt a constant correction of 5% to each flux obtained from circular feed observations only [code 1 in column (13)].

The correction for source-to-beam ratio can be substantial. For the large angular diameter galaxies mapped with the Arecibo flat feed system, the beam-corrected flux S_c is just S_{tot} as derived in Paper II. For observations made with the circular feed and a few taken with the Green Bank 91-m telescope, we have corrected for the variations of the beam response across the solid angle subtended by the source via a factor $f_0 > 1$, which approaches unity when the size of the source is negligible in comparison with the size of the telescope beam. For the 91-m telescope, we assume that the beam is characterized by a Gaussian of HPBW = 10′; the circular feed, a Gaussian of HPBW = 3.3′. Following Paper II, the hydrogen surface-density distribution is taken as the sum of two concentric Gaussians of opposite sign, producing a central depression, for which the characteristic H I scale length is taken as $R_{\mathrm{H\,I}} = 1.2a$. For these smaller galaxies, $S_c = f_0 \int S\,dV$.

In Appendix B, we derive a correction for the internal H I self-absorption f_{H} which is a function of axial ratio and morphological type and which is derived via an examination of the variation of H I surface density with axial ratio. This correction is found to be negligible for types $T \leqslant 3$ and $T > 8$. The corrected H I flux is then given by $f_{\mathrm{H}}\, S_c$.

To summarize, the corrected H I flux $S_{\mathrm{H},c} = f_0 f_{\mathrm{H}} S$, given in column (10), line (2) is then corrected for pointing error, beam attenuation, and internal H I self-absorption if the data were taken with the circular feed (single point). For mapped galaxies, the flux derived in Paper II is listed in column (10), line (1); in these cases, the flux is not affected by pointing errors and beam attenuation. The values after correction for internal absorption are given in line (2) of column (10).

i) rms Noise

Column (11), line (1) gives the rms noise per channel, σ, in mJy, for the dual circular feed observations. This value can be combined with an assumed velocity width to compute the upper limit to the H I mass in the case of nondetections and is an indication of the signal-to-noise ratio.

j) Profile Width

The 21–cm linewidth W in km s^{-1} is given in column (12), line (1). We use as the observed width W_{obs} the average of widths measured (a) at a level equal to 50% of the mean flux over the emission profile and (b) at a level equal to 20% of the peak flux. This value is on the average 4 km s^{-1} larger than the width measured at 50% of the mean flux, 30 km s^{-1} larger than the width measured at 50% of the maximum of the profile, and 8 km s^{-1} smaller than the width measured at a level of 20% of the average of the two horns of the profile. W is then obtained by correcting this hybrid observed width for the effect of redshift broadening:

$$W = W_{obs}/(1 + z). \quad (7)$$

In line (2), the true 21-cm linewidth W_0 in km s^{-1} is corrected for viewing inclination so that $W_0 = W/\sin i$. Corrected widths are given only for detected galaxies with inclinations greater than 30°.

k) Sources for 21-cm Data

The observational samples from which the H I parameters in columns (9) to (12) were derived are identified in column (13) by a numerical code referring to the following:

0	305-m telescope, circular feed, galaxy not detected
1	305-m telescope, circular feed, galaxy detected
2	305-m telescope, circular feed, galaxy detected in absorption
10	305-m telescope, flat feed mapping, Paper II
11	91-m telescope
12	flux from 91-m telescope; other parameters from 305-m telescope, circular feed
13	flux is average of 91- and 305-m telescopes, flat feed mapping; other parameters from 305-m flat feed mapping (Paper II)
14	305-m telescope, flat feed (Haynes 1981)

l) Optical Luminosity

Log(h^2L), where L is the optical luminosity in solar units, as given in column (14), is obtained from the corrected apparent magnitude m_c, given in column (7), line (2), and assuming a solar photographic absolute magnitude of + 5.37 after Stebbins and Kron (1937) via

TABLE II. Galaxies which are not detected in 21-cm line.

UGC #	NGC or IC #	T	a x b (')	m_z	V^{opt} (kms^{-1})	Ref	Det?	log h^2M_H $M_\odot$
(1)	(2)	(3)	(4)	(5)	(6)	(7)	(8)	(9)
151		1	1.3x1.2	14.7				
309	N137	1	1.6x1.6	14.2	5276	CfA		< 7.69
318		7	1.1x1.0	16.5				
558		3	1.7x0.7	15.7				
1194	N656	2	1.5x1.3	13.5	3916	CfA		< 8.31
1482	N781	4	1.7x0.5	14.0	3483	CfA		< 8.12
1631	N821	0	3.3x2.2	12.6	1716	CfA		< 7.90
1903		5	1.0x0.2	15.7	10769	CfA		< 9.85
2964		7	1.3x1.2	15.5				
4276		3	1.1x0.8	15.1				
4341		3	1.1x0.6	15.0				
4432		7	1.7x1.2	15.2				
4524		7	1.4x0.2	15.2				
4791	N2765	1	1.7x1.0	13.3	4250	St		< 8.17
4826		3	1.0x0.1	15.3				
5032		3	1.0x0.2	15.7				
5155	N2954	1	1.7x1.1	13.5	3836	CfA	*	< 7.89
5397		2	2.3x0.6	13.0	1401	CfA		< 7.46
5865		3	1.0x1.0	15.7	23000:	HGC		< 9.86
5891	N3376	1	0.8x0.3	14.4	5837	CfA		< 9.11
6196		2	1.3x1.3	14.6	6400:	HGC		< 8.63
6608		3	1.1x0.7	14.5	6200:	HGC		< 9.51
11618	N6954	1	0.9x0.5	14.2	4011	RC2		< 8.67
11633	N6969	3	1.1x0.3	15.0	4000	CfA		< 8.57
11863		9	1.0x0.8	15.7			*	8.54:
11928		5	1.0x0.8	15.7				
11965	I1457	1	1.1x1.0	14.9			*	< 8.10
12251		1	1.0x0.4	15.4				
12393	I5287	5	1.1x1.0	15.2				
12474		3	1.2x0.4	14.1				
12623	N7683	1	2.0x0.9	14.6				
12729		1	1.3x0.5	15.2				
12794	N7760	0	1.1x1.1	14.8	5000	St		< 7.82
12841	N7785	0	1.8x1.2	13.0	3833	CfA		< 8.35

$$h^2L = 10^{10}(hD)^2 10^{0.4M_\odot} 10^{-0.4m_c}\ L_\odot, \quad (8)$$

where $D = V_0/100h$ is the distance in Mpc. No entry is given in the few cases where no redshift is available.

m) H I Mass

Column (15) contains $\log(h^2 M_{\rm H})$, where $M_{\rm H}$ is the neutral hydrogen mass in solar units, obtained from the corrected 21-cm line flux given in column (10), line (2):

$$h^2 M_{\rm H} = 2.36\times 10^5 (hD)^2 S_{{\rm H},c}\ M_\odot. \quad (9)$$

For nondetected galaxies as listed in Table II, we derive an upper limit to the H I mass by assuming an integrated 21-cm line flux of intensity equal to 1.5 times the rms noise as given in column (12) and having a velocity width of 300 km s^{-1} for those galaxies with optical redshifts. These upper limits are given in Table II only.

n) Total Mass

$\log(hM_T)$, where M_T is the total mass in solar units, listed in column (16), is inferred from the corrected 21-cm linewidth W_0 and assuming a Brandt rotation law of index $n = 1.3$ (flat rotation curve):

$$hM_T = 6.8\times 10^4 (1.5)^{3/n} (hD) R_{\rm max} V^2_{\rm max}\ M_\odot. \quad (10)$$

Here, $R_{\rm max}$ is the radius at which the maximum in the rotation curve occurs. We assume that $R_{\rm max}$ is a fraction of the UGC radius: 0.2 for $T < 5$,0.3 for $T = 6$, 0.4 for $T = 7$, and 0.5 for $T = 8$, 9. $V_{\rm max}$ is just $W_0/2$. The total mass is derived only for detected galaxies with inclinations greater than 30°. While this law has been applied to all galaxies, it may be inappropriate for irregular galaxies.

A number of the galaxies deserve special remarks. These are stated in the notes to Table I.

In combination with Fig. 3, Table I offers a complete summary of the 21-cm line observations of all 324 galaxies in the Arecibo isolated galaxy sample.

V. INTEGRAL PROPERTIES OF ISOLATED GALAXIES

Our original purpose in observing the isolated galaxies was to use them to define the expected H I content for a galaxy with certain optical properties, say morphological class and luminosity. The isolated galaxies were chosen to represent objects which are found in environments which could be considered relatively constant over a Hubble time. In this section, we present the derived integral properties for galaxies in the Arecibo sample.

The isolated galaxy sample is not complete in any magnitude-limited sense. Furthermore, it is affected by a Malmquist bias as illustrated in Fig. 4 in which the luminosity h^2L is plotted versus the corrected velocity V_0. All 306 galaxies with known velocity are included. Clearly, low-luminosity galaxies are observed only in nearby volumes, and likewise, the most distant galaxies tend also to be the most luminous. A concern over this luminosity-distance bias must be kept in mind.

As illustrated in Fig. 1 of Paper I, which plots the distributions of morphological types, the sample is weighted heavily toward later-type galaxies. For the earlier types, the statistics are few and the disparity in the detected H I masses versus upper limits for nondetections is large. The 34 galaxies which were not clearly detected in any of the 21-cm line observations are listed in Table II, along with their morphological type code, angular dimensions, and apparent magnitude. Three of those which are possibly detected are identified by an asterisk in column (8) of Table II. The spectra of the tentative detections are displayed in Fig. 3. When an optical velocity is available, we derive an upper limit to the H I mass, assuming an integrated 21-cm line flux of intensity equal to 1.5 times the rms noise given in column (12) of Table I and having a velocity width of 300 km s^{-1}. Designations are the same as in Table I. Uncertain values are followed by a colon. In Fig. 5, we have plotted the percentage of galaxies in each morphological class which are either undetected or not clearly detected; the fraction of nondetections is also indicated for each type. There is a marked increase in the nondetection rate for the earliest types. Furthermore, many of the upper limits to the H I mass $h^2 M_{\rm H}$ given in Table II are substantially smaller than those derived for detected galaxies. As discussed in Paper I, the early-type galaxies which have detected H I fluxes contain significant H I masses, comparable to those found in later (Sb or Sc) spirals of compara-

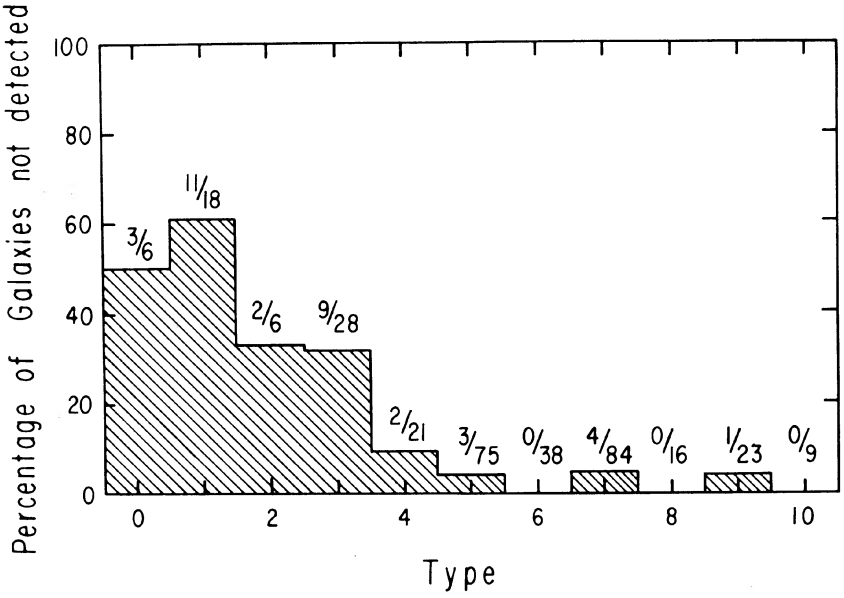

FIG. 4. Observed luminosities h^2L as a function of corrected velocity V_0 showing that a Malmquist bias exists in the isolated galaxy sample. All galaxies with known redshift are included.

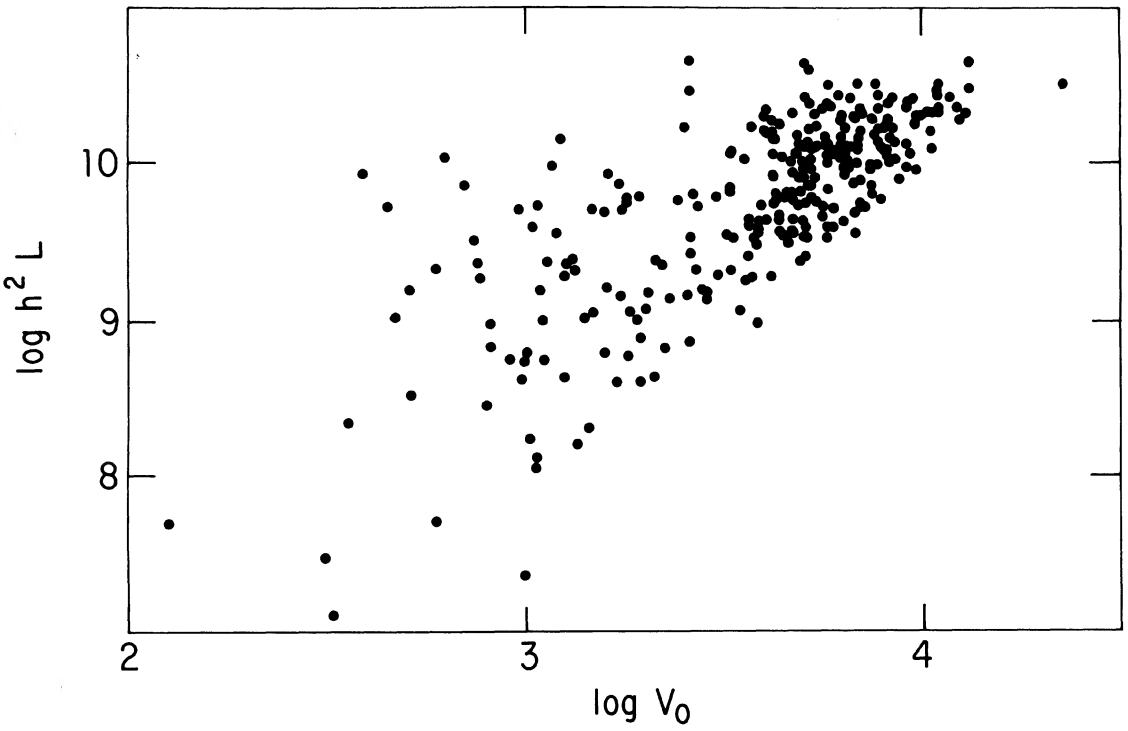

FIG. 5. Percentage of galaxies not detected in the Arecibo 21-cm line survey as a function of morphological type index T; the fraction of nondetections is also given. Galaxies with and without known redshifts are included; nondetections are listed in Table II. It is likely that some of the undetected galaxies have substantial H I fluxes but velocities which are higher than the search range.

ble optical luminosity. Yet, for some of the undetected ones, the absence of detectable H I emission is, by contrast, striking. The relevance of these statistics is hampered by the lack of optical redshifts for some of the galaxies coupled with the cutoff in the velocity regime searched for 21-cm emission of about 13 000 km s^{-1} and the unevenness of the sensitivity over the search range. Some of the galaxies of unknown redshift may be undetected merely because their distance places their H I emission outside the observed range.

Because of the small number of early-type galaxies in the sample and the high rate of nondetections for those types, the results for types E, S0, and S0/a ($T = 0$ to 2) are of marginal statistical significance and will have to be considered separately *vis-à-vis* high-quality plate material. For the later types, however, the Arecibo isolated galaxy sample provides a substantial data base for establishing the H I content of normal galaxies.

Figure 6 shows histograms on a logarithmic scale of the distribution of the major integral properties h^2M_H, h^2L, hM_T, and the ratios M_H/L, hM_H/M_T and M_H/D_l^2 for different morphological subgroups and for the entire sample for which the relevant data are available. The number of galaxies contributing to each histogram is also indicated. For h^2M_H, only detections are used, resulting in relatively biased inferences especially for the early types $T = 0$ to 2. For h^2L, all galaxies in the sample for which a redshift is available are included. For the scaled total mass hM_T, only detections with inclinations greater than 30° are used. To see if inclination problems bias the statistics, we have also restricted the inclination to $i \geqslant 40°$ or $i \geqslant 45°$, but find with those subsamples alone no substantial deviations from the trends indicated in Fig. 6.

In the remainder of our analysis, we exclude U 268 and U 1356 because the measured values of H I flux and velocity width are too uncertain.

For types Sa to Irr, we have already shown in Paper II and in Giovanelli and Haynes (1983) the near constancy of the hydrogen H I surface density M_H/D_{HI}^2, where D_{HI} is the linear H I diameter obtained from a measurement of a characteristic H I size. In practice, however, we are unable to make such a measurement of the H I extent of a galaxy and are limited to an optical diameter. Figure 7 shows the variation of h^2M_H with the linear diameter hD_l derived from the UGC blue major diameter a, after correction for the surface magnitude related bias as discussed in Appendix D. As noted in Paper II and by Shostak (1978), the near proportionality of h^2M_H and $(hD_l)^2$ implies a nearly constant H I surface density averaged over the entire galaxian disk. For the entire Arecibo isolated galaxy sample, we find

$$\log h^2M_H = 7.16 + 1.74 \log hD_l \text{ with } r = 0.89, \qquad (11)$$

similar to that obtained for H I diameters in Eq. (11) of Paper II.

As in all least-squares fits presented in this paper, the coefficients $c_1 = 7.16$ and $c_2 = 1.74$ of (11) correspond to the regression line which minimizes the residuals of the variable to the left of the equal sign, *not* to the average of the two regression lines. The reader may derive the slope of the other regression line

$$\log hD_l = c_1' + c_2' \log h^2M_H$$

from the correlation coefficient $r = (c_1'/c_2')^{1/2}$. In the case of (11), the mean regression line has a slope of 1.97.

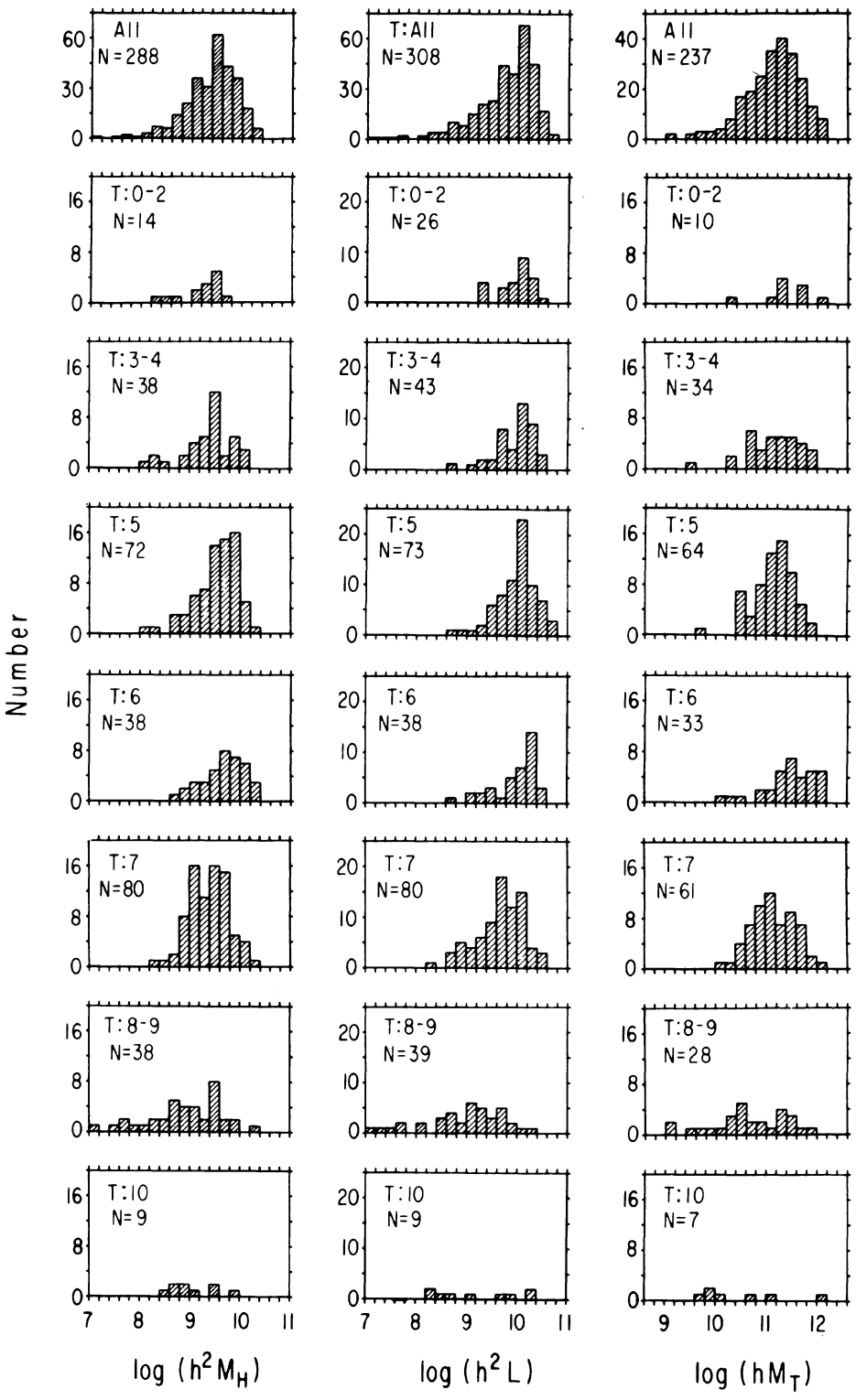

FIG. 6. Histograms showing the distribution of integral properties for different morphological subgroups. Detections only have been used to compute $h^2 M_H$. For luminosities, all galaxies with known redshift are included. Only galaxies with inclinations greater than 30° and which were detected contribute hM_T. Subgroups are identified by their type T and the number N of galaxies included in each histogram is given.

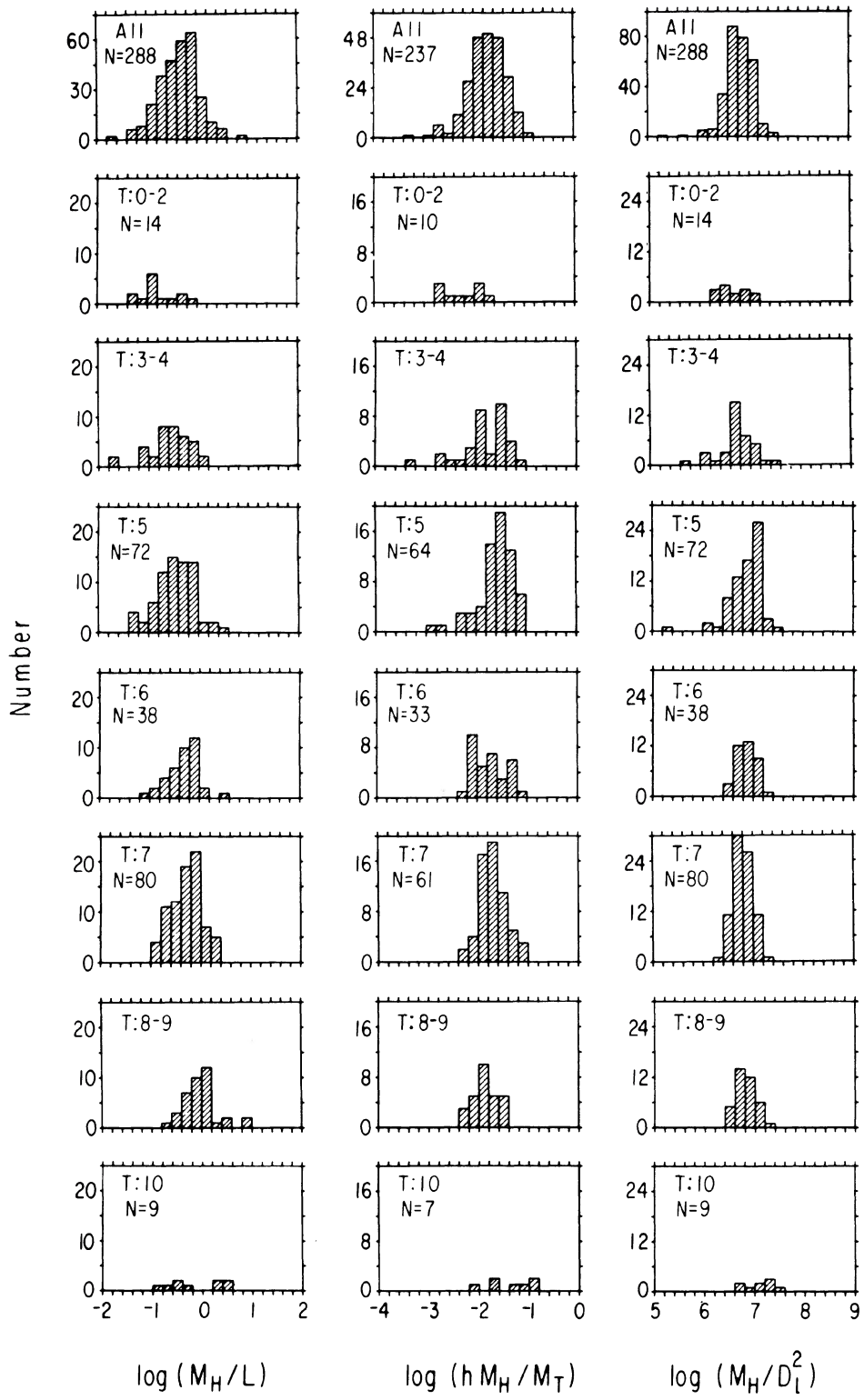

FIG. 6. (continued)

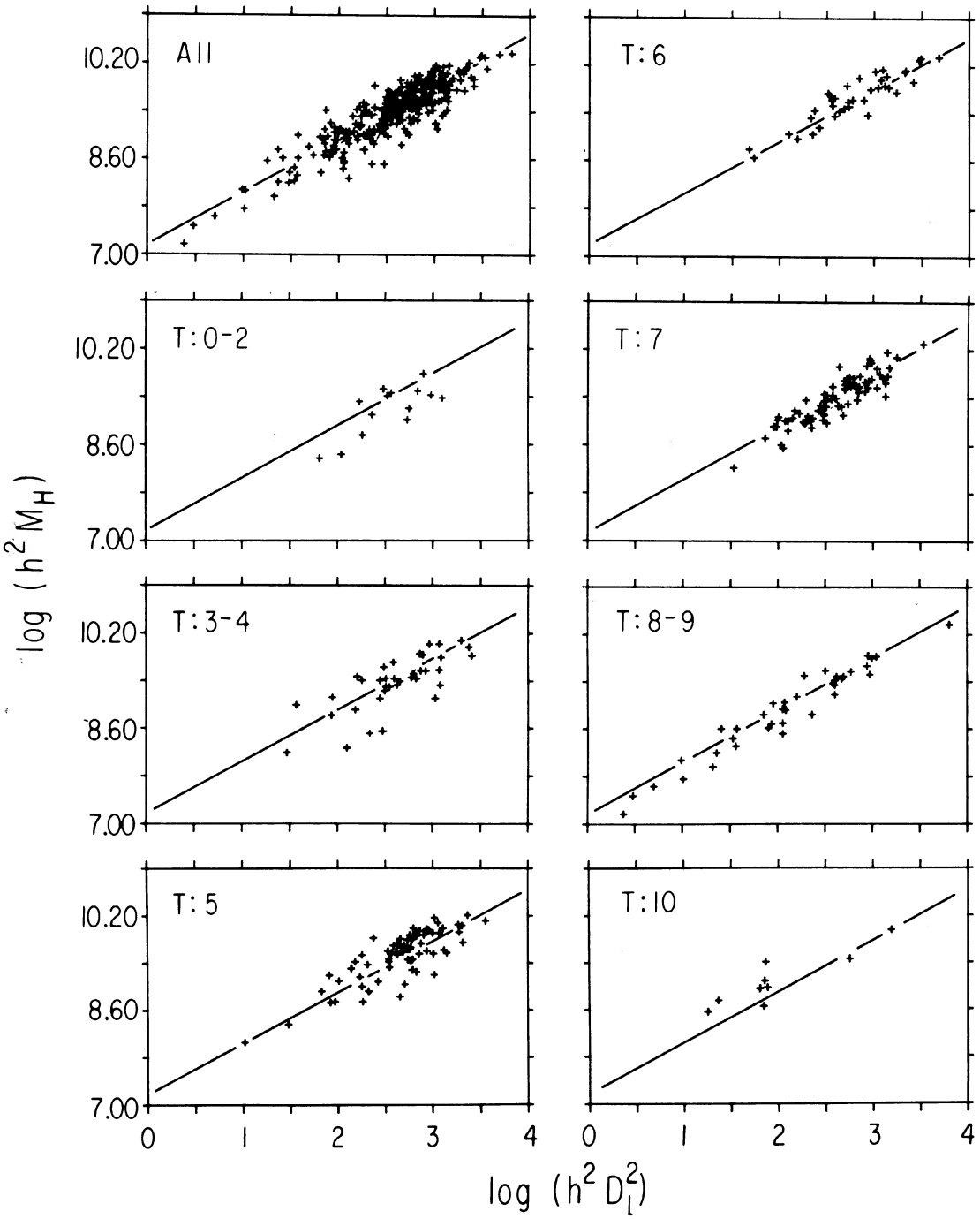

FIG. 7. Relationships between the scaled H I mass $h^2 M_H$ and the squared linear optical diameter hD_l for different morphological groups. Solid lines indicate the single regression line, fit to the set of all detected galaxies (upper left panel), whose coefficients are given in Table V.

A major point of debate is the relationship of the H I profile width corrected for viewing inclination and the intrinsic luminosity of the galaxy, the so-called Tully-Fisher relationship (Tully and Fisher 1977). Richter and Huchtmeier (1983) review the status of a possible type dependence (Roberts 1978; Aaronson and Mould 1983). Figure 8 shows the relationship of the square of the corrected H I profile width W_0 vs derived luminosity $h^2 L$, on a logarithmic scale, for the various morphological subgroups. Only detected galaxies with inclinations larger than 30° are included. We have also restricted the sample to galaxies with inclinations larger than 45° with no discernible changes in the observed slopes, but an increased noise because of the fewer galaxies. Table III lists the coefficients of the fits to the relations

$$\log h^2 L = c_1 + c_2 \log W_0^2, \quad (12)$$

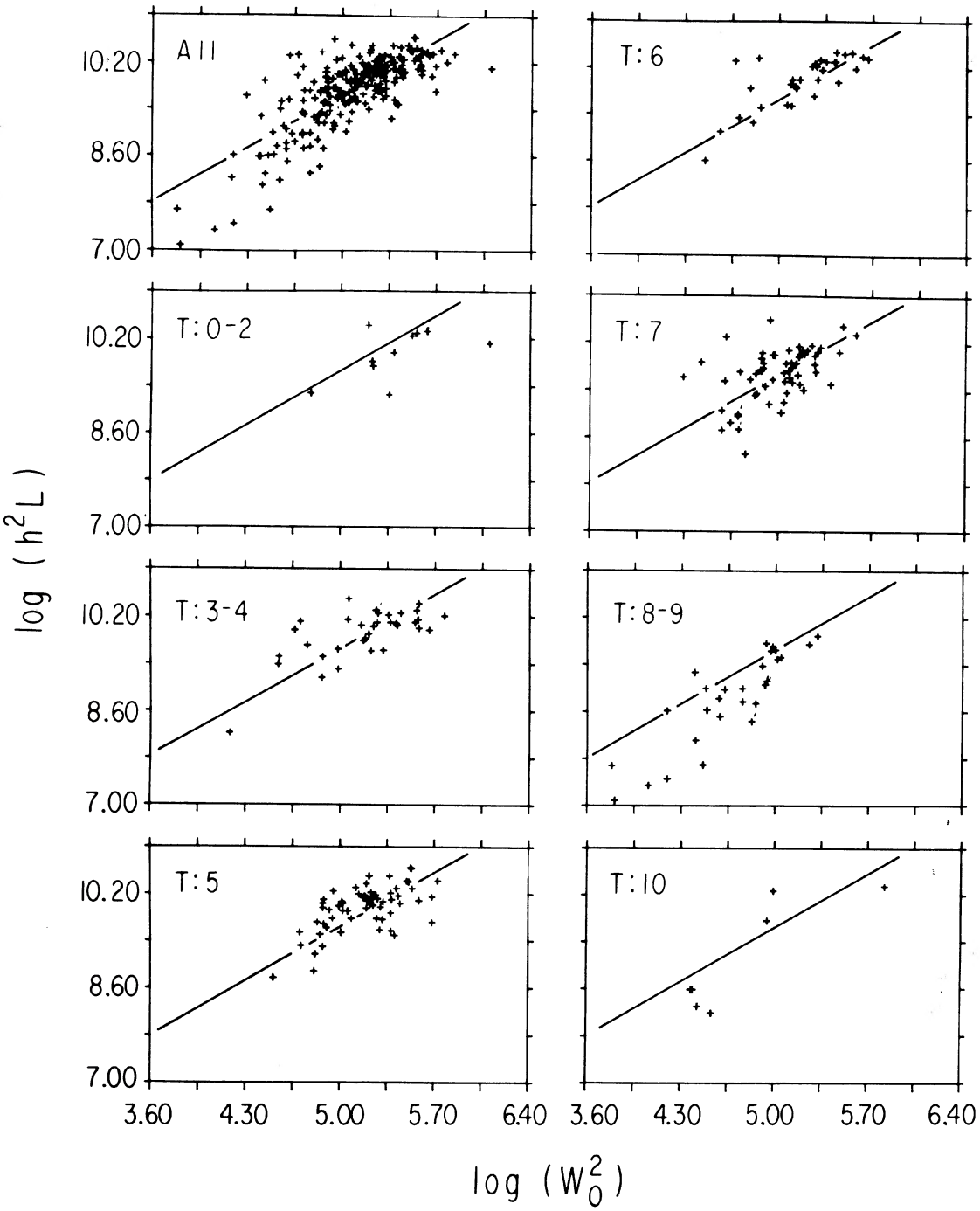

FIG. 8. Relationships between the square of the corrected H I velocity width W_0^2 and the luminosity h^2L for different morphological class groups on a logarithmic scale. Only galaxies with inclinations greater than 30° are included. The solid lines indicate the single regression line fit to the composite set of all morphological types (upper left panel). Coefficients of the fits are given in Table III for the different type groupings.

which are displayed in Fig. 8. We also give in Table III, N, the number of galaxies included, and the correlation coefficient r. Figure 6, giving the total mass hM_T and luminosity h^2L, as well as Fig. 10 and Table III, imply a higher total mass as derived from the corrected velocity width for earlier types, as discussed by Meisels (1983) and others (referenced therein). However, because of the Malmquist bias and the incompleteness of our sample, it is not possible to identify a true variation in the slope of (12) as a function of type, given the poor statistics and the large scatter caused by the inherent variations in the intrinsic mass-to-luminosity ratio or possible shape differences in the rotation curves.

TABLE III. Coefficients of the relation $\log h^2 L = c_1 + c_2 \log W_0^2$.

Type	N	c_1	c_2	r
(1)	(2)	(3)	(4)	(5)
All	236	3.13	1.30	0.77
0-2	10	6.31	0.67	0.55
3,4	34	5.58	0.84	0.70
5	63	5.40	0.88	0.62
6	33	4.50	1.06	0.75
7	61	5.36	0.87	0.50
8,9	28	0.71	1.74	0.87
10	7	1.74	1.55	0.87

VI. ISOLATED GALAXIES AS STANDARDS OF H I CONTENT

As stressed previously, one of the main objectives of this survey of isolated galaxies is to establish standards of normalcy for the H I properties of galactic disks in the absence of external influences on galaxy evolution. Normalcy is obviously a relative matter, to be considered *vis-à-vis* the processes that may result in traumatic alterations of the galactic structure, such as tides, collisions with other galaxies, sweeping, evaporation, or ionization of the interstellar gas in hostile environments. The sample of isolated galaxies is presumably least affected by those processes; thus we shall define as normal the set of H I properties characteristic of this sample.

By H I properties, one refers to the collective information on integral content, extent, and distribution of H I in a galaxy. Here, we shall concern ourselves with the question of the H I content, its operational definition, and its relation to other galactic properties. Our main goal consists of establishing a standard of H I content. We wish to be able to estimate with the highest possible accuracy the degree to which H I content of a galaxy of a given morphology, size, and luminosity deviates from our defined normalcy.

"H I content" is a loosely defined term that has, in different instances, been associated with different quantities, all involving the measured H I flux in some functional form. Let us for the moment associate it with an arbitrary quantity X_H. Using the galaxies in a control sample (in our case, that of isolated galaxies), one can find its most probable value, $\bar{X}_H$. $\bar{X}_H$ will be correlated with other parameters $(x_1, x_2, \ldots)$ which characterize the optical appearance of the galaxy, such as morphological type, luminosity, or size. One can then use such correlations to infer an expected value of the H I content for any galaxy of optical parameters $(x_1, x_2, \ldots)$. After the H I content of that galaxy is measured, one can define a deviation from normalcy, a quantity usually referred to as "deficiency" *Def*, as

$$Def = \bar{X}_H(x_1, x_2, \ldots) - X_H. \quad (13)$$

X_H has variously been equated with the logarithm of the H I mass M_H, or of the ratios M_H/L and M_H/D_l^2, where L and D_l are some optical luminosity and linear diameter. The use of H I mass appears as the most intuitively obvious, but M_H is a distance-dependent quantity, affected by the uncertainties in the value of the Hubble constant and in the magnitude of local deviations from the expansion flow. This defect limits the use of M_H, making it suited mainly to detecting relative variations within a sample of galaxies all at nearly the same distance, such as within a cluster. Thus is the popularity of distance-independent ratios such as M_H/L and M_H/D_l^2 justified, the first ratio being more widely used.

When the H I content is defined as the hydrogen mass to luminosity ratio M_H/L, common wisdom attributes the heaviest weight in the expectation of the standard M_H/L to the galaxy's morphology, while common practice has often simplified the approach to the extent of ignoring any dependence other than the one on type so that

$$X_H(x_1, x_2, \ldots) \equiv \log(M_H/L) \text{ (type)}. \quad (14)$$

Bottinelli and Gouguenheim (1974) cautioned the practitioners of this approach, noting that, if a residual dependence of M_H/L on L exists, the analysis of samples which differ in their luminosity characteristics from the control sample will result in systematic biases in the inferred *Def*, an effect later confimed by Giovanelli *et al.* (1981) in the case of the Hercules clusters.

Table IV gives the average values of $\log M_H$, $\log(M_H/L)$, and $\log(M_H/D_l^2)$, where D_l is the UGC blue major diameter converted to kpc, binned for different morphological classes. The comparison of the standard deviations s.d. (for individual objects, *not* for the mean) also listed in Table IV illustrates the inferior quality of M_H and M_H/L, as compared with M_H/D_l^2 as diagnostic tools for the H I content, if only type-dependences are considered. In fact, the use of M_H/D_l^2 led Chamaraux *et al.* (1980) to the first good-quality measurement of the H I deficiency of galaxies in the Virgo cluster. From Table IV, one can also appreciate the near independence of the hybrid H I surface density M_H/D_l^2 of spiral disks on morphological type: *the diameter of a spiral disk is a much more important diagnostic parameter for the H I mass than is morphological type.* Both M_H and D_l are disk properties, while L refers to the combined contribution of the disk and the (gas-free) spheroidal bulge. The growing importance of the bulge component in earlier morphological types reduces the values of M_H/L. While beyond the scope of this section, it is interesting to ask whether there are morphological dependences left in the ratio between M_H and disk luminosity in spirals.

TABLE IV. Average integral properties.

Type	N	$\log h^2 M_H/M_\odot$	± s.d	$\log(M_H/L)/(M_\odot/L_\odot)$	± s.d.	$\log(M_H/D_l^2)/(M_\odot/\text{kpc}^2)$	± s.d.
(1)	(2)	(3)	(4)	(5)	(6)	(7)	(8)
All	287	9.39	± 0.52	-0.35	± 0.39	6.81	± 0.24
0-2	14	9.19	± 0.42	-0.74	± 0.37	6.61	± 0.27
3,4	38	9.37	± 0.47	-0.55	± 0.41	6.69	± 0.32
5	74	9.67	± 0.42	-0.44	± 0.37	6.83	± 0.26
6	38	9.54	± 0.43	-0.32	± 0.32	6.85	± 0.19
7	72	9.40	± 0.40	-0.28	± 0.31	6.79	± 0.19
8,9	40	8.93	± 0.73	-0.04	± 0.33	6.87	± 0.17
10	9	9.09	± 0.44	-0.13	± 0.53	7.06	± 0.28

TABLE V. Coefficients of the relations between H I mass and luminosity or linear diameter.

		$\log h^2M_H = c_1 + c_2 \log h^2L$				$\log h^2M_H = c_1 + c_2 \log (hD_l)^2$			
Type	N	c_1	c_2	r	s.e.e.	c_1	c_2	r	s.e.e
(1)	(2)	(3)	(4)	(5)	(6)	(7)	(8)	(9)	(10)
All	287	2.94	0.66	0.77	0.33	7.12	0.88	0.89	0.23
0-2	14	2.93	0.63	0.55	0.36	6.88	0.89	0.76	0.28
3,4	37	2.87	0.66	0.60	0.38	7.17	0.82	0.76	0.31
5	71	2.99	0.66	0.56	0.36	7.29	0.83	0.81	0.25
6	38	2.77	0.69	0.73	0.29	7.27	0.85	0.91	0.17
7	80	3.03	0.66	0.75	0.26	6.91	0.95	0.90	0.18
8,9	38	1.40	0.84	0.91	0.30	7.00	0.94	0.97	0.17
10	9	4.99	0.45	0.85	0.25	7.75	0.66	0.91	0.19

Table V illustrates the danger of using type as the only diagnostic variable in the H I content measure. Listed by morphological subgroup are the number of galaxies contributing to each fit, the coefficients of the single linear regression, the correlation coefficient, and the standard error of the estimate (s.e.e.). Log M_H is not linearly related with either log L or log D_l^2: that M_H/L and M_H/D_l^2 have residual dependences on L and D_l is graphically illustrated in Figs. 9 and 10, combining Sbc and Sc ($T = 6$ and 7) for M_H/L in Fig. 9, and for all types (because there is little type dependence of M_H/D_l^2) in Fig. 10. For example, two Sc galaxies which differ in luminosity by one order of magnitude will have M_H/L ratios differing by about a factor of 2. This effect may introduce systematic errors in the analysis of samples consisting of galaxies in distant clusters, which are usually affected by a Malmquist bias and does, in all cases, produce an artificially large scatter of inferred H I contents. The situation is not so severe in the case of M_H/D_l^2, although taking into account the residual dependence illustrated in Figs. 9 and 10 eliminates the advantage of distance independence which motivated the use of M_H/L and M_H/D_l^2 in the first place.

In an attempt to maintain the analysis in terms of distance-independent quantities, one can correct for the residual dependence of M_H/L using the surface magnitude SM as defined in Eq. (4), rather than the luminosity, as the second diagnostic variable. Figure 11, similarly to Fig. 9, illustrates the dependence of $\log(M_H/L)$ on SM for Sbc and Sc galaxies and Table VI lists the coefficients of the fit,

$$\log(M_H/L) = c_1 + c_2\, SM, \tag{15}$$

together with the correlation coefficient and the standard

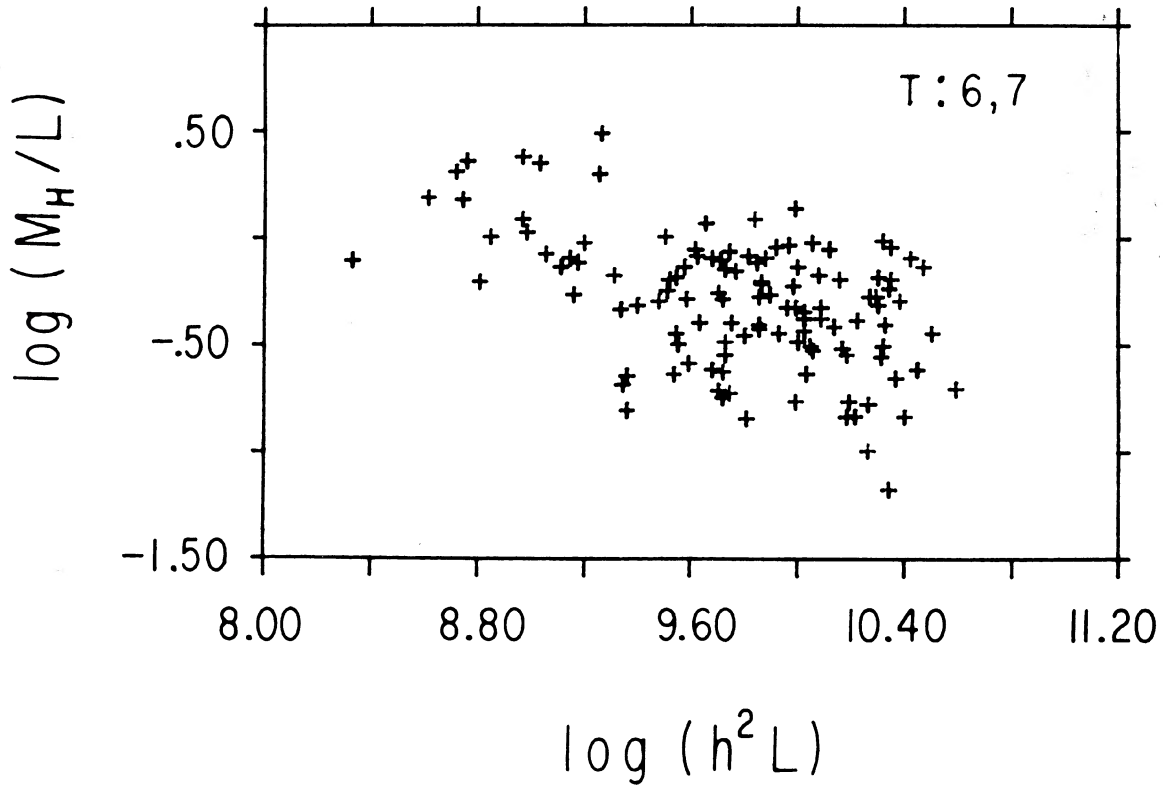

FIG. 9. Residual dependence of the hydrogen mass to luminosity ratio M_H/L on scaled luminosity h^2L, on a logarithmic scale for types $T = 6$ and 7.

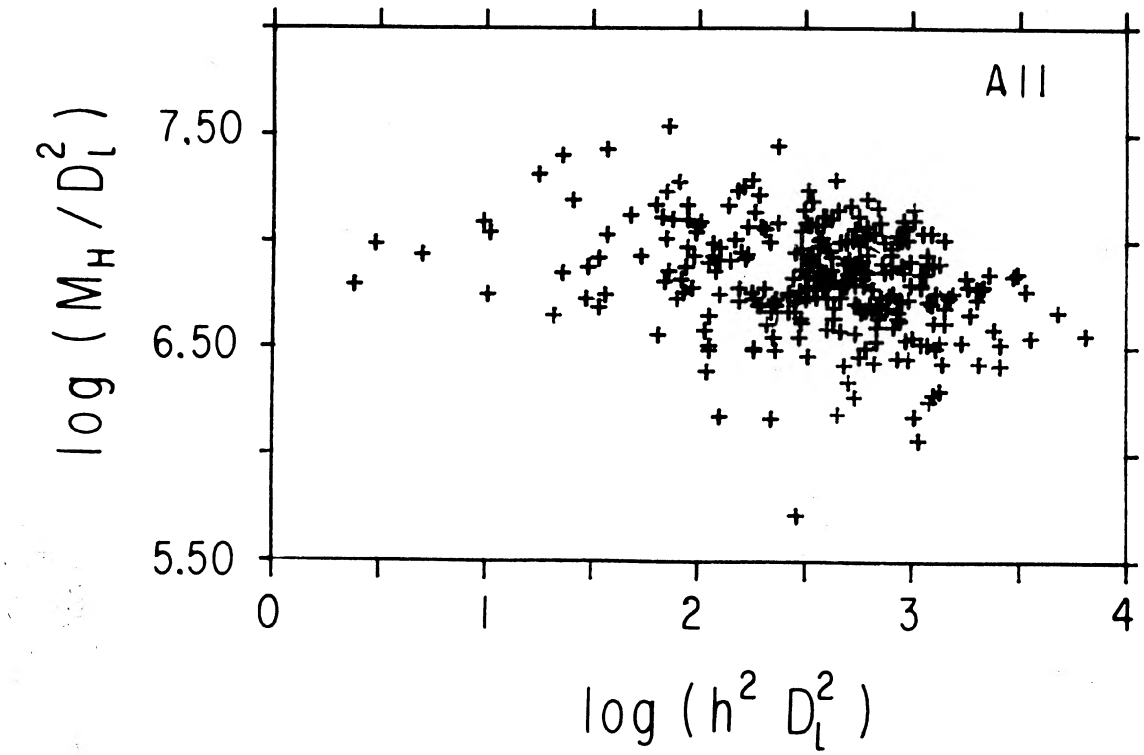

FIG. 10. Residual dependence of the hydrogen surface-density ratio M_H/D_1^2 on scaled linear diameter $(hD_1)^2$ on a logarithmic scale for galaxies of all types.

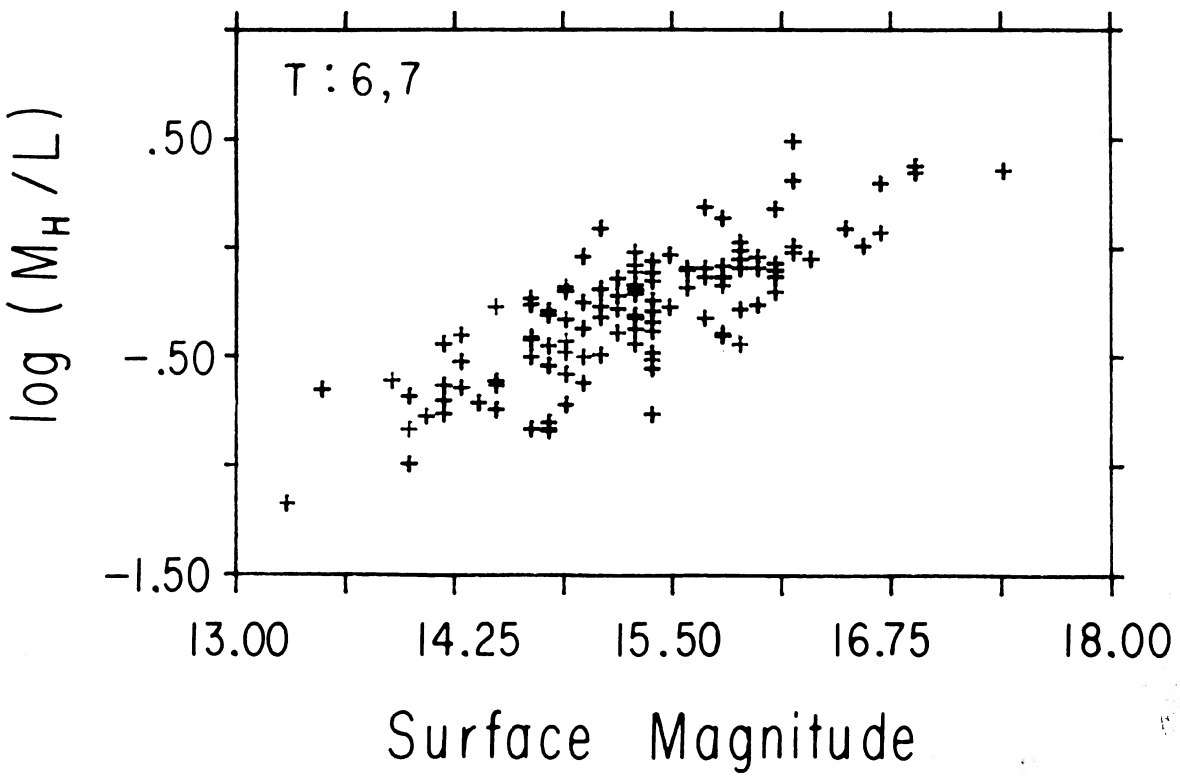

FIG. 11. Residual dependence of the hydrogen mass to luminosity ratio M_H/L on surface magnitude SM for galaxies of types $T = 6$ and 7 on a logarithmic scale.

TABLE VI. Coefficients of the relation $\log(M_H/L) = c_1 + c_2$ SM.

Type	N	c_1	c_2	r	s.e.e
(1)	(2)	(3)	(4)	(5)	(6)
All	287	-5.58	0.35	0.78	0.24
0-2	14	-5.97	0.36	0.69	0.28
3,4	37	-4.82	0.29	0.63	0.32
5	71	-5.75	0.36	0.72	0.26
6	38	-5.68	0.36	0.80	0.19
7	80	-5.55	0.34	0.82	0.18
8,9	38	-5.13	0.32	0.85	0.17
10	9	-4.86	0.32	0.84	0.30

error of the estimate for each set of morphologies. Again, these coefficients correspond to the single fit of (15), not to the average of the two regression lines. The improvement in the quality of the inferred H I contents can be appreciated by comparing the values of the standard deviations in Table IV with the s.e.e. in Table VI, from 0.4 to about 0.25. Notice also that the morphological type dependence becomes a second-order effect, as compared with SM dependence, and because of the way L is folded into both sides of (15), the value of c_2 near 0.4 in (15) is mainly a relation between the hydrogen mass and size. Thus, to use

$$X_H(x_1,x_2,\ldots) \equiv \log M_H/D_l^2 \text{ (type, } D_l) \quad (16)$$

is a simpler approach. The breach of distance independence in the analysis introduced by correcting for the small residual dependence on D_l constitutes a factor of uncertainty which is small in comparison with the errors in the measurements of H I fluxes and optical diameters. The advantages of (16) are, on the other hand, substantial. Unlike luminosity, diameter is a disk property. While magnitudes are severely affected by internal and galactic absorption, sizes are thought to be much less so. Moreover, angular sizes are measured relatively more easily than magnitudes on the PSS prints, so that this technique may be applied to galaxies for which accurate measurements of magnitudes are not available. Most importantly, uncertainties by one or two steps in the morphological-type scale have little effect on the inferred *Def*; such uncertainties can produce serious errors when analysis is carried on via (14).

Throughout this paper, we have avoided the use of magnitudes and angular diameters in any system other than those provided by the CGCG (after removal of systematic biases as described in Sec. IV*f*) and the UGC, the largest sources for the two quantities. However, conversion to standard photometric systems, such as that of Holmberg (1958), for objects for which direct measurements in those systems are not available, has been a common practice in the literature. While those conversions are justifiable for bright, large angular diameter galaxies, they involve daring extrapolations when applied to faint or small galaxies (typically $m > +14.0$ and a smaller than 2.5), introducing large conversion errors. CGCG magnitudes, when properly corrected for systematic biases, are quite reliable, involving random errors on the order of 0.25 mag or less (Giovanelli and Haynes 1984). UGC major diameters for sizes of less than two arcminutes are affected by relative errors that we estimate to be on the order of 10% to 15%, while H I flux integrals of profiles with signal-to-noise ratios larger than about 5 are accurate to within 20% to 30% (Paper II). One should therefore expect the standard errors around the estimate of *Def* using (16), for example, to be on the order of 0.20, caused by purely random errors in the determination of the observed quantities, well in agreement with the s.e.e. obtained for all types except $T = 5$ and $T = 10$ in Table VI and the right-hand side correlation in Table V. The errors are larger for galaxies of type 10 (peculiars) and, to some extent, for those of type 5, which includes not only true Sb's but also vaguely classified spirals (S . . . , S: . . ., etc.). It is surprising that the fit quality is as good as it appears to be for the earlier morphological types, although we remind the reader that we have used *only detections* to derive the coefficients; because the detection rate is low for early types $T < 3$, the use of upper limits as well would certainly increase the spread of points around any fit (cf. Paper I).

We can draw the following conclusions from this section:

(1) The H I content of normal spiral galaxies can be predicted with an accuracy characterized by a standard error of about 0.20 in the log of either the integrated flux or the H I mass, if a dependence on the size of the disk, besides the type, is properly taken into account.

(2) The accuracy of the prediction is better for late spiral types, and for those is basically limited by random errors in the observed parameters rather than by hidden dependences of the residuals.

(3) The use of diameters via (16) to diagnose the expected H I content is preferable. Utilizing M_H/L via (15) will give results which are almost as satisfactory, but it represents an unnecessarily convoluted way of taking into account a basic size dependence which (16) applies explicitly.

VI. CONCLUSION

A 21-cm line survey of isolated galaxies has provided a substantial data base for the future comparison of the integral properties of galaxies in differing intergalactic environments. The sample itself is composed of 324 galaxies of which 288 (89%) have been detected; redshifts are known for a total of 306. The undetected galaxies may include some whose emission lies outside the frequency range searched by the 21-cm observations.

The nondetection percentage increases dramatically for the earliest types. Because of the few detected early-type galaxies, the results of the H I content for types earlier than Sa are of marginal significance. In fact, while some of the early types contain substantial H I masses (Paper I), several of the others are undetected to limits substantially smaller than the lowest detected masses, similar to the bimodal distribution of H I masses in elliptical galaxies discussed by Sanders (1981). The question of the reliability of morphological classifications for faint, small angular diameter galaxies is raised again.

In providing the measure of normal H I content, the Arecibo isolated galaxy sample has several limitations. Because it is heavily weighted to the later morphological classes and because of the lack of available redshifts for some of the undetected galaxies, it can be used only for types Sa and later. The sample is not complete in any magnitude-limited sense and is affected by a Malmquist bias as seen in Fig. 4. However, it does contain a substantial number of later-type relatively distant objects which can serve as a representative population for comparison with galaxies in the nearer Abell clusters.

As discussed previously in Paper II and by Shostak (1978), the H I surface density averaged over the disk is found to be nearly constant and the relationship between the H I mass

$h^2 M_H$ and the square of the linear optical diameter $(hD_1)^2$ is independent, in the first approximation, of morphological type. Because of uncertainties in catalogued magnitudes and in the corrections to the observed magnitudes in converting to luminosities, the use of the hydrogen mass to luminosity ratio M_H/L as the measure of H I content is subject to doubt. We find a residual dependence of M_H/L on L in the sense that more luminous galaxies have lower values of M_H/L as noted by Bottinelli and Gouguenheim (1974). This effect may become quite important in the analysis of samples affected by the Malmquist bias. The best approach to the use of M_H/L as the standard of H I content includes removal of the residual dependence of that ratio on the surface magnitude SM.

The diameter of a spiral disk is a much more important parameter in predicting the H I mass than is the morphological type. The type dependence of M_H/L is largely affected by type variations in $h^2 L$, rather than in $h^2 M_H$. Undoubtedly, the relative importance of the disk and bulge components as a function of morphological type plays an important role; $h^2 L$ is a combined measure of the contributions from both the disk and the gas-free bulge. If a disk luminosity only could be measured, the type-dependence of M_H/L might be substantially reduced.

As both $h^2 M_H$ and hD_1 are disk parameters, the comparison of the standard deviations in the average integral properties shows that the H I surface density M_H/D_1^2 is a better diagnostic tool for the H I content than either M_H/L or the H I mass $h^2 M_H$ alone. For the later-type spirals, the accuracy of the H I content derived from the Arecibo isolated galaxy sample is basically limited by random errors in the observed quantities rather than by hidden dependences.

The Arecibo isolated galaxy sample, as presented herein, describes the standard H I properties of galaxies least affected by their environment and hence provides a valid comparison for others which exist in regions of higher intergalactic density.

The observations required for this study could not have been accomplished without the dedicated assistance of the telescope operations staff of the Arecibo Observatory and the flexible allocation of telescope time by the schedulers, Dr. H. D. Craft, Jr. and Dr. D. B. Campbell. We are especially grateful to Carmen Segarra for her help in making Fig. 3. Various contributions to the project were made by students Leslie K. Hunt, Jacqueline N. Hewitt, and Thomas S. Norton. We are especially appreciative to the numerous Arecibo staff members who gave us their observing time when equipment failures or poor weather conditions prevented them from undertaking their own experiments. We thank J. Huchra, J. Stocke, and G. L. Chincarini for providing redshifts in advance of publication, and D. Burstein for his special tape version of the UGC. Long and fruitful discussions on the best way to determine the H I content of galaxies have been contributed by M. S. Roberts, N. Thonnard, D. Burstein, G. L. Chincarini, and all the participants of the 1982 Green Bank workshop.

APPENDIX A: CORRECTION TO OPTICAL MAGNITUDE FOR INTERNAL ABSORPTION

An examination of the relationship between axial ratio (or inclination) and the observed surface magnitude gives an estimate of the amount of internal absorption within the galactic disk. Much disagreement prevails among various authors who have tried to estimate the corrections to the observed magnitude to account for internal absorption. In his 1958 study, Holmberg found a morphological type dependence in the magnitude correction such that type Sa–Sb spirals show a greater amount of internal obscuration than do Sc's. Presumably, the absorption is caused by dust within the disk. Recent results on the dust content of galaxies (Jura 1981) have shown that the amount of potential obscuring material varies greatly from galaxy to galaxy, even within a single morphological class. Sandage and Tammann (1981) note that Holmberg's sample may have included predominantly dusty Sa's. Furthermore, Heidmann *et al.* (1972b) have found no type dependence and a lesser internal absorption effect for their sample, and argued that part of Homberg's result was influenced by the so-called "perception effect", the underestimate of the axial ratio with decreasing axial ratio, or the dependence of the measured angular diameter on the axial ratio. Because of the uncertainties in Holmberg's coefficients, perhaps the result of sample bias, and because of the distinct differences in terms of size and apparent magnitude of galaxies in our sample and any of the other studies, we have tried to derive appropriate corrections for internal absorption based on the UGC material alone. In order to increase the size of the statistical sample, we extend it to include all galaxies in the UGC. We define a surface magnitude SM as in Eq. (4) (minus the K correction which requires the redshift to be known) which is the surface magnitude the galaxy would exhibit if seen at face-on appearance and with no internal absorption correction. Separately, for each morphological type or group of types, we analyze the dependence of SM on the intrinsic axial ratio $r_i = b'/a'$, as derived from the UGC diameters a and b according to the specifications of Sec. IV *e*. In order to increase the statistical weight of the relatively scarcer but more significant high-inclination systems, we compute averages of SM over bins of $\log r_i$ and then use those to obtain least-squares fits for the relation

$$\mathrm{SM} = c_1 + c_2 \log r_i . \qquad (17)$$

Table VII lists the coefficients c_1 and c_2 for each morphological type or types that exhibit disk structure, as well as the value of the correlation coefficient of the fit and the total number of galaxies used. Data and the computed fits corresponding to the entries in Table VII are illustrated in Fig. 12.

Relations were obtained also for restricted samples excluding all galaxies that are included in Volume I of the CGCG, because of the anomaly with magnitudes in that volume as discussed by Kron and Shane (1976) and discussed in Sec. IV *f*. We find, however, that if the Kron and Shane correction Δm_s is applied, the coefficients c_1 and c_2 obtained from these restricted samples are statistically indistinguish-

TABLE VII. Coefficients of the relation $\mathrm{SM} = c_1 + c_2 \log r_i$.

Type	N	c_1	c_2	r
(1)	(2)	(3)	(4)	(5)
1,2	1283	15.10	-0.40	-0.81
3	652	15.18	-0.59	-0.89
4	530	15.09	-1.01	-0.96
5	3484	15.12	-1.22	-0.99
6	635	15.26	-1.12	-0.95
7	2465	15.50	-1.17	-0.98
8	133	15.37	-1.06	-0.92

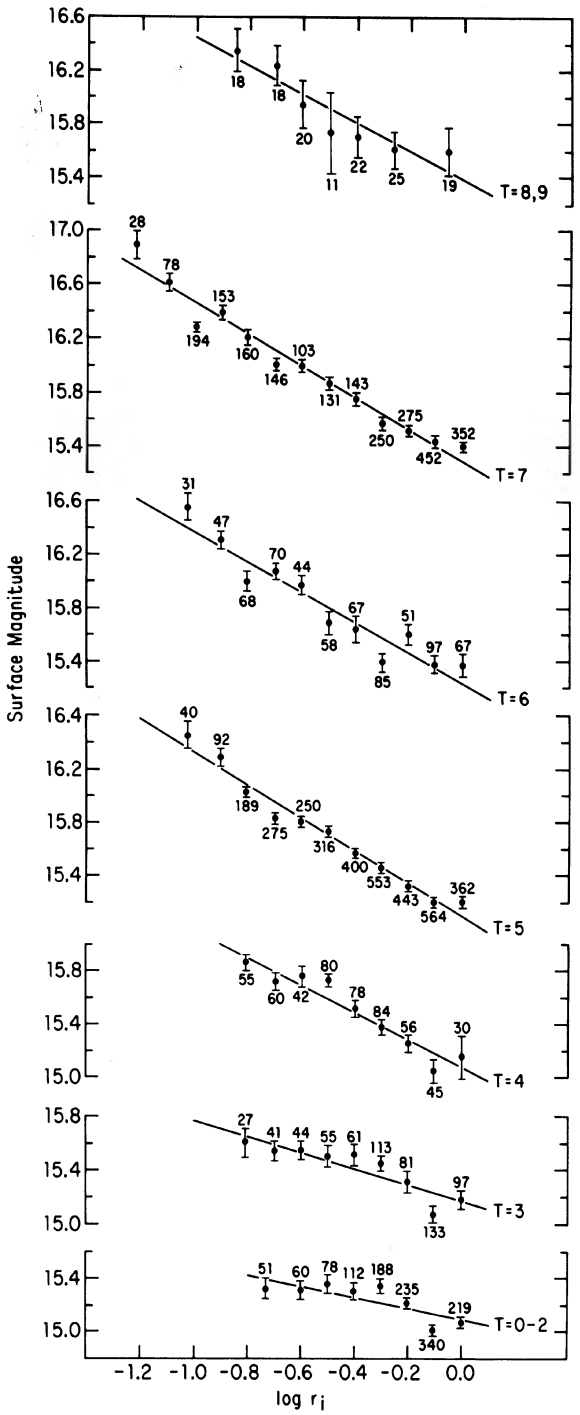

FIG. 12. Variation in the surface magnitude SM as defined in Eq. (4) with axial ratio $r_i = b'/a'$ for different morphological subgroups. All galaxies in the UGC have been used. In order to increase the statistical weight of the scarcer high-inclination systems, averages have been computed over bins of $\log r_i$. The number of galaxies used in computing each average is given along with error bars. The computed fits are listed in Table VII.

able from those derived if galaxies in Volume I are not ignored.

The internal absorption for type $T = 0$ (ellipticals) is assumed to be negligible. No significant dependence of SM on r_i is discernible for dwarf and Magellanic spirals; hence no internal absorption Δm_i is applied for galaxies of type 9. The technique of utilizing Eq. (17) to infer Δm_i is not appropriate for irregular and peculiar galaxies, because the UGC diameters do not reflect the inclination of a disk. In the case of irregulars, because of their similarity in mass, luminosity, and gas content with dwarf and Magellanic spirals, we assume the internal absorption Δm_i to be negligible. In the case of peculiars, a tentative correction Δm_i can be applied only if a disk structure and its inclination can be discerned and a rough guess of the disk morphology made. For all peculiars in our sample of isolated galaxies, we have qualified our estimate of the disk morphology underlying the peculiarity; if such a qualification is not possible, Δm_i is arbitrarily assumed to be zero.

As evident in Fig. 12, galaxies with low values of r_i are uncommon among early morphological types in the UGC. The simplest interpretation is that for early spirals the catalogued axial ratios are heavily affected by the presence of bulges which in inclined systems determine the measured minor diameters. The correction for the observed axial ratio takes into account the occurrence of thicker disks, but not of bulges. As a result, highly inclined systems with large bulge-to-disk ratios may appear in bins of r_i which are not representative of the actual disk inclination. If true inclinations could be measured, the slopes of the relations shown in Fig. 12 and Table VII might be even lower. Thus the inferred increase in the amount of internal extinction for Sb's and Sc's reflects not only the increase of absorbing material in the disk but also the diminishing importance of the bulge contribution to the total light, since the bulge luminosity is largely unabsorbed.

On the assumption that the dependence of SM on r_i is purely the result of internal absorption within the galaxy disk, the correction to face-on magnitude is given by $\Delta m_i = c_2 \log r_i$, where c_2 is the appropriate coefficient from Table VII corresponding to the morphological type of each galaxy.

APPENDIX B: CORRECTION TO H I FLUX FOR INTERNAL H I SELF-ABSORPTION

H I self-absorption within the disk affects to some degree the measured fluxes, especially of highly inclined galaxies. A correction law may be inferred by modeling the distribution of gas within the galaxy. The self-absorption model requires a detailed knowledge not only of the average values of H I densities, spin temperatures, velocity dispersions, and disk geometry as a function of morphological type, but also of the degree of clumping, the spectrum of spin temperatures, and the dependence of those parameters on location in the disk. A simplified model was adopted by Heidmann *et al.* (1972a), who obtained a correction law of the form

$$S_{H,c} = S_c K/(1 - e^{-K}), \tag{18}$$

where $S_{H,c}$ is the H I flux corrected for H I self-absorption, S_c is the observed flux corrected for instrumental effects, and K is a mean optical depth which depends on the inclination of the disk i. Heidmann *et al.* derived a correction of about two percent for the observed flux at inclinations less than 60°, a value which rises to 6%, 9%, and 19%, respectively at $i = 75°$, 80°, and 85°. The comparison of absorption and emission H I spectra within our own galaxy allows an estimate of the amount by which column densities of H I inferred from emission spectra alone (on the assumption of optical thinness) differ from the real column densities. Dick-

TABLE VIII. Average correction factor for galactic H I emission profiles to account for self-absorption (after Dickey and Benson 1982).

range of $\lvert b^{II} \rvert$ (1)	csc $\lvert b^{II} \rvert$ (2)	avg. factor (3)	N (4)
30°	2.00	1.04 ± 0.04	10
15° to 30°	2.0 to 3.9	1.11 ± 0.14	6
10° to 15°	3.9 to 5.8	1.18 ± 0.16	11
5° to 10°	5.8 to 11.5	1.15 ± 0.06	7
3° to 5°	11.5 to 19.1	1.12 ± 0.08	5
3°	19.1	1.52 ± 0.25	6

ey and Benson (1982) have determined such correction factors for a number of lines of sight at different galactic latitudes. In Table VIII, we have averaged them by interval of galactic latitude. The values listed in Table VIII are comparable with the predictions of Eq. (18), although the former constitute only indicative lower limits on the self-absorption correction to the H I fluxes of galaxies such as ours, because of our location *within* the Milky Way. We can infer that for late-type giant spirals, the correction law of Heidmann *et al.* probably underestimates the amount of self-absorption.

TABLE IX. Coefficients of the relation $\log S/a^2 = c_1 + c_2 \log r_i$.

Type (1)	N (2)	c_1 (3)	c_2 (4)	r (5)
0-2	33			
3,4	134	0.219	0.04	0.20
5	420	0.376	0.16	0.79
6	130	0.405	0.14	0.71
7	527	0.395	0.14	0.88
8,9	254	0.306	-0.02	-0.11
10	50			

On the other hand, the self-absorption can be derived following a statistical approach, similar to that for the optical internal absorption in Appendix A, in which we now investigate a correlation between the H I surface density S_c/d^2 and the inclination. Such a correlation may occur for more than one reason, however. Heidmann *et al.* (1972b) advocate a dependence of the measured optical diameter $d(r)$ on the axial ratio r_i of the form

$$\log d(r) = \log d(0) + c \log r_i, \qquad (19)$$

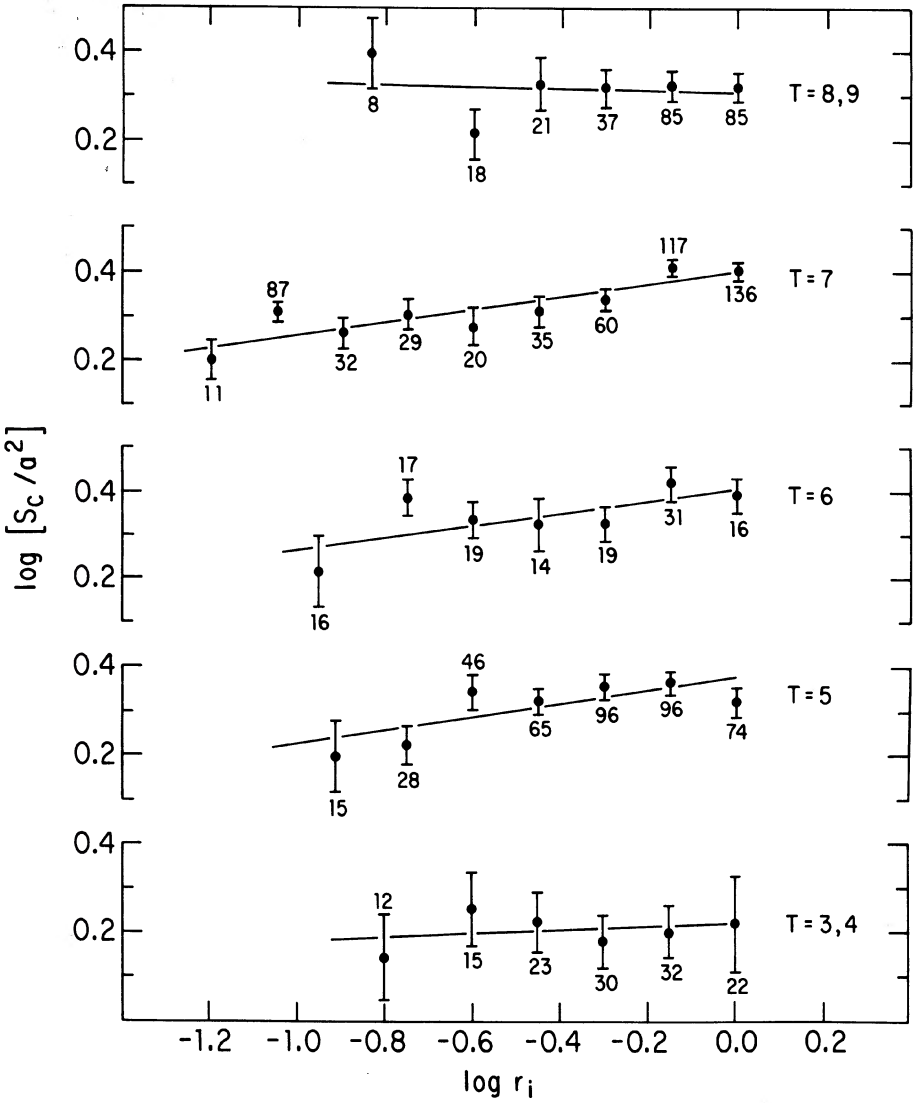

FIG. 13. Correlation between the H I surface density S_c/a^2 and the axial ratio $r_i = b'/a'$ for different morphological subgroups. Data for a total sample of 1500 galaxies detected by us at Arecibo have been included. The H I flux S_c is corrected for instrumental effects but not for H I self-absorption: UGC diameters are used. Data have been binned for intervals of $\log r_i$, and error bars and the number of galaxies used to derive the average values are indicated. Coefficients of the linear regressions are given in Table IX.

where $d(0)$ is the face-on diameter, and r_i is the axial ratio as before. (Notice r_i is the ratio of minor to major diameters, corrected for the "perception effect.") The value of c in Eq. (19) has been much debated in the literature. The results of Heidmann *et al.* (1972b) and of de Vaucouleurs *et al.* (1976) give a value $c = -0.2$, although others (Tully 1972; Lewis 1980) conclude that more likely $c = 0$. The importance of this correction may be underscored by the fact that for an axial ratio of 1/8, $c = -0.2$ implies $d(r) = 1.52d(0)$, which would result in a value of S_c/d^2 less than half as large as the face-on value, even in the absence of H I self-absorption. Given the inclinations usually inferred from catalogued axial ratios, and the relatively large scatter of observed quantities, it makes practical sense to attempt to fit the self-absorption correction by a power law, rather than by an expression of type (18), obtaining

$$\log(S_c/d^2) = c_1 + c_2 \log r_i, \tag{20}$$

where c_1 is the logarithm of the surface density after correction for the inclination bias. We separately investigate the dependences of S_c, d, and the ratio (20) on r_i. For this end, however, the sample of isolated galaxies alone will not suffice, as the subdivision into morphological groups produces statistically poor subsamples. We then utilize a larger sample of over 1500 galaxies observed by us at Arecibo.

For diameters, we use the UGC blue major diameter a. In order to give added weight to the relatively scarcer points of high axial ratio, data have been binned for intervals of $\log r_i$ and a fit obtained to these averaged values; the values of the coefficients of these fits for seven morphological type groups are given in Table IX and the correlations are shown in Fig. 13. Types Sa and Sab were grouped together in Fig. 13 and Table IX; however, although the statistical samples are less reliable, there is an indication that type Sab might resemble more closely the type Sb relation. We shall then for Sab galaxies use a value of 0.10 for c_2, intermediate between that derived for Sb's and that for the combination of Sa's and Sab's. For each group, we also list in Table IX the number of galaxies utilized and the correlation coefficient. Table IX indicates that the effect of the overestimate of the angular diameter with increasing axial ratio as given in Eq. (19) appears to have been largely overestimated by Heidmann *et al.* (1972b), and we can preliminarily conclude that $c > -0.07$. Furthermore, if the H I self-absorption correction to the flux is as large as implied by (18) and by the values listed in Table VIII, then the value of c is indistinguishable from zero as proposed by Tully (1972) and Lewis (1980).

We can attempt to separate the dependences on r_i of S_c and a, by choosing a subsample of galaxies within a narrow range of redshifts, so that the biases introduced by the uncertainties in the distance scale are minimized. Because our sample's velocity distribution sharply peaks at about 5000 km s^{-1}, we have selected the 165 galaxies with velocities between 4500 and 5500 km s^{-1}, of types Sbc and Sc, which can be lumped together because of the similarity of their behavior, as illustrated in Table IX and Fig. 13. We have then verified that for this subsample, there is no preference for galaxies of either end of the axial ratio range to lie on either end of the chosen redshift range (no distance dependence). We have already shown in Paper II and in Sec. V that the H I mass and linear diameter are well correlated. So, we can fit separately

$$\log M_{\rm H} = c_3 + c_4 \log r_i \tag{21}$$

and

$$\log D^2 = c_5 + c_6 \log r_i, \tag{22}$$

where $M_{\rm H}$ is the H I mass and D is the linear optical diameter, inferred from S_c and a. The values obtained for the coefficients upon binning to give weight to the fewer points of high axial ratio are

$$c_3 = 9.54, \quad c_4 = -0.128,$$

and

$$c_5 = 2.72, \quad c_6 = +0.012.$$

The comparison of c_4 and c_6 indicates that most of the inclination dependence of S_c/a^2 is to be attributed to H I self-absorption effects, and that the inclination bias in the measure of the UGC blue diameters is negligible.

A few other observations based on Fig. 13 and Table IX merit mention. The derived inclination correction for Sa galaxies is about a factor of 3 smaller than that for Sb's and Sc's. At the same time, we also notice that the scatter is larger for early morphological types for which there is a marked paucity of objects with high axial ratios. As discussed in Appendix A, the higher values of r_i observed for early-type galaxies may reflect not only the presence of thicker disks, but also the existence of dominating bulge components which are not accounted for in converting from observed axial ratio to disk inclination. As before, highly inclined disks appear in bins of r_i which are not representative of disk inclination, thus increasing the scatter and mildly altering the slope of the corresponding fits. At the other end, the lack of a measurable inclination effect may be the result of two sets of circumstances. On the one hand, disks of very late, Magellanic, and dwarf spirals may indeed be less opaque than those of intrinsically larger Sa to Sc galaxies; this possibility appears to be supported by two facts: first, that face-on H I surface densities, averaged over the optical disk, are significantly smaller for galaxies of types 8 and 9 than for spirals of earlier types; and second, that those late types exhibit little evidence of internal absorption of starlight, as discussed in Appendix A, indicating the scarcity of dust and therefore of densely clumped interstellar gas. Unless H I disks are substantially less extended with respect to their optical counterparts in galaxies of types 8 and 9, then the characteristic H I column densities across the disks of these galaxies are low. On the other hand, inclinations of galaxies in this group as inferred from the observed axial ratio may be uncertain, as the subsample is contaminated by objects of irregular morphology.

Summarizing, we derive a correction for the H I internal self-absorption using an expanded sample of H I observations which is similar in its results to those obtained for optical internal extinction. The correction for H I absorption for types $T < 3$ and $T > 8$ is taken to be zero. For intermediate types, we use the relations in Table IX giving the self-absorption correction factor $f_{\rm H}$:

$$f_{\rm H} = S_{{\rm H},c}/S_c = r_i^{-c_2}, \tag{23}$$

so that the corrected H I flux is just $f_{\rm H}\, S_c$.

APPENDIX C: APPARENT OPTICAL DIAMETERS AND GALACTIC EXTINCTION

The measured values of isophotal diameters of galaxies will be affected by galactic extinction, higher extinctions obviously resulting in smaller diameters. This effect has been analyzed by Heidmann *et al.* (1972b). The extent to which UGC diameters are affected by this bias is more uncertain. UGC diameters are the result of subjective estimates and, although much agreement exists on the high quality of these

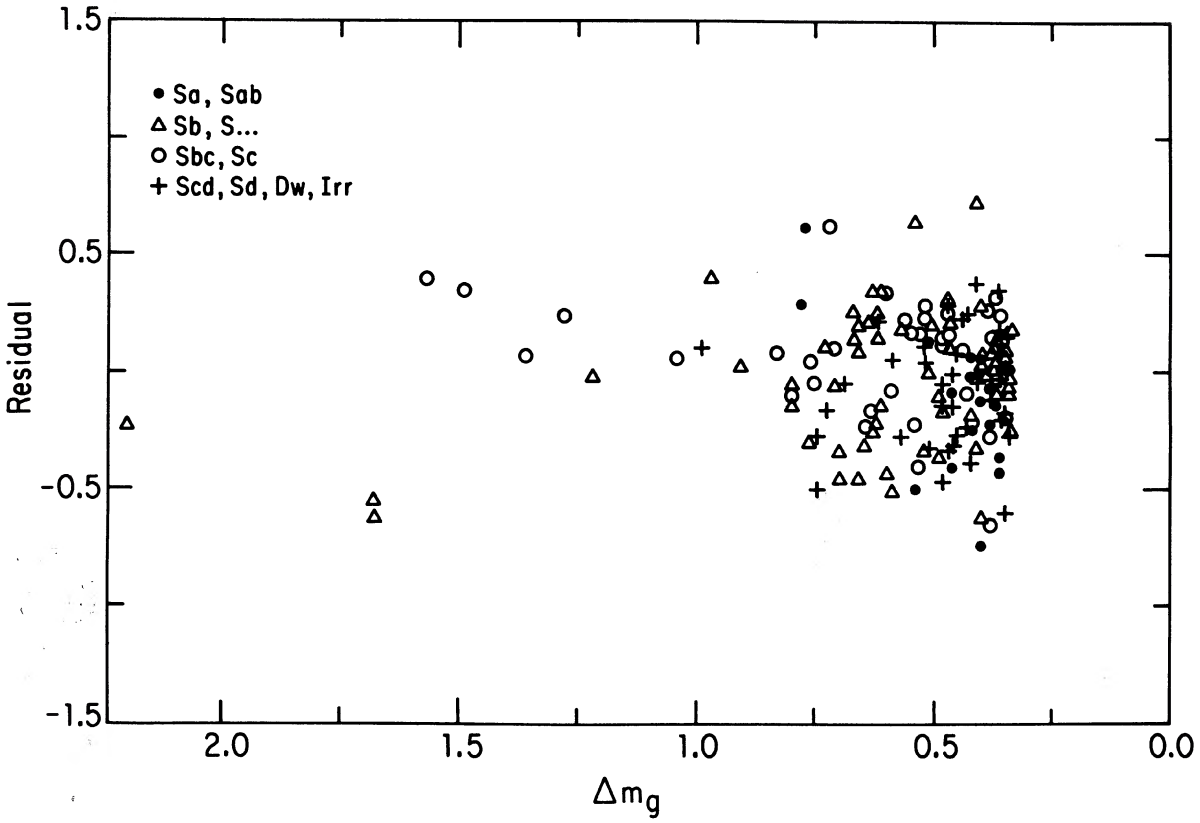

FIG. 14. The residuals of the fit to Eq. (20) against the galactic extinction Δm_g for galaxies within the sample of 1500 which have Δm_g greater than 0.35.

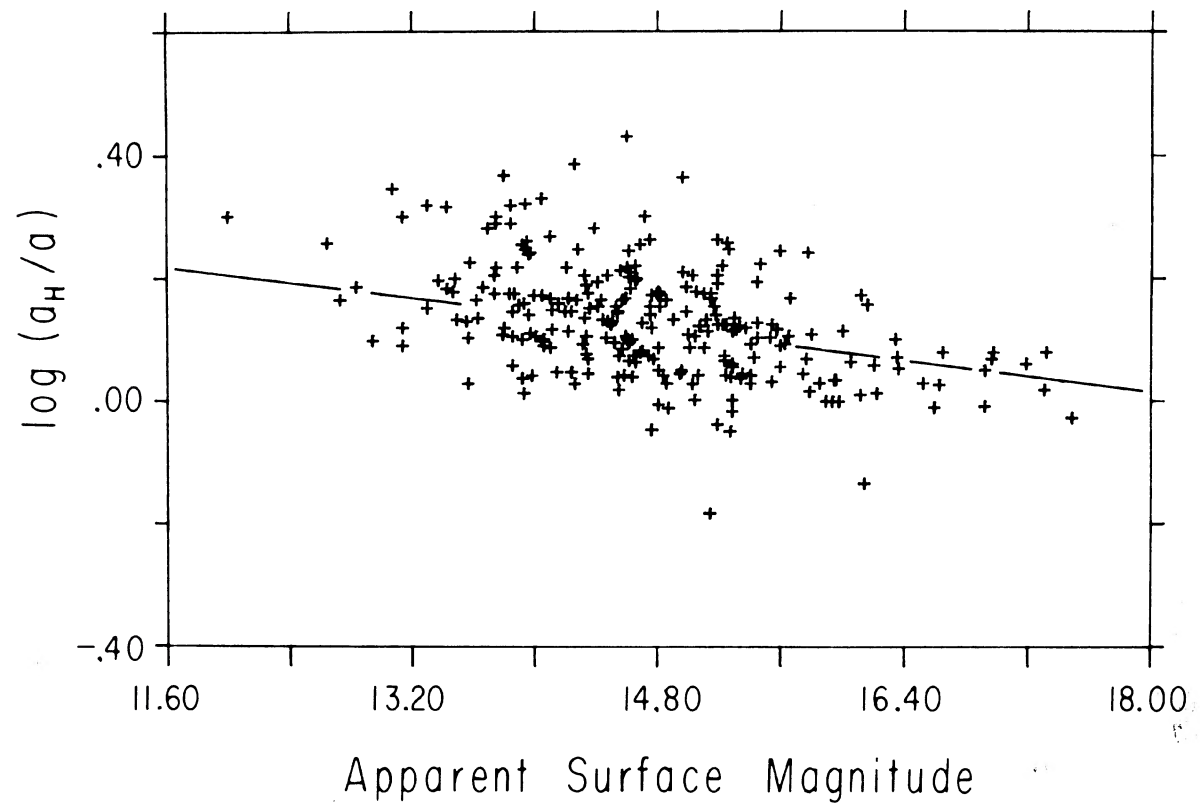

FIG. 15. Relationship between the ratio of the Holmberg to UGC major diameter and UGC apparent surface magnitude, $m + 2.5 \log(ab)$.

estimates, the approximate isophotal level corresponding to them may differ depending on the average surface brightness of the image or on its gradient.

We have tried to determine statistically the magnitude of such an effect by following the same procedure utilized by Heidmann *et al.*, that is, by plotting the residuals of the fit to Eq. (20) against the galactic extinction Δm_g. We did that separately for different morphological types, and used for the fit the coefficients c_1 and c_2 from Table IX. Figure 14 exhibits the residuals with different symbols for different morphological types, for galactic extinction larger than 0.35 mag (for values of extinction smaller than 0.35, the superposition of symbols makes the plot unusable; no effect can be discriminated there anyway). While for extinctions of more than 0.75 mag the majority of points show positive residuals, as one would expect for apparently diminished optical diameters, the three points with highest extinction all show *negative* residuals, leaving the question unanswered. At any rate, it appears that for extinctions of less than 1.5 mag, one can safely state that the underestimate of the optical angular diameter does not exceed 40%.

APPENDIX D: VISUAL OPTICAL DIAMETERS AND SURFACE MAGNITUDE

The visual perception of the angular size of an optical image may depend on such characteristics as its average surface brightness and the gradient in the brightness profile in the outer regions. Romanishin *et al.* (1983) find a relationship between isophotal diameter and UGC diameter, for low surface brightness spirals, which is different from the one obtained for higher surface brightness galaxies. Here, we use the galaxies in the Holmberg (1958) catalog which are in common with the UGC to investigate the mentioned bias in the UGC diameters. Figure 15 displays the logarithm of the ratio between the Holmberg diameter a_H and the UGC major blue diameter a (a_H/a) vs the apparent surface magnitude as derived from UGC data, $\mathrm{SM_{UGC}} = m + 5\log(ab)$, for that sample. The line fit to reproduce the systematic relationship is described by

$$\log(a_H/a) = 0.598 - 0.0326[2.5\log(ab)]. \quad (24)$$

UGC diameters are measured at a lower isophotal level when the average surface brightness is low. The magnitude of the bias is such that for a difference of two surface magnitudes, the disagreement between the UGC diameter and that measured at a constant isophote of 26.5 mag arcsec^{-2} amounts to 18%.

Since we are particularly interested in the correction as applied to spirals, we assume as a standard the UGC diameter measured at a value of apparent surface magnitude $\mathrm{SM_{UGC}}$ of 15.1. Then, for a galaxy of UGC diameter a and apparent surface magnitude $\mathrm{SM_{UGC}}$, we derive a corrected diameter

$$a_c = a(10^{-0.0326(\mathrm{SM_{UGC}} - 15.1)}). \quad (25)$$

REFERENCES

Aaronson, M., and Mould, J. (1983). Astrophys. J. **265**, 1.
Adams, M. T., Jensen, E. B., and Stocke, J. T. (1980). Astron. J. **85**, 1010.
Auman, J. R., Hickson, P., and Fahlman, G. G. (1982). Publ. Astron. Soc. Pac. **94**, 19.
Balkowski, G. (1973). Astron. Astrophys. **29**, 43.
Bothun, G. (1983). Preprint.
Bothun, G., and Schommer, R. A. (1982). Astrophys. J. Lett. **255**, L23.
Bottinelli, L. (1982). In *Comparative H I Content of Normal Galaxies*, proceedings of a Green Bank workshop, p. 5.
Bottinelli, L., and Gouguenheim, L. (1974). Astron. Astrophys. **36**, 461.
Bridle, A. H., Davis, M. M., Fomalont, E. R., and Lequeux, J. (1972). Astron. J. **77**, 405.
Briggs, F. H. (1982). Astrophys. J. **259**, 544.
Burstein, D., and Heiles, C. (1978). Astrophys. J. **225**, 40.
Chamaraux, P., Balkowski, C., and Gerard, S. (1980). Astron. Astrophys. **83**, 38.
Chincarini, G. L., and Rood, H. J. (1979). Astrophys. J. **230**, 648.
Davies, R. D., and Lewis, B. M. (1973a). Mon. Not. R. Astron. Soc. **165**, 213.
Davies, R. D., and Lewis, B. M. (1973b). Mon. Not. R. Astron. Soc. **165**, 231.
Dickey, J. M., and Benson, J. M. (1982). Astron. J. **87**, 278.
Dressel, L. L., and Condon, J. J. (1976). Astrophys. J. Suppl. **31**, 187.
Einasto, J., Joeveer, M., and Saar, E. (1980). Mon. Not. R. Astron. Soc. **193**, 353.
Fesenko, B. I. (1977). Sov. Astron. **20**, 387.
Giovanelli, R., and Haynes, M. P. (1983). Astron. J. **88**, 881.
Giovanelli, R., and Haynes, M. P. (1984). Astron. J. **89**, 1.
Giovanelli, R., Chincarini, G. L., and Haynes, M. P. (1981). Astrophys. J. **247**, 383.
Giovanelli, R., Haynes, M. P., and Chincarini, G. L. (1982). Astrophys. J. **262**, 442.
Haynes, M. P. (1978). Ph.D. thesis, Indiana University.
Haynes, M. P. (1981). Astron. J. **86**, 1126.
Haynes, M. P., and Giovanelli, R. (1980). Astrophys. J. Lett. **240**, L87 (Paper I).
Haynes, M. P., and Giovanelli, R. (1983). Astrophys. J. **275**, 472.(Paper III).
Haynes, M. P., Giovanelli, R., and Chincarini, G. L. (1984a). Annu. Rev. Astron. Astrophys. (to be published).
Haynes, M. P., Giovanelli, R., and Chincarini, G. L. (1984b). In preparation.
Heidmann, J., Heidmann, N., and de Vaucouleurs, G. (1972a). Mem. R. Astron. Soc. **76**, 85.
Heidmann, J., Heidmann, N., and de Vaucouleurs, G. (1972b). Mem. R. Astron. Soc. **76**, 105.
Hewitt, J. N., Haynes, M. P., and Giovanelli, R. (1983). Astron. J. **88**, 272 (Paper II).
Holmberg, E. (1946). Medd. Lund. Astron. Obs. Ser. II, No. 117.
Holmberg, E. (1958). Medd. Lund. Astron. Obs. Ser. II, No. 136.
Huchra, J., and Thuan, T. X. (1977). Astrophys. J. **216**, 694.
Huchra, J., Davis, M., Latham, D., and Tonry, J. (1983). Astrophys. J. Suppl. **52**, 89.
Jura, M. (1981). Astrophys. J. **243**, 108.
Karachentseva, V. E. (1973). Comm. Spec. Astrophys. Obs. **8** (CIG).
Karachentseva, V. E. (1980). Sov. Astron. **24**, 665.
Karachentseva, V. E., and Karachentsev, I. D. (1979). Astrofizika **15**, 589.
Karachentseva, V. E., and Karachentsev, I. D. (1980). Sov. Astron. Lett. **7**.
Kirschner, R. P., Oemler, A., Schechter, P. L., and Schectman, S. A. (1981). Astrophys. J. Lett. **248**, L57.
Knapp, G. R., Kerr, F. J., and Williams, B. A. (1978). Astrophys. J. **222**, 800.
Kron, G. E., and Shane, C. D. (1976). Astrophys. Space Sci. **39**, 401.
Lewis, B. M. (1980). Preprint.
Meisels, A. (1983). Astron. Astrophys. **118**, 21.
Nilson, P. (1973). *Uppsala General Catalogue of Galaxies*, Uppsala Astron. Obs. Ann. **6** (UGC).
Pence, W. D. (1976). Astrophys. J. **203**, 39.
Peterson, S. D. (1979). Astrophys. J. Suppl. **40**, 527.
Richter, O.-G., and Huchtmeier, W. K. (1983). Preprint.
Roberts, M. S. (1969). Astron. J. **74**, 859.
Roberts, M. S. (1975). In *Galaxies and the Universe*, edited by A. Sandage, M. Sandage, and J. Kristian (University of Chicago Press, Chicago), p. 309.
Roberts, M. S. (1978). Astron. J. **83**, 1026.

Romanishin, W., Stron, K. M., and Strom, S. E. (1983). Astrophys. J. Suppl. **53**, 105.
Sandage, A. (1978). Astron. J. **83**, 904.
Sandage, A., and Tammann, G. A. (1981). *Revised Shapley-Ames Catalog of Bright Galaxies* (Carnegie Institution of Washington, Washington, D.C.).
Sanders, R. H. (1978). Astrophys. J. **244**, 820.
Shostak, G. S. (1978). Astron. Astrophys. **68**, 321.
Soneira, R. M., and Peebles, P. J. E. (1977). Astrophys. J. **211**, 1.
Stocke, J. (1978). Astron. J. **83**, 348.
Stocke, J. (1979). Private communication.
Tully, R. B. (1972). Mon. Not. R. Astron. Soc. **159**, 35P.
Tully, R. B., and Fisher, J. R. (1977). Astron. Astrophys. **54**, 661.
Turner, E. L., and Gott, J. R. (1976). Astrophys. J. Suppl. **32**, 409.
de Vaucouleurs, G. (1975). In *Galaxies and the Universe*, edited by A. Sandage, M. Sandage, and J. Kristian (University of Chicago Press, Chicago), p. 557.
de Vaucouleurs, G., de Vaucouleurs, A., and Corwin, H. G. (1976). *Second Reference Catalog of Bright Galaxies* (University of Texas, Austin).
Zwicky, F., Herzog, E., Karpowicz, M., Kowal, C. T., and Wild, P. (1960–1968). *Catalog of Galaxies and Clusters of Galaxies* (California Institute of Technology, Pasadena, Calif.), six volumes (CGCG).